Fall 1-1-2019

In-quest of Biomarkers For Alzheimer's Disease And Pharmacokinetic Profile of Anticancer Agents Using Lc-ms In Human Plasma

Chandana Mannem
Cleveland State University

IN-QUEST OF BIOMARKERS FOR ALZHEIMER'S DISEASE AND PHARMACOKINETIC PROFILE OF ANTICANCER AGENTS USING LC-MS IN HUMAN PLASMA

CHANDANA MANNEM

Bachelor of Science in Pharmaceutical Sciences

Jawaharlal Nehru Technological University, India

April 2010

submitted in partial fulfillment of requirements for the degree

DOCTOR OF PHILOSOPHY IN CLINICAL-BIOANALYTICAL CHEMISTRY

at

CLEVELAND STATE UNIVERSITY

December 2019

We hereby approve this dissertation for

Chandana Mannem

Candidate for the Doctor of Philosophy in Clinical-Bioanalytical Chemistry degree

for the Department of Chemistry
And
CLEVELAND STATE UNIVERSITY
College of Graduate Studies

_____

Dissertation Chairperson, Dr. Yan Xu

_____

Department of Chemistry & 26 Nov 2019

_____

Dissertation Committee Member, Dr. Anthony Berdis

_____

Department of Chemistry & 26 Nov 2019

_____

Dissertation Committee Member, Dr. Xue-Long Sun

_____

Department of Chemistry & 26 Nov 2019

_____

Dissertation Committee Member, Dr. Yana Sandlers

_____

Department of Chemistry & 26 Nov 2019

_____

Dissertation Committee Member, Dr. Yuping Wu

_____

Department of Mathematics & 26 Nov 2019

Student's Date of Defense: November 26, 2019

Dedicated to my loving family Kalpana Mannem, Prabhakar Reddy Mannem and Krishna Kanth Reddy Mannem

and

to my dear husband, Shashank Gorityala

ACKNOWLEDGEMENT

I am grateful that I have Dr. Yan Xu as my advisor and mentor while pursuing my doctoral study. I first met him in his "Chromatography and Separations" class and then decided to join the group. I was stubborn to join his group, and I have a fond memory of being rejected three times by Dr. Xu before he says "Yes" to me. I was given a small project over summer to do and then joined the group. Initially, I feared to communicate with him, but he is patient and kind enough to teach me and guide me throughout the process of learning and molding my thinking process as an analytical scientist. I quote, he always says, "Ph.D. is a process of becoming independent from dependent" in terms of the thinking process, writing, and doing work meticulously. I enjoyed working in his lab and gave me more extensive exposure to critical thinking. Without his guidance, supervision, and persistent push and encouragement, this would not have been possible.

I want to take this opportunity and thank Dr. Shuming Yang, who taught me the techniques of research during my initial phase. He is kind enough to teach me all of the minor techniques, which made my life easy on the day-to-day research process.

I would like to thank my committee members, Dr. Anthony Berdis, Dr. Xue-Long Sun, Dr. Yana Sandlers, and Dr. Yuping Wu, for providing me their valuable suggestions on every aspect of my research. It was my pleasure to work with you all.

I would like to thank Dr. Jagan A Pillai for collaboration and for providing samples for my research work. I would like to take this opportunity and thank Dr. Mundell, for all the support and help during my duties as a TA. I would like to thank Dr.Xiang Zhou for his support with instrument training.

I appreciate the input from my previous group members, Dr. Girish Avula, Dr. Sandeep Kunati, Dr. Shashank Gorityala, Dr. Sujatha Chilakala, Dr. Gang Xu, and current lab members.

A special and heartfelt thanks to my husband, Shashank Gorityala. This work would not have been possible without his support.

IN-QUEST OF BIOMARKERS FOR ALZHEIMER'S DISEASE AND PHARMACOKINETIC PROFILE OF ANTICANCER AGENTS USING LC-MS IN HUMAN PLASMA

CHANDANA MANNEM

ABSTRACT

In this dissertation work, a semi-quantitative assay using a lipidomics approach and an absolute quantitative assay using liquid chromatography-mass spectrometry techniques were developed (LC-MS). In the lipidomics approach, ultra-high pressure liquid chromatography in tandem with quadrupole time of flight (UHPLC-QTOF) mass spectrometry was used to profile, compare and quantitate the human plasma lipids in Alzheimer's disease subjects (AD) and normal cognitive controls (NCCs). The purpose of this study is to identify potential plasma lipid markers of AD and to explore the relationships between AD and lipid pathways in humans by using bioinformatic tools. The plasma samples of study subjects were first spiked with a mix of 12 synthetic-lipid internal standards, then total lipids were extracted using a modified Blight-Dyer method and fractionated into phospholipids (PL) and neutral lipids (NL) using the aminopropyl cartridge. The UHPLC-QTOF-MS/MS data were processed and analyzed with corrections of retention time and mass shifts. Molecular features were extracted for lipid identifications based on mass-to-charge ratios, isotopic patterns, adducts, and charge states. Venn diagrams were plotted to group the common and the unique features of lipids between AD patients and NCCs. The common significant molecular features between these two study groups were analyzed using principal component analysis (PCA), partial least

squares-discriminant analysis (PLS-DA), and non-parametric Wilcoxon rank-sum *t*-test with false discovery rate calculated *p*-values. Quantitative lipidomics was performed on the twenty-eight identified significant common lipids. Our results indicate these significant common lipids between AD patients and NCCs were belong to glycerophospholipids, glycerolipids, and sphingolipids. Gene-lipid centric pathway analysis was performed on these significant lipids to obtain the implicated pathways in AD and to understand it's relation to AD.

In absolute quantitation work, an assay using a liquid chromatography system in tandem with triple quadrupole mass spectrometry (LC-QqQ) was developed and validated to measure the O^6Benzylguanine (O^6BG) and its metabolite, 8-oxo-O^6Benzylguanine (8-oxo-O^6BG) in human plasma. O^6BG and 8-oxo-O^6BG along with the analog internal standard, *p*Cl-O^6BG, were extracted from alkalinized human plasma by liquid-liquid extraction (LLE) using ethyl acetate, dried under nitrogen and reconstituted in the mobile phase. Reverse-phase chromatographic separation was achieved using isocratic elution with a mobile phase containing 80% acetonitrile and 0.05% formic acid in water at a flow rate of 0.600 mL/min. Quantification was performed using multiple-reaction-monitoring (MRM) mode with positive ion-spray ionization. The linear calibration ranges of the method for O^6BG and 8-oxo-O^6BG were 1.25 to 250 ng/mL and 5.00 to 1.00×10^3 ng/mL respectively with acceptable assay accuracy, precision, recovery and matrix factor. The method was validated as per the Food and Drug Administration (FDA) guidelines and was applied to the measurement of O^6BG and 8-oxo-O^6BG in patient plasma samples from the prior phase I clinical trial.

TABLE OF CONTENTS

Page

LIST OF TABLES

LIST OF FIGURES

CHAPTER I

APPLICATION OF LIQUID CHROMATOGRAPHY-MASS SPECTROMETRY IN HUMAN PHARMACOKINETIC AND BIOMARKER ANALYSIS

1.1. Pharmacokinetic (PK) analysis of drugs using mass spectrometry

1.1.1. Introduction

Pharmacokinetics (PK) is the study of absorption, distribution, metabolism, and excretion (ADME) of drugs which is of fundamental importance in determining the drug's effect on the biological system and the response incurred by the drug administration [1–3]. With the advances in the drug development and the regulatory requirements surrounding this space has increased the need of reliable analytical techniques as well as methodologies. Mass spectrometry has played a central role in the pharmacokinetic studies to gain the drug's quantitative information thus able to estimate the drug distribution, metabolism, excretion and half-life of the drug [4–7]. Pharmacodynamics (PD) deals with the study of the relationships between the concentration of the drug at the effective site such as receptor and the extent of the pharmacological effect evident. The primary goal of PD is to establish

the dose-response profile of the drug in the biological system and is often carried out in parallel to PK study [8–10].

Liquid chromatography coupled with the soft ionization techniques like electrospray ionization (ESI) or atmospheric pressure chemical ionization (APCI) with triple quadrupole mass spectrometry is the most common type of analytical methodology applied for the pharmacokinetic studies of the drugs. The major reason being the capability of Liquid Chromatography-Mass Spectrometry (LC-MS/MS) to simultaneously get the structural as well as quantitative information of the drug in its various stages of metabolism. With the advent of more potent drugs, the administration dose levels have significantly reduced which in turn circumvents the need for more reliable, accurate and sensitive quantitative methods in complex biomatrices like plasma, serum, urine and tissue which can be easily achieved by LC-MS/MS [11–13]. This is carried out in three distinct phases *i.e.*, bioanalytical method development, validation and sample analysis.

1.1.2. Workflow of bioanalytical method development

The bioanalytical method development comprises of two key aspects, sample extraction/preparation and instrumentation.

1.1.3. Biological sample extraction

With the advancements of the drug modalities, the potency of the drug has increased which requires a sensitive quantitative method for the analysis of the drug. Quantitative bioanalytical methods are focused to meet the requirements of detecting the trace quantities of drugs or endogenous compounds in complex biomatrices like urine,

plasma, serum, saliva and tissues. To achieve this goal, the major challenge is encountered from the interfering compounds present in these matrices such as proteins, lipids, metabolites, salts and endogenous compounds. Essentially the success of the quantitative method is dependent on the selective extraction of the analytes of interest form the other endogenous components of the matrix. The community has been employing some common extraction methods to meet these requirements such as protein precipitation (PPT), liquid-liquid extraction (LLE), solid phase extraction (SPE), solid-liquid extraction (SLE) [14–16]. This work used the sample preparation techniques of liquid-liquid extraction (LLE), which along with other extraction techniques will be discussed in brief.

1.1.3.1. Protein precipitation (PPT)

This is the most common method of extraction for the sample clean-up of analytes form the blood products such as whole blood, plasma, serum. It is usually applied to the various species such as dogs, rats, mice and human universally in spite of the matrices differences. PPT usually allows the disruption of drug binding to the proteins by either acidifying or basifying the protein precipitation solvents, which basically denatures the protein and inhibits the drug binding capacity depending on the binding mechanism. Usually the organic solvents like methanol, acetonitrile or a combination of organic solvents and organic salts are used for the precipitation of the samples. This step is followed by the centrifugation step which settles down the precipitated protein as sediment and the supernatant can be isolated and used for the analysis.

A protein in solution is acted upon by the attractive forces form the induced dipoles, and repulsive forces resulting from the hydration layer around protein. The

balance between these forces is responsible for the non-aggregation of protein in the solution. The principle of protein precipitation is based on disrupting the balance between the attractive and repulsive forces on the protein in the aqueous solution, and this is achieved by the organic solvents by reducing the hydration layer around protein leading to the aggregation and precipitation of the protein. Though this sample preparation technique is quite efficient in extracting the analyte of interest, the major limitation of this is its inability to remove salts form the sample [17–21].

1.1.3.2. Liquid-Liquid extraction (LLE)

The physical and chemical properties of the components in the matrix are different, and these differences determine the differential solubility of these components. LLE exploits the differential solubility of different matrix components and selectively extracts the analytes of interest. This extraction is based on the principle that the separation is based in the differences in the distribution of the analyte in the water-immiscible organic phase. The aqueous mixture of the matrix along with the analyte is mixed with the water immiscible organic solvents and agitated, so that two distinct layers of immiscible layers are formed, and the analytes of interest are partitioned between these layers depending on the properties of the components. The hydrophilicity and the hydrophobicity drive this partitioning. This partitioning is complete at a state of equilibrium when the ratio of the concentrations in the two solvents no longer change. This is represented by the distribution constant (K_D) with the following equation

$$K_D = C_o/C_{aq} \quad \text{(Equation 1.1)}$$

where C_o = concentration of the analyte in the organic phase

C_{aq} = concentration of the analyte in the aqueous phase.

The partitioning of the compound is dependent on the K_D value. Higher being the indication of better partitioning between the phases and lower being the prerequisite for repeated extraction. K_D can be increased by altering the strength of the organic solvent. Hydrophobic molecules can be dissolved by adding a much non-polar solvents such as hexane, carbon tetrachloride, whereas the polar molecules can be extracted using polar solvents such as ethyl acetate and chloroform. Alternative strategy to decrease the solubility of the molecule in the aqueous phase is 'salting out'. This is achieved by suppressing the ionic nature of the molecule by changing the pH that can bring about the change in the solubility of the molecule in that phase [22–24].

The primary advantage of using LLE over protein precipitation is the ability of LLE to remove the salts and other interfering components of the matrix. However, on the down side LLE required significant amount of organic solvents and sometimes time consuming. There has also been reports of the emulsion formation when LLE is performed.

1.1.3.3. Solid-Phase extraction (SPE)

Solid-Phase extraction is the most intensive and efficient sample preparation technique for the bioanalytical assays. This offers higher degree of selectivity, cleaner sample extracts and ability to automate. This technique uses a sorbent bed where the analytes are retained on the bed, and the bed is washed to remove the interfering components and finally the analytes are eluted using the elution solvents. The choice of the SPE system is dependent on the nature of the analyte and the type of the interactions possible with the sorbent bed. The most common type of interactions involved in this type

of extraction are Vander Waals forces, hydrogen bonding, dipole-dipole interactions and cation-anion interactions. Most commonly used SPE sorbent is reverse phase which is employed when a nonpolar analyte is present in a polar matrix. Reverse phase SPE cartridges uses the alkyl- or aryl-bonded silicas (C-18, C-8, C-4) reverse phases. Normal phase is less common and used when a polar analyte is present in the non-polar to mid-polar matrix. The typical media used for the normal phase cartridges are polar functionalized bonded silica like LC-CN, LC-NH_2, and LC-Diol. Ion exchange chromatography is used for the analytes which are ionized in the solution. Cationic (positive) compounds are separated using the silica with sulphonic acid groups whereas the anionic negative) charged analytes are separated using aliphatic quaternary amine group bonded to silica surface [25–28].

The major advantage of this technique is the efficient removal of the interfering components of the matrix and relatively higher recoveries. It must be noted that this is also a complicated process and need careful optimization of the conditions and elution parameters. Careful evaluation of the interactions between the chromatographic bed and the analyte must be made before choosing the SPE variant. This offers the flexibility of automation [29,30].

1.1.4. Liquid chromatography- mass spectrometry (LC-MS)

LC-MS has gained significance as the primary technique of choice for the quantitative and qualitative analytical workflow. This has gained an important position in the drug research and development. The basic components of LC-MS are represented in Fig. 1.1.

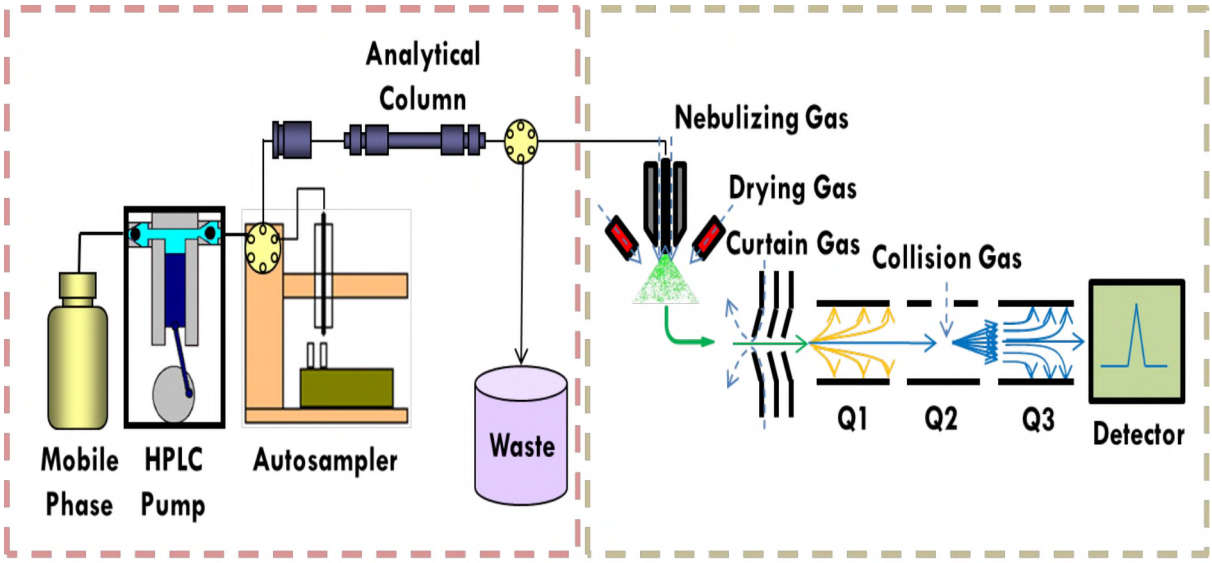

Figure 1.1. Basic components of LC-MS instrument [103].

1.1.4.1. Liquid chromatography (LC)

Liquid chromatography is a separation technique to separate the analytes of interest from the complex mixtures and biological matrices. It comprises of the mobile phase, pumping mechanism, an autosampler, and an analytical column, which is connected to the detector. Mobile phase constitutes the liquid component whose constant flow is maintained by the binary pumps, autosampler is for the injection of the sample and an analytical column for the actual separation of analytes from the complex mixtures. Sometimes the guard column is used optionally to protect the analytical column.

The most commonly used modes of LC are reverse-phase chromatography RPC), normal-phase chromatography (NPC), hydrophilic interaction chromatography (HILIC), and ion-pair chromatography (IPC). Based on the nature of the analyte, different modes of LC separation are employed [31,32]. As mentioned, this work used the RPC, which will be further discussed.

Reverse-phase chromatography (RPC) consists of a C-8 or C-18 non-polar alkyl hydrocarbons that are bonded to silica support as stationary phase and mobile phases are mixture of aqueous and organic solvents. RPC is based on the principle of analyte partitioning between the mobile phase and the stationary phase. The retention of the analyte in this is dependent on the pH, polarity and the organic content in the mobile phase. These factors contribute to the selectivity to the separation. When compared to the other separation techniques like NPC and IEC which need the use of nonvolatile salts like phosphates or additives like ion pairing reagents, RPLC is more compatible with MS with respect to the composition of mobile phase [33,34].

1.1.4.2. Mass spectrometry

Mass spectrometry (MS) is the detection technique which identifies the molecules based on their mass to charge (m/z) ratio. In recent times, this technique has gained significance in the pharmacokinetic research. Mass spectrometry hyphenated with liquid chromatography is used for the structure elucidation, accurate quantification of the metabolites in the biological systems. The working of the mass spectrometry is a combined events of sample ionization and vaporization in the ion source followed by the separation of the produced ions in the mass analyzer based on the respective m/z ratio. The ions produced are finally detected by the detector which is read out as mass spectrum.

Nature of the analyte and the complexity of the matrix dictates the type of the ion source employed for the LC-MS analysis. The most commonly used ion sources are electrospray ionization (ESI) and atmospheric pressure chemical ionization (APCI). In this work, we used the ESI ion source where the sample passes through the charged needle to produce a spray of droplets at the atmospheric pressure. The droplets are either charged positive or negative in the solvent, and the heated nebulization gases aids in the evaporation of the solvents. The produced ions travel the mass analyzers.

Mass analyzers help in the separation of ions based on the mass-to-charge (m/z) ratios in presence of electric and magnetic field. The common mass analyzers used are quadrupole MS, ion trap MS, and time-of-flight (TOF) MS. This work used the triple quadrupole (QqQ) analyzer for the quantification of drug in the biomatrix (Fig.1.2). QqQ analyzer mainly consists of three quadrupoles in which Q1 and Q3 are the mass filters whereas Q2 acts as the collision cell which is the non-mass resolving quadrupole.

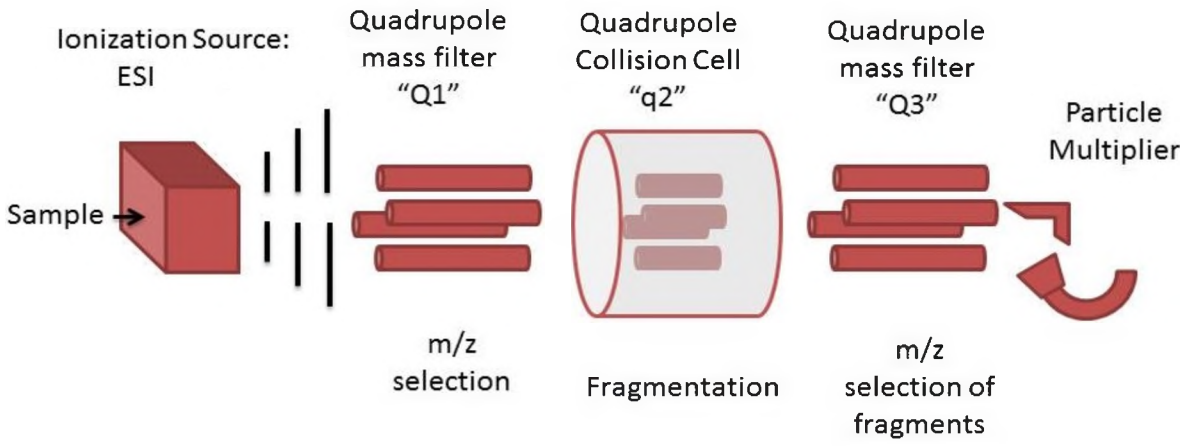

Figure 1.2. Components of a triple quadrupole mass spectrometer [103].

Each set of the quadrupole rods in Q1 and Q3 are applied with DC voltage and radiofrequency. This voltage imparts the electromagnetic field between the electrodes. This electromagnetic filed acts as the filter for the ions of particular m/z. Q2 is the collision cells where the ions are fragmented via collision induced dissociation (CID). Essentially, Q1 selects the parent or precursor ions, Q2 fragments them and passes them to Q3, and finally Q3 filters the daughter ions to reach the detector [35–37].

1.1.5. Bioanalytical method development and validation

Method development and validation are the key aspects of a successful analysis of the study samples. The method that is developed for the quantitative determination of the analytes of interest has to be validated for its accuracy and reproducibility before the application of the developed method for the analysis of the incurred samples [38–40].

1.1.5.1. Method development

During the method development, the major focus is the optimization of the mass spectrometer parameters, LC and sample preparation. The first step of the method development is the tuning of mass spectrometer by direct infusion or by LC flow-injection of the analytes in mobile phases to determine the mass spectrometric variables. Full MS scans are performed to identify the molecular and adduct ions which is followed by the fragmentation of these ions to determine the fragmentation pattern of the analyte. To enhance the specificity, multiple reaction monitoring (MRM) are used based on the fragmentation of the analyte. Thus, specific MRM transitions are selected for the analyte and its respective internal standard.

LC optimization includes selection of the mobile phase, type of column, flow rate, pH, elution profile, etc. The main aim is to achieve baseline separation of the analytes from the matrix interfering components. The peak shape and consistency are determined to ensure the method accuracy and reproducibility [38,39,41,42].

The most important aspect of the method development is the sample extraction. Sample extraction is designed to selectively extract the analyte of interest and its corresponding internal standard from complex matrices such as blood, plasma, serum, tissues, etc. Recovery and matrix effect evaluations determine the quality of the developed sample extraction method. Based on the analyte's polarity and chemical properties, the extraction method is optimized for the best signal-to-noise ratio. Sometimes, a combination of sample extraction techniques may be required to obtain the optimized signal-to-noise-ratio. Finally, the developed method is subjected to method validation based on the FDA-ICH guidelines for industrial bioanalytical method validation.

1.1.5.2. Method validation

The U.S Food and Drug administration (FDA) has formulated the guidelines for the validation of quantitative bioanalytical methods developed for the small molecules before their application to the preclinical and clinical studies. These guidelines constitute the standard procedures along with the acceptance criteria for the development of accurate and reliable bioanalytical methods for the small molecules in biomatrices. These guidelines consist of selectivity, sensitivity, linearity of the calibration curve, matrix effect, recovery, accuracy, precision, and stability studies.

The following is the brief discussion on the guidelines used for this work.

I. Selectivity

Selectivity is described as the ability of an analytical method to differentiate and quantify the analyte in the presence of other components in the sample. To ensure the selectivity of the assay the following tests are performed.

a. Blank matrices from 6 individual sources are used and the mass chromatograms at m/z of analyte and m/z of internal standard (IS) is evaluated in 5 replicates.

b. In case of the interference in the blank matrix at the same retention time (t_R) of the analyte and IS, their mean peak area must be $\leq$ 20% of the mean peak area of the analyte at lower limit of quantitation (LLOQ), and $\leq$ 5% of the IS.

c. Sensitivity of the method is a measure of LLOQ. It is the lowest amount that can be quantified with acceptable accuracy and precision using the method developed.

d. LLOQ must be determined by evaluating at least 5 replicates of the sample at the

e. LLOQ concentration on at least one of the validation days. The acceptance criteria for this is the intra-run precision (%CV) and accuracy (%RE) should be $\leq \pm$ 20%.

f. Apart from the above condition, the LLOQ is also evaluated in 6 sources of blank

g. matrix with 5 replicated of each sample. The acceptance criteria being the %CV and %RE $\leq \pm$ 20%.

II. Calibration standards

The calibration standards constitute the calibration curve which includes.

a. Matrix blank: matrix sample without IS, also known as the double blank.

b. Zero standard: matrix sample with IS, also known as blank.

c. 6 to 8 non-zero standards, which are calibrators.

d. The acceptance criteria for considering the calibration curve are at least 75% of standards/calibrators should meet the criteria; LLOQ $\leq$ 20% and all other calibrators $\leq$ 15%.

III. Upper limit of quantitation (ULOQ)

This is not a mandatory test that must be included in the validation. However, this is included to demonstrate the ruggedness of the developed method. The accuracy and precision may be determined in a similar manner as LLOQ but %CV and %RE should be $\leq$ 15%.

IV. Validation batches

The validation batches are analyzed at least 3 batches (i.e., calibration curves), typically 5 for accuracy (%RE) and precision (%CV). These are performed in two types, intra-day (compared within the same day) and inter-day (compared on different days).

V. QC samples

The QC samples are analyzed to evaluate the calibration curve performance in measuring the unknown samples.

a. QCs are analyzed in three different concentrations (low, mid, and high) with either 6 or a minimum of 5% of the total number of unknown samples in each analytical batch.

b. The acceptance criteria for the QCs is at least 67% (4 out of 6) of the QC samples should meet the acceptance criteria i.e., LLOQ $\leq$ 20%, all others $\leq$ 15%. It is also important to note that 33% of the QC samples which cannot be all the replicates at the same concentration, can be outside the acceptance criteria.

c. If more than 2 QC samples at a concentration fail to meet the criteria, then 50% of QC samples at each concentration should meet the acceptance criteria.

VI. Preparation of calibration standards and QC samples

Calibration standards and QC samples must be prepared from different spiking stock solutions. A single source of matrix may also be used if selectivity has been verified.

VII. Positional differences

While performing a validation batch, the calibrators and the quality controls are analyzed in a predefined sequence

a. One set of calibrators is place at the beginning of the run (front curve).

b. The quality controls and other validation related samples are arranged after the first calibration curve. The validation samples and the quality controls are randomized in positions.

c. Another set of calibrators is analyzed at the end of the run (back curve). This makes it a dual curve.

d. To assess the carryover effect, a blank matrix sample or zero standard is placed after the high concentration sample (ULOQ).

VIII. Placement of samples

The calibrators, blanks, QCs and the unknown study samples are arranged in an appropriate sequence based on the needs of the study. Usually it is recommended to randomly spread the unknown study samples among the QCs for a better estimate of the method performance.

IX. Recovery

The recovery of an analyte in an assay is the detector response obtained from an amount of the analyte added to and extracted from the biological matrix, compared to the detector response obtained for the true concentration the pure authentic standard. Recovery gives an estimate of the extraction efficiency of an analytical method within the limits of variability. Recovery of the analyte in a bioanalytical method is not expected to be 100% however the recovery of an analyte and of the internal standard should be consistent, precise and reproducible. The following are the criteria for the recovery

a. The recovery of the analyte and IS must be reproducible and consistent.

b. The samples included in this test are blank matrix spiked with analyte and IS; extracted blank matrix spiked with analyte and IS.

c. These samples are prepared at all the three QC concentrations and analyzed in the replicates of 5.

d. Peak areas (PA) of analyte and IS are calculated/obtained from the chromatograms and recovery is calculated using the following equations

$Recovery_{analyte}$ = [(PA of analyte in matrix)/(PA of analyte in extracted matrix)] X 100%

$Recovery_{IS}$ = [(PA of IS in matrix)/(PA of IS in extracted matrix)] X 100%

IS normalized recovery or $Recovery_{normalized}$ = (Recovery of analyte)/(Recovery of IS)

X. Matrix effect

Matrix factor, also termed as matrix effect is a measure of the suppression or enhancement of ionization by co-eluting compounds, which is common in ESI source. This parameter provides the information on the interference of endogenous compounds in the matrix on the quantitation of the analyte of interest.

a. It is ideal to have an absolute MF or IS-normalized MF of about 1 for the assay to be reliable and reproducible. However, it is not a requirement. If IS is a heavy isotope labeled compound, IS normalized MF is expected to be close to 1.

b. It is a requirement to determine absolute MF (or IS-normalized MF) in 6 individual matrix lots and %CV should be less than 15%. If a stable isotope labeled IS is employed, this requirement does not apply.

c. The samples included in this test are spiked with analyte and IS in the extracted blank matrix and the solvent.

d. These samples are prepared at all the three QC concentrations and analyzed in the replicates of 5.

e. Peak areas (PA) of analyte and IS are obtained from the chromatograms and matrix factor (MF) is calculated using the following equations

$MF_{analyte}$ = [(PA of analyte in extracted matrix)/(PA of analyte in solvent)]

MF_{IS} = [(PA of IS in extracted matrix)/(PA of IS in solvent)]

IS normalized MF or $MF_{normalized}$ = ($MF_{analyte}$)/(MF_{IS})

XI. Accuracy and precision

The accuracy of an analytical method is defined by the closeness of the mean test results obtained by the method to the true value (concentration) of the analyte. Accuracy is determined by the replicate analysis of the samples containing known amounts of the analyte. The precision of an analytical method id defined by the closeness of individual measures of an analyte when the procedure is applied repeatedly to multiple aliquots of a single homogenous volume of the biological matrix.

a. Three level concentration QC samples (low, mid, and high) plus dilution QC are included in this test.

b. Low QC is the concentration level near the LLOQ (up to 3 x LLOQ).

c. Mid QC is the concentration level which is middle of the calibration range (at about the geometric mean of low and high QC concentration)

d. High QC is the concentration range which is close to the high end of the calibration range, about 70% to 85% of ULOQ.

e. Dilution QC is the concentration level which covers the highest anticipated dilution.

f. Intra-run accuracy and precision is performed at least 5 replicates at each concentration and the mean, SD, %CV, and %RE are determined. The criteria for acceptance are %CV and %RE $\leq$ 15%.

g. Inter-run accuracy and precision is performed at least 5 parallels at each concentration and the mean, SD, %CV, and %RE are determined. The criteria for acceptance are %CV and %RE $\leq$ 15%.

XII. Stability

The stability of the analytes in the biological fluid is a function of the storage/shipping conditions, the chemical properties of the analytes, the matrix, and the container system. Stability testing must evaluate the stability of the analytes during sample collection and handling, after long-term (frozen at the intended storage temperature) and short-term (bench top at room temperature and auto-sampler) storage. The conditions for the stability testing must be designed in such a way that they are as close as possible to that are encountered during actual sample handling and analysis. The best possible scientific rationale must be applied while choosing the test conditions. In general, the following tests are included in the stability evaluation.

a. The stability of the stock solution is determined at a minimum of 6 h at room temperature.

b. Post-preparative (extracted samples/autosampler tray) stability test is performed to cover the longest duration from the sample preparation through sample analysis. In this test, the stability samples are assessed against fresh standards, except for autosampler re-injection reproducibility, in which the re-injected batch is compared to the previous acquired data from the same batch.

c. Benchtop stability of analyte in matrix is assessed at ambient temperature (or the conditions used for the sample preparation) to cover the duration of time taken to accomplish the sample preparation typically ranging from 4-24 h.

d. Freeze-thaw cycle evaluation is performed using QC samples at minimum of 2 concentrations (low, high) which undergo at least 3 freeze-thaw cycles. The temperature used in this test is the sample storage temperature with at least 12 h between each freeze-thaw cycle with an exception of first freeze-thaw of 24 h post QC preparation.

e. Long-term stability is performed in such a way that it covers longest time from collection to final analysis for any sample in study. In this test, 3 aliquots at low and high concentrations (LQC, HQC) are analyzed with fresh prepared calibration curve. Long-term stability can be completed post validation.

XIII. Replicate analysis

Replicate analysis is not required if the method developed has acceptable variability according to the criteria. It becomes a requirement when the developed method suffers from the irreproducibility and difficult to achieve acceptable accuracy and precision.

XIV. Multiple analytes in a run

This tells us about the acceptance criteria for the samples which involves multiple analytes in a run. In case of multiple analytes in a run, the run cannot be rejected on the basis of one analyte failing the criteria. The failed analyte can be reevaluated in such case. This tells us about the acceptance criteria for the samples which involves multiple analytes in a run.

XIV. Rejected run

It is not a requirement to document the data from the rejected runs, however the rejection and the reason for rejection must be documented and reported. Scientific rationale must be used before a batch can be reinjected to avoid duplication of the sample analysis data.

1.2. Lipidomics

1.2.1. Introduction

LIPIDOMICS is an emerging field of biomedical research which primarily deals with the complex lipidome analysis especially the cellular lipids based on analytical chemistry principles and technological tools, mass spectrometry in particular. Lipidome is defined as the comprehensive and quantitative description of the lipids present in an organism. Lipidomics deals with identification and quantitation of system-level pathways, intricate networks of cellular lipids and their interactions with other lipids, proteins and other in vivo entities thus finding its application in health and disease. Lipidomics emerged in 2003 and has greatly advanced in recent years, largely due to the development of mass spectrometry [43–48]. It is considered as the subgroup of metabolomics and is subdivided into membrane-lipidomics and mediator-lipidomics (Fig. 1.3).

1. **Membrane-lipidomics**: Aims to study the comprehensive and quantitative description of membrane lipid constituents.
2. **Mediator-lipidomics**: Aims to study the structural characterization and quantification of low abundant bioactive lipid species.

Lipids are basically hydrophobic or amphipathic small molecules which constitute monoglycerides, diglycerides, fats, waxes, phospholipids, sterols, and fat-soluble vitamins such as vitamins A, D, E and K. Lipoproteins are crucial components of cellular membranes and play essential roles in cellular functions, including cellular barriers, membrane matrices, signaling, and energy depots. Cellular lipids are highly complex; that is, there are tens to hundreds of thousands molecular species at concentrations ranging from pmol to nmol/mg protein [49–51]. Cellular lipids are dynamic in nature which change constantly with physiological, pathological, and environmental conditions [52,53].

1.2.2. Goals

The primary goal of lipidomics to determine the lipid composition and the changes occurring in the biological system in response to the physical and chemical changes. This is majorly achieved by the profiling experiments performed on the biological systems in various stages. An extension of this primary goal is the identification of metabolic pathways that play a major role in the pathophysiological changes occurring in the biological system. Fulfillment of these goals will help us to identify and utilize the biomarkers for the early diagnosis and screening. In this work, we profiled the lipids in Alzheimer's patient plasma samples, semi-quantitated and build the prediction models with the quest for identifying the probable biomarkers for the early diagnosis of AD. The probable biomarkers identified will need to be validated with a much defined and larger dataset.

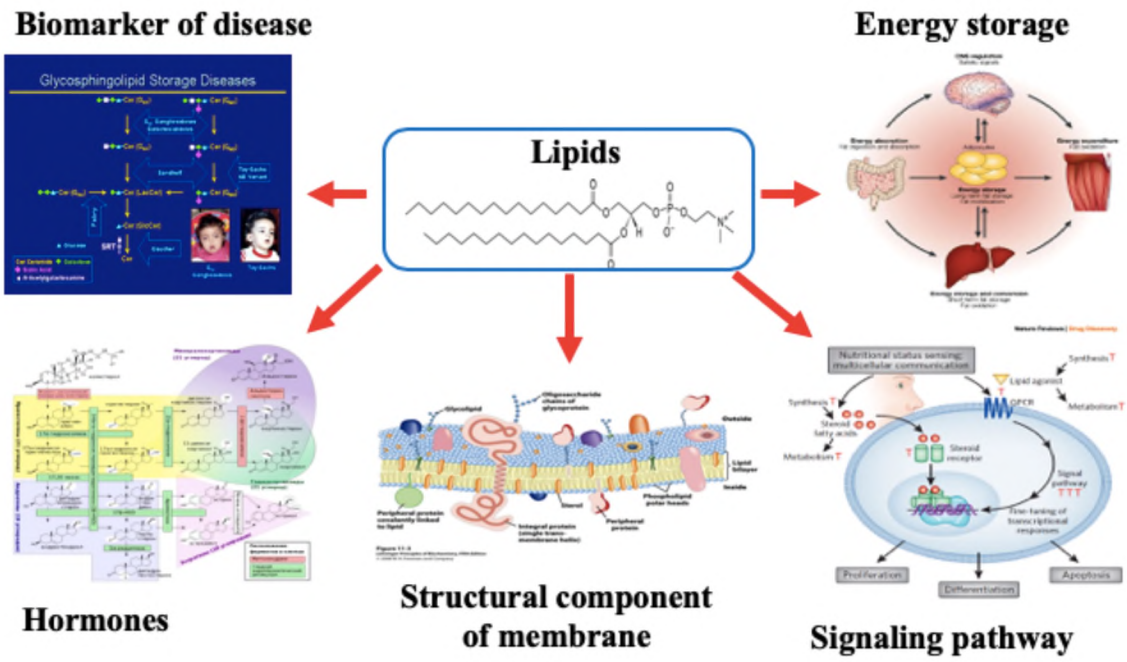

Figure 1.3. Role of lipids in biological systems [104].

1.2.3. Lipid nomenclature

Lipids are abbreviated as follows: sterol lipids – cholesteryl ester (CE), oxidised cholesteryl ester (oxCE); sphingolipids – ceramide (Cer), dihydroceramide (DHCer), ganglioside GM3 (GM3), hexa-ceramides with differing glycan chains (Hex1Cer, Hex2Cer, Hex3Cer), sphingomyelin (SM); glycerolipids – diacylglyceride (DG), triacylglyceride (TG); glycerophospholipids – phosphatidylcholine (PC), phosphatidylethanolamine (PE), phosphatidylglycerol (PG), phosphatidylinositol (PI), phosphatidylserine (PS) and the lyso (L) species (LPC and LPE). Alkyl ether and plasmalogen linkages are denoted by O- and P- respectively.

Lipids are named according to the LIPID MAPS classification system 'Headgroup(*sn*1/*sn*2)', where *sn* refers to the radyl side-chains [54,55]. The side-chain structures are denoted as carbon chain length:number of double bonds and are provided for each chain where they could be determined, or as a total number of all carbons and double bonds where individual chains could not be determined. If the position of the individual fatty acid side chain on glycerol backbone could not be determined by the technique, the it is represented as 'Headgroup(*sn*1_*sn*2)'.

1.2.4. Workflow of Lipidomics

The typical workflow of lipidomics includes the sample preparation, lipid analysis which includes data acquisition, and finally data processing (Fig. 1.4). Recent advances in lipidomics have greatly enhanced the novel applications of lipidomics in the field of biomedical research [56].

1.2.5. Sample preparation

The sample preparation for the lipidomic analysis involves the lipid extraction followed by either the total lipid analysis, or fractionation of the extracted lipids into various fractions. We will briefly discuss the lipid extraction techniques and the fractionation procedures in this work.

1.2.5.1. Lipid extraction

Lipid extraction is an important step in the sample preparation as it eliminates most of the interfering components from the matrix, making our extracts rich in lipids. During lipid extraction, the choice and addition of appropriate internal standards is critical to the accurate quantitation of lipids extracted. The internal standards are used for the normalization of the lipid signal in the extracted matrix and are added by normalization of the total protein, wet/dry tissue, or fluid volume for lipid quantitation. Unbiased recovery of lipid species is another critical aspect of the lipid quantitation. The most commonly used extraction methods in lipidomics are modified Bligh and Dyer method, modified Folch method, methyl *tert*-butyl ether (MTBE method), butanol/methanol (BUME method). In this work we used the modified Bligh and Dyer method, however all the extractions are discussed in brief below [57,58].

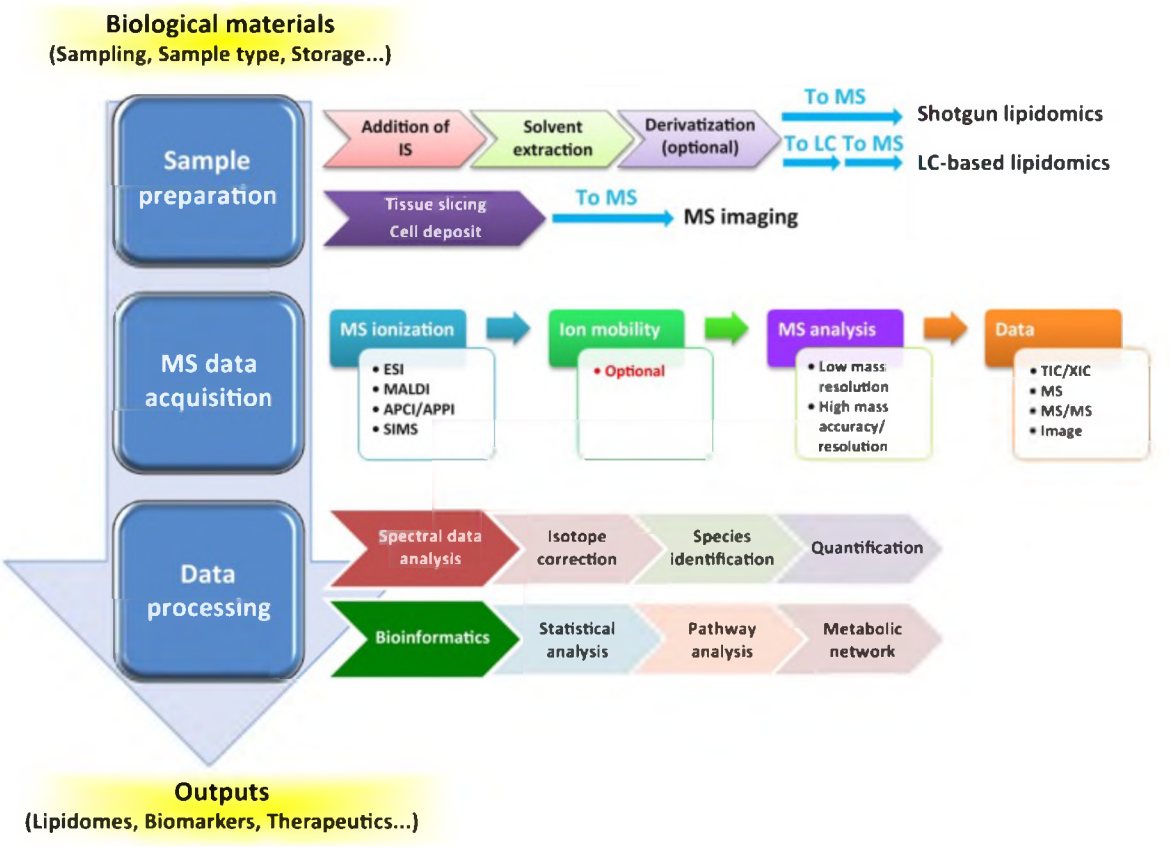

Figure 1.4. General workflow of lipidomics [104].

1.2.5.1.1. Modified Bligh and Dyer method

This extraction method uses chloroform/methanol/water (1: 1: 0.9, v/v/v) for the extraction of total lipids from the biological samples. After phase separation, the total lipids are present in the chloroform phase which is transferred to a separate tube for the downstream process. This extraction is well-established standard method and is most commonly used. The major drawbacks of this extraction are the use of the hazardous chloroform, and the practical challenge of collecting the bottom chloroform layer which may cause the carry-over of the water-soluble impurities. These aspects pose challenges in the automation of this extraction procedure [59–61].

1.2.5.1.2. Modified Folch method

This extraction method uses chloroform/methanol (2: 1, v/v) for the extraction of the total lipids from the biological samples. This method uses the water or 0.9% NaCl to wash the solvent extract. This has similar advantages and disadvantages as the modified Bligh and Dyer method [59,62–64].

1.2.5.1.3. MTBE method

This extraction method uses MTBE/methanol/water (5: 1.5: 1.45, v/v/v) for the extraction of total lipids form the biological samples. This method helps to overcome the challenges posed by the chloroform extraction as MTBS is present in the top layer after phase separation, thus making it more feasible for high throughput and automation. The drawback of this method is the presence of water-soluble impurities as MTBE has a

significant amount of aqueous component that carryover the water-soluble contaminants [65–67].

1.2.5.1.4. BUME method

This extraction method uses the addition of butanol/methanol (3: 1, v/v) to a small amount of aqueous phase followed by the addition of the equal volume of heptane/ethyl acetate (3: 1, v/v). Finally, 1% acetic acid is added in equal amounts of BUMS to induce phase separation. This method offers the advantage of less water-soluble contaminants in the extracted organic phase. The only drawback of this method is the difficulty/longer drying time of butanol component in the organic phase.

After the extraction of the total lipids, some additional steps may be applied to simplify the complexity of the extracts depending on the choice of mass spectrometry analysis. This additional clean up step is importantly especially for the shotgun lipidomics approach which do not employ any chromatographic separation/enrichment prior to MS analysis. This additional clean-up process can be done either by physical processes like liquid/liquid partitioning, solid phase extraction to separate polar *vs.* non-polar lipids or by chemical approaches like base hydrolysis for the enrichment of low-abundance phospholipids and/or glycerolipids [68–70]. For the lipids which lack the inherent charged moieties and prevent efficient ionization, derivatization is the most commonly used approach. In this work, we used the fractionation of lipids by solid-phase extraction to isolate different classes of lipids.

1.2.5.2. Fractionation of lipids

Followed by the extraction of total lipids, the next step involved the fractionation of the complex mixture into various classes of lipids. This allows the isolation of each lipid component that can be used for individual analysis. This technique allows most comprehensive and accurate profiling and quantitation of unknown lipids. Thus, this fractionation procedure can be adopted depending on the aim of the study. The neutral lipids can be separated from the polar lipids. And it is also common to separate the complex lipid mixtures into phospholipid and glycolipid fractions [71–75].

Solid phase extraction (SPE) is the most common sample preparation technique used for the fractionation of lipids. Due to the ease of use, cost effectiveness and the decreased requirements of the solvent usage, SPE has rapidly replaced the other conventional methods like liquid-liquid extraction, liquid-solid column chromatography and thin later chromatography that were used for the fractionation of lipids in the past. The application of SPE for the lipid analysis commonly uses silica bonded aminopropyl and C-18 reverse phase columns, alumina, microporous carbon and ion-exchange phases. There are also availability of the mixed mode separation mechanisms and a large amount of proprietary stationary phases in the market which are designed for specific applications [76,77]. This work used the bonded aminopropyl sorbent-based fractionation of lipids, which is discussed in brief.

1.2.5.2.1. Bonded aminopropyl sorbents

The bonded phases are formed by the treatment of the surface silanol groups of silica with the siloxane derivatives. Commercially numerous bonded phases are available

and classified as nonpolar (reverse phase), polar (normal phase), or ion exchange. Depending on the number of layers of the bonding reagent the bonded phases are either monomeric or polymeric phases and the choice is dictated by the specific application.

Aminopropyl bonded phase are polar and are classified as the normal-phase sorbents. Lipids with polar functional groups have stronger interaction with the primary amine through hydrogen bonding. The amino group present also offers the advantage of ion exchange chromatography as it can impart the weak anion exchange properties. Owing to the polarity of these phases, they have acquired a common usage for the fractionation of lipids. Methodology for the rapid separation of the total lipids into the neutral and polar lipids was developed in late 1900s and the modifications of this method was widely applied based on the specific needs of the analysis. The neutral lipids can be separated and further fractionated by gradual increase of the polarity of the elution solvents. Free fatty acids and the phospholipids are bound to the column by ionic interactions, which can be disrupted by changing the pH of the elution solvents. The polarity and the pH play a crucial role in the efficient separation of lipids onto defined fractions. Studies have shown that consecutive usage of aminopropyl columns have resulted in a very efficient separation of total lipids into neutral lipids, free fatty acids, phospholipids, cholesterol (or other sterol) esters, triglycerides, cholesterol (or other sterols), diglycerides, and monoglycerides [78,79].

1.2.6. Lipidomics techniques

Mass spectrometry (MS) and nuclear magnetic resonance (NMR) are the two key techniques for the lipidomics advancement, with mass spectrometry being the major player in this field. NMR spectroscopy is a technique used for the structural elucidation of lipids. The sample preparation for this is relatively less time consuming and uses a non-destructive approach. However, the major drawback of this technique being the low sensitivity and its limitation to detect only the most abundant species of lipids. These drawbacks have made the mass spectrometry a spearhead technique for the lipid analysis [80–82]. In this work, the primary technique used for the analysis of lipids is mass spectrometry which will be the primary focus in the future discussion.

The variants of mass spectrometry that are used in the lipid analysis are Shotgun analysis, Liquid chromatography-mass spectrometry (LC-MS), and gas chromatography-mass spectrometry (GC-MS). The shotgun lipidomic analysis deals with the direct infusion of the lipid solutions into the mass spectrometer without the chromatography involved whereas LC-MS and GC-MS are chromatography-based approaches. GC-MS is the most widely used technique, however with the advancement of ionization techniques, LC-MS has gained popularity in terms of the flexibility to identify and quantitate multiple classes of lipids in a single injection. Direct infusion MS or shotgun lipidomics is performed by the direct infusion of the samples into the mass spectrometer for the identification and quantification of lipid species. The identification of lipids is based on the accurate mass of the species [83–85]. In this work, LC-MS based lipidomic analysis was performed using reverse phase chromatography and Agilent QTOF 6540 mass spectrometer. The mass

spectrometer was operated in both positive and negative mode in data dependent acquisition mode.

1.2.6.1. Reverse phase liquid chromatography

Liquid chromatography is the separation technique that is used to separate the analytes from the analyte of interest from the biological matrix components or the complex compound mixtures. A LC system comprises of a liquid mobile phase, pumping mechanism to pump the mobile phases, an autosampler to inject the sample of interest, an analytical column to separate the analytes of interest from the complex mixtures, and finally a detector to detect the signal of the analyte. The most commonly used modes of LC are reverse-phase chromatography RPC), normal-phase chromatography (NPC), hydrophilic interaction chromatography (HILIC), and ion-pair chromatography (IPC). Based on the nature of the analyte, different modes of LC separation are employed [86]. As mentioned, this work used the RPC, which was briefly discussed in the previous sections.

1.2.6.2. Quadrupole time-of-flight mass spectrometry

Mass spectrometry (MS) is a technique that identifies the molecules based on their mass to charge (m/z) ratio. Mass spectrometer works in a step-wise events which starts with the sample vaporization and ionization in the ion source which is followed by the separation or resolution of the ions in the mass analyzer depending on the m/z ratio and ultimately the ions are detected by the detector producing the mass spectrum.

The ion source used in the mass spectrometer is dependent on the nature of the analyte. Commonly used ion sources in mass spectrometry are electrospray ionization (ESI) and atmospheric pressure chemical ionization (APCI). In ESI the sample passes through an ion spray needle to which a high voltage is applied. This produces a spray of droplets which are charged with either positive or negative charge depending on the potential applied. These ions produced then travel into mass analyzer. The specialty of ESI with Agilent Jet Stream Technology (Fig. 1.5) is it uses super-heated nitrogen sheath gas to confine the electrospray which improves the ion density and desolvation leading to higher MS signal intensities and reduced noise. The MS and MS/MS sensitivity can improve 5 to 10-fold by Agilent Jet Stream technology at optimal LC flow rates.

In the mass analyzer, the ions interact with the electric and magnetic field and are separated based on the mass-to-charge (m/z) ratio. The most commonly used mass analyzers are quadrupole MS, ion trap MS, and time-of-flight (TOF) MS. This lipidomic work used the Agilent 6540 quadrupole time-of-flight (Q-TOF) (Fig. 1.6). Q-TOF consists of a quadrupole, a collision cell and time-of-flight mass analyzer. The quadrupole essentially acts as a mass filter and consists of four parallel metal rods where only selected ions pass through them and the other ions decay by colliding the rods. The ions are guided from the quadrupole into the collision cell by the hyperbolic rods. Collision cell as the name suggests is the component which aids in the ion fragmentation. This cell is a high pressure hexapole assembly where the collision energy voltage is applied over the selected ions to generate fragments or product ions. The generated fragment ions are guided into the mass analyzer by the ion beam shaper.

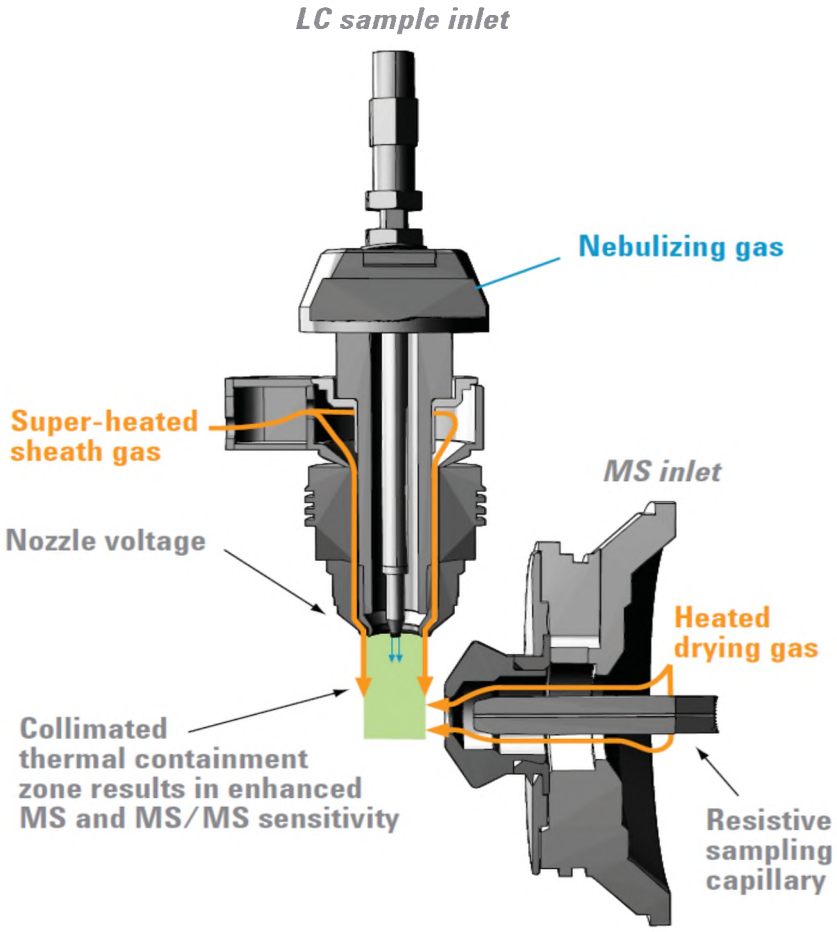

Figure 1.5. ESI with Agilent Jet Stream Technology [105].

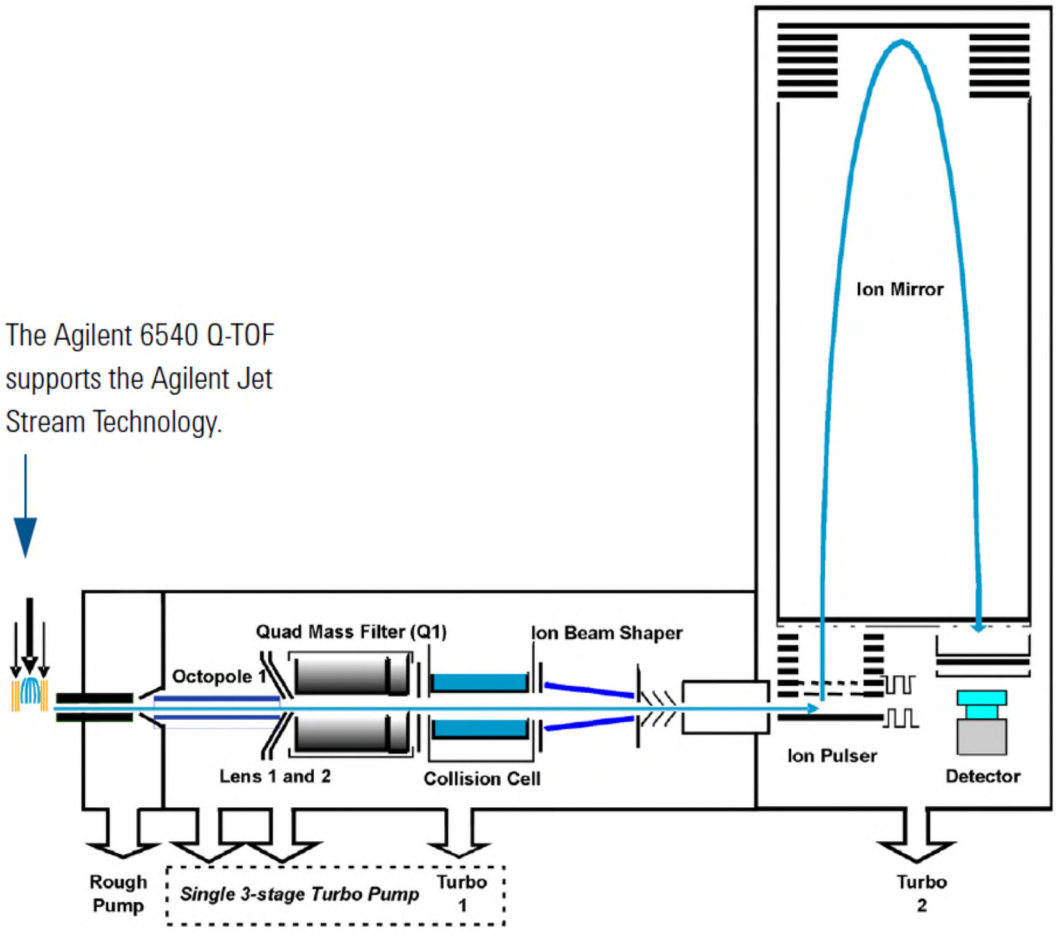

Figure 1.6. Components of quadrupole time-of-flight mass spectrometer [105].

The parallel beam of the ions reaches the time of flight analyzer where high voltage is applied at the pulser of TOF to start the flight of ions to the detector. The ions leave the pulser to travel through the flight tube to reach the ion mirror called 'reflectron' at the end of the tube. This reflectron reflects the ions thus increasing the resolving power of the instrument by doubling the flight path in the same space. It also performs the refocusing operation so that the ions with different velocities still reach the detector at the same time. This analyzer determines the mass-to-charge ratio based on the time taken by the ion to travel the flight tube. Ions with higher charge possess more kinetic energy compared to ions with lower charge. Thus mass-to-charge determines the velocity of the ions i.e., the lighter ions reach the detector earlier than the heavier ions. However, the reflectron TOF analyzer which consists of a series of ring electrodes with high voltage are able to efficiently correct the kinetic energy distribution in the direction of ion flight thus increasing resolution. The ions which possess the greater energy penetrate deeper into the reflectron while those with lesser energy and same m/z penetrate a shorter distance. This enables the ions with same m/z reach the detector at the same time (Fig. 1.7). Q-TOF instruments offer the advantage of high mass resolution and wide m/z range, which makes these instruments an ideal tool for the discovery mode of work such as identification of molecules, peptide, protein and oligonucleotide analysis [87,88].

The mass spectrometer was operated in auto MS/MS mode. In this mode, the instrument can automatically perform secondary mass spectrometry on qualified ions based on the parameters set by the user. When a particular ion or set of ions meet the preset conditions, the quadrupole assumes the selected ion monitoring (SIM), and the collision cell can fragment ions [89–91]. This is followed by the scanning of the fragments to get

the mass spectrum. This mode is commonly used for the identification and structure analysis of unknown compounds.

1.2.7. Data processing tools and resources

The major part of lipid analysis is the data processing where the large sets of data generated is curated at multiple levels to profile, perform qualitative, quantitative, and multivariate analysis to build statistical models. Some of the processing steps include spectral feature picking, spectral alignment, smoothing, de-isotoping, detecting adduct formation, peak identification, subjecting to statistical analysis and finally the lipid identification. With the increasing demands and complexity of data processing, numerous open-source and commercial software are available [92]. The tools used for the data processing in this work are briefly described below.

1.2.7.1. MassHunter Qualitative Analysis

This is a proprietary software from Agilent, which was used to perform qualitative check on the retention time drift and correct it. The version used for this work was B.06.00.

A

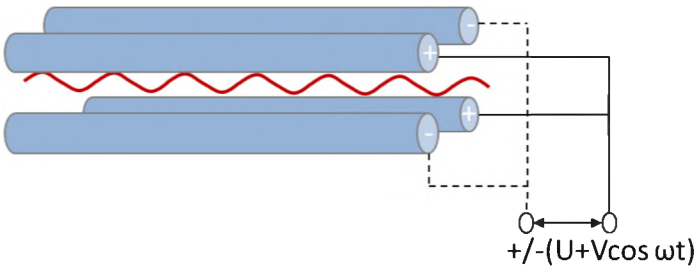

B

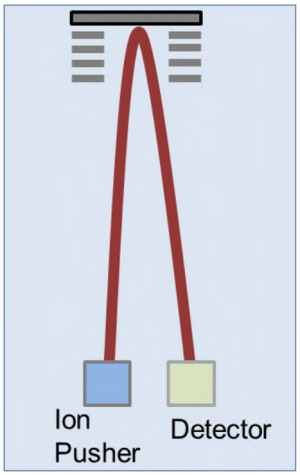

The derivation process of the time that ions pass through field free region in the liner TOF analyzer:

- The potential energy : E=zeV (ze is the charge of the particle, and V is the voltage)
- The kinetic energy of ions: $E=1/2mv^2$
- The potential energy is converted into kinetic energy: $zeV=1/2mv^2$
- Thus, $v = \sqrt{\frac{2zeV}{m}}$
- The time taken by ions to reach the detector: $t=\frac{d}{v}$
- Finally, $t= d\sqrt{\frac{m}{2zeV}}$

Figure 1.7. Schematic diagram of (A) Quadrupole mass analyzer and (B)Reflector TOF analyzer [105].

1.2.7.2. MassHunter Profinder

Agilent MassHunter Profinder software is a stand-alone program used for batch feature extractions from Q-TOF based profiling data files. It basically picks the features from the raw data based on the adducts chosen and performs spectral refining. Feature extraction along with the chromatographic data alignment across multiple data files from replicates is a crucial step in peak finding and data reduction workflow. This helps to minimize the false positive and false negative features by "binning" the features in the chromatographic time domain. This software majorly helps to reduce the acquired data size and complexity by removing the redundant and non-specific information by identifying the relevant variables associated with the data. Thus, feature extraction is performed to produce a smaller data set without losing the information quality, and is easy to perform analysis. Profinder is optimized to provide an intuitive user interface to inspect and review and compare extracted ion chromatograms, mass spectral data, and isotopologies associated with each feature. The feature files generated by Profinder (CEF files) can be imported into Agilent Mass Profiler Professional (MPP) for further analysis. The version used for this work was B.06.00.

1.2.7.3. Mass Profiler Professional (MPP)

Agilent Mass Profiler Professional (MPP) software is a powerful chemometrics platform which is designed to use the high information content of mass spectra (MS) data and can be used in any MS-based differential analysis to determine relationships among two or more sample groups and variables. MPP provides advanced statistical analysis and visualization tools for GC/MS, LC/MS, CE/MS, and ICP-MS data analysis. It also offers

the integrated identification/ annotation of compounds and integrated pathway analysis for metabolomic and proteomic studies. It allows the differential analysis of the data obtained from two or more sample sets, with guided and advanced workflows. It provides the comprehensive statistical tools like ANOVA, PCA, volcano plots, hierarchical trees, and multiple methods for class prediction models. It also facilitates the identification of the unknown compounds by generating the inclusion lists for the subsequent MS/MS-based analysis. It also offers the additional help in predicting the biochemical pathways associated with the identified features via a module called Pathway Architect. MPP is ideally suited for applications characterized by complex sample matrices such as metabolomics, proteomics, natural products, food, beverages, flavors, fragrances, and environmental analyses.

1.2.7.4. SimLipid®

SimLipid® is a high throughput informatics tool from Premier Biosoft for identification and relative quantitation of lipids using data from LC-MS, MALDI, Shotgun-MS. The major challenge posed by the mass spectrometry based lipidomic data is the complexity and the large range of concentrations of thousands of lipid species found in the biological samples. Due to the complexity of the lipid structure the identification of lipids requires sophisticated software for the interpretation of lipid MS/MS spectra. The fragmentation pattern and the ionization efficiencies are specific to each class of lipid.

This tool is capable of processing the raw data from hundreds of LC-MS and MS/MS experimental runs for LC peak detection, peak-picking, molecular feature finding and retention time alignment. Though this tool is capable of these, in this study these

functions were carried out by the Agilent software as discussed earlier. Structure elucidation can be performed by MS and MS/MS based database search. The isobaric candidate structures for each MS/MS scan can be distinguished using a proprietary scoring system. The SimLipid® database contains 40,312 lipids, and 1,508,293 structure-specific in-silico MS/MS characteristic ions. Apart from this, the database also stores 5,227 transitions of precursor ion scan and neutral loss scan triple quadrupole mass spectrometry methods corresponding to 1,179,393 and 221 unique fatty acyls from glycerophospholipids, glycerolipids, and sphingolipids respectively. Correction of experimental peak intensities for their isotopic overlaps can be performed for the identified peaks. This software also allows the relative quantitation of the profiled lipids based on user-specific internal standards [93–95].

Apart from SimLipid®, LIPIDMAPS is an open-source platform for the lipid database that can be used for the same purpose. LIPIDMAPS is an US based consortium of lipids that comprises of around 1.6 million lipids and is the most comprehensive database of lipids. It comprises procedures for extraction of lipids, their purification, analysis, fragmentation patterns, standard protocols. Though the functionality of this tool is limited, the fact that it is an open source platform enables researchers to use the database [96–98].

1.2.7.5. MetaboAnalyst®

MetaboAnalyst® is a set of online tools for metabolomic data analysis and interpretation which provides a range of analysis methods tailored for metabolomic data. The analysis methods in this tool include metabolomic data processing, normalization, multivariate statistical analysis and data annotation. In this work, MetaboAnalyst® is used

for the multivariate analysis and generation of the statistical models *i.e.,* Principal Component Analysis (PCA), Partial Least Square -discriminant analysis (PLS-DA).

MetaboAnalyst® supports a wide variety of data input types commonly generated by metabolomic studies including GC/LC-MS raw spectra, MS/NMR peak lists, NMR/MS peak intensity table, NMR/MS spectral bins, and metabolite concentrations. MetaboAnalyst® has four modules:

1. Data processing
2. Statistical analysis (one-factor, two-factor, and time-series data)
3. Functional enrichment analysis
4. Metabolic pathway analysis

The main features of the data processing include peak detection, retention time correction, peak alignment, baseline filtering, data integrity check and missing value imputation. These features help to provide the quality check on the data for the reliable statistical analysis. The statistical analysis features offered by this tool include univariate analysis, dimension reduction, feature selection, cluster analysis, classification, two-way ANOVA and temporal comparison. Functional enrichment analysis includes over representation analysis, single sample profiling and quantitative enrichment analysis. Metabolic pathway analysis includes enrichment analysis, topology analysis and interactive visualization [99–102].

1.3. Conclusion

This chapter is majorly focused on providing the basic information and background on the type of work described in this dissertation work. This work is focused on depicting

the application of mass spectrometry in the clinical studies *i.e.,* quantitative method development and validation for the PK analysis of anticancer drug, and the identification of the probabilistic biomarkers for the early diagnosis of Alzheimer's disease in human. The workflows, principles and the techniques used for accomplishing this work are briefly introduced in this chapter. FDA-ICH guidelines for the industrial bioanalytical method development and validation were used to validate the quantitative method developed for the PK analysis, which was briefly discussed.

1.4. REFERENCES

1. Loucks, J.; Yost, S.; Kaplan, B. An introduction to basic pharmacokinetics. *Transplantation* **2015**, *99*, 903–907.
2. Smith, B.S.; Yogaratnam, D.; Levasseur-Franklin, K.E.; Forni, A.; Fong, J. Introduction to drug pharmacokinetics in the critically ill patient. *Chest* **2012**, *141*, 1327–1336.
3. Urso, R.; Blardi, P.; Giorgi, G. A short introduction to pharmacokinetics. *Eur Rev Med Pharmacol Sci* **2002**, *6*, 33–44.
4. Shou, W.Z.; Zhang, J. Recent development in high-throughput bioanalytical support for in vitro ADMET profiling. *Expert Opin Drug Metab Toxicol* **2010**, *6*, 321–336.
5. Janiszewski, J.S.; Liston, T.E.; Cole, M.J. Perspectives on bioanalytical mass spectrometry and automation in drug discovery. *Curr. Drug Metab.* **2008**, *9*, 986–994.
6. Feng, W.Y. Mass spectrometry in drug discovery: a current review. *Curr Drug Discov Technol* **2004**, *1*, 295–312.
7. Cuyckens, F. Mass spectrometry in drug metabolism and pharmacokinetics: Current trends and future perspectives. *Rapid Commun. Mass Spectrom.* **2019**, *33 Suppl 3*, 90–95.
8. Beierle, I.; Meibohm, B.; Derendorf, H. Gender differences in pharmacokinetics and pharmacodynamics. *Int J Clin Pharmacol Ther* **1999**, *37*, 529–547.
9. Schmidt, S.; Gonzalez, D.; Derendorf, H. Significance of protein binding in pharmacokinetics and pharmacodynamics. *J Pharm Sci* **2010**, *99*, 1107–1122.

10. Currie, G.M. Pharmacology, Part 1: Introduction to Pharmacology and Pharmacodynamics. *J Nucl Med Technol* **2018**, *46*, 81–86.
11. van Nuland, M.; Rosing, H.; Schellens, J.H.M.; Beijnen, J.H. Bioanalytical LC-MS/MS validation of therapeutic drug monitoring assays in oncology. *Biomed. Chromatogr.* **2019**, e4623.
12. Iwamoto, N.; Shimada, T. Regulated LC-MS/MS bioanalysis technology for therapeutic antibodies and Fc-fusion proteins using structure-indicated approach. *Drug Metab. Pharmacokinet.* **2019**, *34*, 19–24.
13. Xu, X.; Ji, Q.C.; Jemal, M.; Gleason, C.; Shen, J.X.; Stouffer, B.; Arnold, M.E. Fit-for-purpose bioanalytical cross-validation for LC-MS/MS assays in clinical studies. *Bioanalysis* **2013**, *5*, 83–90.
14. Wu, Q.; Xu, Y.; Ji, H.; Wang, Y.; Zhang, Z.; Lu, H. Enhancing coverage in LC-MS-based untargeted metabolomics by a new sample preparation procedure using mixed-mode solid-phase extraction and two derivatizations. *Anal Bioanal Chem* **2019**, *411*, 6189–6202.
15. Liakh, I.; Pakiet, A.; Sledzinski, T.; Mika, A. Modern Methods of Sample Preparation for the Analysis of Oxylipins in Biological Samples. *Molecules* **2019**, *24*.
16. Zhang, Z.; Cheng, H. Recent Development in Sample Preparation and Analytical Techniques for Determination of Quinolone Residues in Food Products. *Crit Rev Anal Chem* **2017**, *47*, 223–250.

17. Xu, R.N.; Fan, L.; Rieser, M.J.; El-Shourbagy, T.A. Recent advances in high-throughput quantitative bioanalysis by LC-MS/MS. *J Pharm Biomed Anal* **2007**, *44*, 342–355.

18. Polson, C.; Sarkar, P.; Incledon, B.; Raguvaran, V.; Grant, R. Optimization of protein precipitation based upon effectiveness of protein removal and ionization effect in liquid chromatography-tandem mass spectrometry. *J. Chromatogr. B Analyt. Technol. Biomed. Life Sci.* **2003**, *785*, 263–275.

19. Xue, Y.-J.; Akinsanya, J.B.; Liu, J.; Unger, S.E. A simplified protein precipitation/mixed-mode cation-exchange solid-phase extraction, followed by high-speed liquid chromatography/mass spectrometry, for the determination of a basic drug in human plasma. *Rapid Commun. Mass Spectrom.* **2006**, *20*, 2660–2668.

20. Comert, F.; Malanowski, A.J.; Azarikia, F.; Dubin, P.L. Coacervation and precipitation in polysaccharide-protein systems. *Soft Matter* **2016**, *12*, 4154–4161.

21. Kole, P.L.; Venkatesh, G.; Kotecha, J.; Sheshala, R. Recent advances in sample preparation techniques for effective bioanalytical methods. *Biomed. Chromatogr.* **2011**, *25*, 199–217.

22. The science and practice of liquid-liquid extraction, edited by J . D. Thornton, 1992, Vol. 1, 603 + xvi pages; Vol. 2, 436 + xv pages, Oxford University Press, U.K. ISBN 0-19-856237-3. Price: Can. $291.95 (2-volume set). - Baird - 1993 - The Canadian Journal of Chemical Engineering - Wiley Online Library Available online: https://onlinelibrary.wiley.com/doi/abs/10.1002/cjce.5450710330 (accessed on Oct 20, 2019).

23. Tajabadi, F.; Ghambarian, M. Carrier-mediated extraction: Applications in extraction and microextraction methods. *Talanta* **2020**, *206*, 120145.

24. Purohit, T.J.; Wu, Z.; Hanning, S.M. Simple and reliable extraction and a validated high performance liquid chromatographic assay for quantification of amoxicillin from plasma. *J Chromatogr A* **2019**, 460611.

25. Telepchak, M.J.; August, T.F.; Chaney, G. Introduction to Solid Phase Extraction. In *Forensic and Clinical Applications of Solid Phase Extraction*; Telepchak, M.J., August, T.F., Chaney, G., Eds.; Forensic Science and Medicine; Humana Press: Totowa, NJ, 2004; pp. 1–39 ISBN 978-1-59259-292-0.

26. Solid-Phase Extraction - an overview | ScienceDirect Topics Available online: https://www.sciencedirect.com/topics/chemistry/solid-phase-extraction (accessed on Oct 20, 2019).

27. Advances in Solid Phase Microextraction and Perspective on Future Directions | Analytical Chemistry Available online: https://pubs.acs.org/doi/10.1021/acs.analchem.7b04502 (accessed on Oct 20, 2019).

28. Faraji, M.; Yamini, Y.; Gholami, M. Recent Advances and Trends in Applications of Solid-Phase Extraction Techniques in Food and Environmental Analysis. *Chromatographia* **2019**, *82*, 1207–1249.

29. Thurman, E.M.; Snavely, K. Advances in solid-phase extraction disks for environmental chemistry. *TrAC - Trends in Analytical Chemistry* **2000**, *19*, 1826.

30. Calderilla, C.; Maya, F.; Leal, L.O.; Cerdà, V. Recent advances in flow-based automated solid-phase extraction. *TrAC Trends in Analytical Chemistry* **2018**, *108*, 370–380.

31. Advances in Liquid Chromatography | Methods in Chromatography Available online: https://www.worldscientific.com/worldscibooks/10.1142/2489 (accessed on Oct 20, 2019).
32. Gama, M.R.; Bottoli, C.B.G. Chapter 9 - Nanomaterials in Liquid Chromatography: Recent Advances in Stationary Phases. In *Nanomaterials in Chromatography*; Hussain, C.M., Ed.; Elsevier, 2018; pp. 255–297 ISBN 978-0-12-812792-6.
33. Aguilar, M.-I. Reversed-Phase High-Performance Liquid Chromatography. In *HPLC of Peptides and Proteins: Methods and Protocols*; Aguilar, M.-I., Ed.; Methods in Molecular Biology™; Springer New York: Totowa, NJ, 2004; pp. 9–22 ISBN 978-1-59259-742-0.
34. Reversed-Phase Chromatography - an overview | ScienceDirect Topics Available online: https://www.sciencedirect.com/topics/biochemistry-genetics-and-molecular-biology/reversed-phase-chromatography (accessed on Oct 20, 2019).
35. Tandem-in-space and tandem-in-time mass spectrometry: triple quadrupoles and quadrupole ion traps | Analytical Chemistry Available online: https://pubs.acs.org/doi/abs/10.1021/ac00219a003 (accessed on Oct 20, 2019).
36. Triple quadrupole mass spectrometry for direct mixture analysis and structure elucidation | Analytical Chemistry Available online: https://pubs.acs.org/doi/abs/10.1021/ac50048a002 (accessed on Oct 20, 2019).
37. Triple Quadrupole Mass Spectrometer - an overview | ScienceDirect Topics Available online: https://www.sciencedirect.com/topics/biochemistry-genetics-and-molecular-biology/triple-quadrupole-mass-spectrometer (accessed on Oct 20, 2019).

38. Viswanathan, C.T.; Bansal, S.; Booth, B.; DeStefano, A.J.; Rose, M.J.; Sailstad, J.; Shah, V.P.; Skelly, J.P.; Swann, P.G.; Weiner, R. Quantitative Bioanalytical Methods Validation and Implementation: Best Practices for Chromatographic and Ligand Binding Assays. *Pharm Res* **2007**, *24*, 1962–1973.
39. Bioanalytical Method Development and Validation: A Review | IntechOpen Available online: https://www.intechopen.com/books/recent-advances-in-analytical-chemistry/bioanalytical-method-development-and-validation-a-review (accessed on Oct 20, 2019).
40. Research, C. for D.E. and Bioanalytical Method Validation Guidance for Industry Available online: http://www.fda.gov/regulatory-information/search-fda-guidance-documents/bioanalytical-method-validation-guidance-industry (accessed on Oct 20, 2019).
41. LC-MS/MS Bioanalysis Method Development, Validation, and Sample Analysis: Points to Consider When Conducting Nonclinical and Clinical Studies in Accordance with Current Regulatory Guidances Available online: https://www.omicsonline.org/lc-ms-ms-bioanalysis-method-development-validation-and-sample-analysis-points-to-consider-2155-9872.S4-001.php?aid=1745 (accessed on Oct 20, 2019).
42. Moein, M.M.; El Beqqali, A.; Abdel-Rehim, M. Bioanalytical method development and validation: Critical concepts and strategies. *J. Chromatogr. B Analyt. Technol. Biomed. Life Sci.* **2017**, *1043*, 3–11.

43. Sethi, S.; Hayashi, M.A.; Sussulini, A.; Tasic, L.; Brietzke, E. Analytical approaches for lipidomics and its potential applications in neuropsychiatric disorders. *World J. Biol. Psychiatry* **2017**, *18*, 506–520.

44. Zhao, Y.-Y.; Cheng, X.; Lin, R.-C. Lipidomics applications for discovering biomarkers of diseases in clinical chemistry. *Int Rev Cell Mol Biol* **2014**, *313*, 1–26.

45. Sethi, S.; Brietzke, E. Recent advances in lipidomics: Analytical and clinical perspectives. *Prostaglandins Other Lipid Mediat.* **2017**, *128–129*, 8–16.

46. Zhao, Y.-Y.; Cheng, X.-L.; Lin, R.-C.; Wei, F. Lipidomics applications for disease biomarker discovery in mammal models. *Biomark Med* **2015**, *9*, 153–168.

47. Stephenson, D.J.; Hoeferlin, L.A.; Chalfant, C.E. Lipidomics in translational research and the clinical significance of lipid-based biomarkers. *Transl Res* **2017**, *189*, 13–29.

48. Lipidomics: Techniques, Applications, and Outcomes Related to Biomedical Sciences: Trends in Biochemical Sciences Available online: https://www.cell.com/trends/biochemical-sciences/fulltext/S0968-0004(16)30127-X (accessed on Oct 20, 2019).

49. Yang, K.; Cheng, H.; Gross, R.W.; Han, X. Automated lipid identification and quantification by multidimensional mass spectrometry-based shotgun lipidomics. *Anal. Chem.* **2009**, *81*, 4356–4368.

50. Han, X.; Jiang, X. A review of lipidomic technologies applicable to sphingolipidomics and their relevant applications. *Eur J Lipid Sci Technol* **2009**, *111*, 39–52.

51. Yetukuri, L.; Katajamaa, M.; Medina-Gomez, G.; Seppänen-Laakso, T.; Vidal-Puig, A.; Oresic, M. Bioinformatics strategies for lipidomics analysis: characterization of obesity related hepatic steatosis. *BMC Syst Biol* **2007**, *1*, 12.

52. van Meer, G.; Voelker, D.R.; Feigenson, G.W. Membrane lipids: where they are and how they behave. *Nat Rev Mol Cell Biol* **2008**, *9*, 112–124.

53. Dynamics and functions of lipid droplets | Nature Reviews Molecular Cell Biology Available online: https://www.nature.com/articles/s41580-018-0085-z (accessed on Oct 20, 2019).

54. A comprehensive classification system for lipids - Fahy - 2005 - European Journal of Lipid Science and Technology - Wiley Online Library Available online: https://onlinelibrary.wiley.com/doi/abs/10.1002/ejlt.200405001 (accessed on Oct 28, 2019).

55. Fahy, E.; Cotter, D.; Sud, M.; Subramaniam, S. Lipid classification, structures and tools. *Biochim Biophys Acta* **2011**, *1811*, 637–647.

56. Han, X.; Yang, K.; Gross, R.W. Multi-dimensional mass spectrometry-based shotgun lipidomics and novel strategies for lipidomic analyses. *Mass Spectrom Rev* **2012**, *31*, 134–178.

57. Gros, V.; Lupette, J.; Jouhet, J. Extraction and Quantification of Lipids from Plant or Algae. *Methods Mol. Biol.* **2018**, *1829*, 213–240.

58. Li, Y.; Ghasemi Naghdi, F.; Garg, S.; Adarme-Vega, T.C.; Thurecht, K.J.; Ghafor, W.A.; Tannock, S.; Schenk, P.M. A comparative study: the impact of different lipid extraction methods on current microalgal lipid research. *Microb. Cell Fact.* **2014**, *13*, 14.

59. Akondi, R.N.; Trexler, R.V.; Pfiffner, S.M.; Mouser, P.J.; Sharma, S. Modified Lipid Extraction Methods for Deep Subsurface Shale. *Front. Microbiol.* **2017**, *8*.

60. Breil, C.; Abert Vian, M.; Zemb, T.; Kunz, W.; Chemat, F. "Bligh and Dyer" and Folch Methods for Solid–Liquid–Liquid Extraction of Lipids from Microorganisms. Comprehension of Solvatation Mechanisms and towards Substitution with Alternative Solvents. *Int J Mol Sci* **2017**, *18*.

61. Iverson, S.J.; Lang, S.L.; Cooper, M.H. Comparison of the Bligh and Dyer and Folch methods for total lipid determination in a broad range of marine tissue. *Lipids* **2001**, *36*, 1283–1287.

62. Folch, J.; Lees, M.; Sloane Stanley, G.H. A simple method for the isolation and purification of total lipides from animal tissues. *J. Biol. Chem.* **1957**, *226*, 497–509.

63. Akondi, R.N.; Trexler, R.V.; Pfiffner, S.M.; Mouser, P.J.; Sharma, S. Modified Lipid Extraction Methods for Deep Subsurface Shale. *Front Microbiol* **2017**, *8*.

64. Washburn, K.W. A Modification of the Folch Method of Lipid Extraction for Poultry. *Poult Sci* **1989**, *68*, 1425–1427.

65. Pellegrino, R.M.; Di Veroli, A.; Valeri, A.; Goracci, L.; Cruciani, G. LC/MS lipid profiling from human serum: a new method for global lipid extraction. *Anal Bioanal Chem* **2014**, *406*, 7937–7948.

66. Matyash, V.; Liebisch, G.; Kurzchalia, T.V.; Shevchenko, A.; Schwudke, D. Lipid extraction by methyl-tert-butyl ether for high-throughput lipidomics. *J Lipid Res* **2008**, *49*, 1137–1146.

67. Zhang, H.; Gao, Y.; Sun, J.; Fan, S.; Yao, X.; Ran, X.; Zheng, C.; Huang, M.; Bi, H. Optimization of lipid extraction and analytical protocols for UHPLC-ESI-HRMS-

based lipidomic analysis of adherent mammalian cancer cells. *Anal Bioanal Chem* **2017**, *409*, 5349–5358.

68. Total Lipid Extraction For Lipidomics Made Easy - The BUME Method | 26390 Available online: https://www.omicsonline.org/proceedings/total-lipid-extraction-for-lipidomics-made-easy--the-bume-method-26390.html (accessed on Oct 20, 2019).
69. The BUME method: a new rapid and simple chloroform-free method for total lipid extraction of animal tissue | Scientific Reports Available online: https://www.nature.com/articles/srep27688 (accessed on Oct 20, 2019).
70. Improved Butanol-Methanol (BUME) Method by Replacing Acetic Acid for Lipid Extraction of Biological Samples Available online: https://www.ncbi.nlm.nih.gov/pmc/articles/PMC4904733/ (accessed on Oct 20, 2019).
71. Katyal, S.L.; Eapen, S.; Venkitasubramanian, T.A. Fractionation of lipids on thin-layer plates and its comparison with silicic acid column chromatography. *Indian J Biochem* **1969**, *6*, 84–87.
72. St John, L.C.; Bell, F.P. Extraction and fractionation of lipids from biological tissues, cells, organelles, and fluids. *BioTechniques* **1989**, *7*, 476–481.
73. Sajilata, M.G.; Singhal, R.S.; Kamat, M.Y. Fractionation of lipids and purification of γ-linolenic acid (GLA) from Spirulina platensis. *Food Chemistry* **2008**, *109*, 580–586.
74. Catchpole, O.J.; Tallon, S.J.; Eltringham, W.E.; Grey, J.B.; Fenton, K.A.; Vagi, E.M.; Vyssotski, M.V.; MacKenzie, A.N.; Ryan, J.; Zhu, Y. The extraction and

fractionation of specialty lipids using near critical fluids. *The Journal of Supercritical Fluids* **2009**, *47*, 591–597.

75. Therriault, D.G. Fractionation of Lipids by Countercurrent distribution. *J Am Oil Chem Soc* **1963**, *40*, 395–399.
76. Targeted lipidomics profiling of acute arsenic exposure in mice serum by on-line solid-phase extraction stable-isotope dilution liquid chromatography–tandem mass spectrometry |SpringerLink Available online: https://link.springer.com/article/10.1007/s00204-017-1937-6 (accessed on Oct 20, 2019).
77. The dispersive micro-solid phase extraction method for MS-based lipidomics of human breast milk - ScienceDirect Available online: https://www.sciencedirect.com/science/article/pii/S0026265X19319198 (accessed on Oct 20, 2019).
78. Use of solid phase extraction in the biochemistry laboratory to separate different lipids - Flurkey - 2005 - Biochemistry and Molecular Biology Education - Wiley Online Library Available online: https://iubmb.onlinelibrary.wiley.com/doi/full/10.1002/bmb.2005.49403305357 (accessed on Oct 20, 2019).
79. Pernet, F.; Pelletier, C.J.; Milley, J. Comparison of three solid-phase extraction methods for fatty acid analysis of lipid fractions in tissues of marine bivalves. *J Chromatogr A* **2006**, *1137*, 127–137.
80. Zarini, S.; Barkley, R.M.; Gijón, M.A.; Murphy, R.C. Overview of Lipid Mass Spectrometry and Lipidomics. In *High-Throughput Metabolomics: Methods and*

Protocols; D'Alessandro, A., Ed.; Methods in Molecular Biology; Springer New York: New York, NY, 2019; pp. 81–105 ISBN 978-1-4939-9236-2.

81. Lee, S.-H.; Hong, S.-H.; Tang, C.-H.; Ling, Y.S.; Chen, K.-H.; Liang, H.-J.; Lin, C.-Y. Mass spectrometry-based lipidomics to explore the biochemical effects of naphthalene toxicity or tolerance in a mouse model. *PLOS ONE* **2018**, *13*, e0204829.
82. Köfeler, H.C.; Fauland, A.; Rechberger, G.N.; Trötzmüller, M. Mass Spectrometry Based Lipidomics: An Overview of Technological Platforms. *Metabolites* **2012**, *2*, 19–38.
83. Zhao, Y.-Y.; Cheng, X.; Lin, R.-C. Lipidomics applications for discovering biomarkers of diseases in clinical chemistry. *Int Rev Cell Mol Biol* **2014**, *313*, 1–26.
84. Sethi, S.; Brietzke, E. Recent advances in lipidomics: Analytical and clinical perspectives. *Prostaglandins Other Lipid Mediat.* **2017**, *128–129*, 8–16.
85. Hu, T.; Zhang, J.-L. Mass-spectrometry-based lipidomics. *J Sep Sci* **2018**, *41*, 351–372.
86. Reversed-Phase Chromatography - an overview | ScienceDirect Topics Available online: https://www.sciencedirect.com/topics/biochemistry-genetics-and-molecular-biology/reversed-phase-chromatography (accessed on Oct 20, 2019).
87. Hybrid quadrupole/time-of-flight mass spectrometers for analysis of biomolecules. - PubMed - NCBI Available online: https://www.ncbi.nlm.nih.gov/pubmed/16401506 (accessed on Oct 20, 2019).
88. Chernushevich, I.V.; Loboda, A.V.; Thomson, B.A. An introduction to quadrupole-time-of-flight mass spectrometry. *J Mass Spectrom* **2001**, *36*, 849–865.

89. Quantitative Profiling of Phospholipids by Multiple Precursor Ion Scanning on a Hybrid Quadrupole Time-of-Flight Mass Spectrometer | Analytical Chemistry Available online: https://pubs.acs.org/doi/10.1021/ac015655c (accessed on Oct 20, 2019).

90. Sandra, K.; Pereira, A.D.S.; Vanhoenacker, G.; David, F.; Sandra, P. Comprehensive blood plasma lipidomics by liquid chromatography/quadrupole time-of-flight mass spectrometry. *J Chromatogr A* **2010**, *1217*, 4087–4099.

91. Ståhlman, M.; Ejsing, C.S.; Tarasov, K.; Perman, J.; Borén, J.; Ekroos, K. High-throughput shotgun lipidomics by quadrupole time-of-flight mass spectrometry. *Journal of Chromatography B* **2009**, *877*, 2664–2672.

92. Checa, A.; Bedia, C.; Jaumot, J. Lipidomic data analysis: tutorial, practical guidelines and applications. *Anal. Chim. Acta* **2015**, *885*, 1–16.

93. Rajanayake, K.K.; Taylor, W.R.; Isailovic, D. The comparison of glycosphingolipids isolated from an epithelial ovarian cancer cell line and a nontumorigenic epithelial ovarian cell line using MALDI-MS and MALDI-MS/MS. *Carbohydr. Res.* **2016**, *431*, 6–14.

94. Seyer, A.; Boudah, S.; Broudin, S.; Junot, C.; Colsch, B. Annotation of the human cerebrospinal fluid lipidome using high resolution mass spectrometry and a dedicated data processing workflow. *Metabolomics* **2016**, *12*.

95. Koelmel, J.P.; Kroeger, N.M.; Ulmer, C.Z.; Bowden, J.A.; Patterson, R.E.; Cochran, J.A.; Beecher, C.W.W.; Garrett, T.J.; Yost, R.A. LipidMatch: an automated workflow for rule-based lipid identification using untargeted high-resolution tandem mass spectrometry data. *BMC Bioinformatics* **2017**, *18*.

96. Sud, M.; Fahy, E.; Cotter, D.; Brown, A.; Dennis, E.A.; Glass, C.K.; Merrill, A.H.; Murphy, R.C.; Raetz, C.R.H.; Russell, D.W.; et al. LMSD: LIPID MAPS structure database. *Nucleic Acids Res.* **2007**, *35*, D527-532.

97. Schmelzer, K.; Fahy, E.; Subramaniam, S.; Dennis, E.A. The lipid maps initiative in lipidomics. *Meth. Enzymol.* **2007**, *432*, 171–183.

98. Fahy, E.; Sud, M.; Cotter, D.; Subramaniam, S. LIPID MAPS online tools for lipid research. *Nucleic Acids Res.* **2007**, *35*, W606-612.

99. Xia, J.; Wishart, D.S. Using MetaboAnalyst 3.0 for Comprehensive Metabolomics Data Analysis. *Curr Protoc Bioinformatics* **2016**, *55*, 14.10.1-14.10.91.

100. Marco-Ramell, A.; Palau-Rodriguez, M.; Alay, A.; Tulipani, S.; Urpi-Sarda, M.; Sanchez-Pla, A.; Andres-Lacueva, C. Evaluation and comparison of bioinformatic tools for the enrichment analysis of metabolomics data. *BMC Bioinformatics* **2018**, *19*.

101. Xia, J.; Sinelnikov, I.V.; Han, B.; Wishart, D.S. MetaboAnalyst 3.0—making metabolomics more meaningful. *Nucleic Acids Res* **2015**, *43*, W251–W257.

102. Chong, J.; Soufan, O.; Li, C.; Caraus, I.; Li, S.; Bourque, G.; Wishart, D.S.; Xia, J. MetaboAnalyst 4.0: towards more transparent and integrative metabolomics analysis. *Nucleic Acids Res.* **2018**, *46*, W486–W494.

103. Bhanot, D.D. How LC – MS/MS Scores over LC – MS? *Lab-Training.com* 2016.

104. Yang, K.; Han, X. Lipidomics: Techniques, Applications, and Outcomes Related to Biomedical Sciences. *Trends in Biochemical Sciences* **2016**, *41*, 954–969.

105. Proteomics, C. Agilent 6540 UHD Quadrupole Time-of-Flight Accurate-Mass Mass Spectrometer Available online: https://www.creative-

proteomics.com/support/agilent-6540-uhd-quadrupole-time-of-flight-accurate-mass-mass-spectrometer.htm (accessed on Dec 15, 2019).

CHAPTER II

IN-QUEST OF BIOMARKERS FOR ALZHEIMER'S DISEASE IN HUMAN PLASMA USING LIQUID CHROMATOGRAPHY IN TANDEM WITH HIGH RESOLUTION MASS SPECTROMETRY (QUADRAPOLE TIME-OF-FLIGHT(Q-TOF))

2.1. Introduction

Alzheimer's disease (AD) is an age-related progressive multifarious neurodegenerative disease. Pathologically it is defined by extensive cerebral cortical atrophy, accumulation of extracellular amyloid beta (Aβ) plaques and intracellular neurofibrillary tangles (NFTs), chronic inflammation and neuronal loss [1,2]. Loss of neuronal communication is attributed to the overproduction of amyloid beta and its inability to be cleared from the brain resulting in plaques, toxic oligomers, and fibrils. Neuronal toxicity and loss of neurons (death of neurons) are attributed to NFTs [3,4]. There are four types of AD's *i.e.,* type1, 2, 3 and 4. Familial AD (early-onset) is associated with inheritance of genetic mutations which includes type 1 AD caused due to mutation in *APP* gene, type 3 AD caused due to mutation in *PSEN1* gene, type 4 AD caused due to

mutation in *PSEN2* gene. SporadicAD which include type 2 AD (late-onset, LOAD) is also associated with *ApoE4* gene along with multiple factors like diet, exercise, disease conditions and environmental. Clinical staging of the AD disease includes preclinical (AD-P), mild cognitive impairment (MCI-AD) and dementia [5–7]. The pathophysiological process of AD begins many years before the diagnosis of clinical MCI due to AD. This long haul preclinical phase of AD can be used for therapeutic intervention if appropriate plasma biomarkers were available for early diagnosis of this stage. Currently, available biomarkers for AD reflect the presence or the progression of the disease but not it's early diagnosis. The proposed biomarker models for the diagnosis of AD-P stage reported in previous studies are either invasive or expensive [8–10].

There are reported studies which reiterate the crucial link between the brain lipids and AD. Genome-wide association (GWAS) have identified several other genes associated with AD risk, which are involved in affecting pathways related to lipid metabolism (*ApoE, CLU*, and *ABCA7)*, the inflammatory response (*CR1*, *CD33*, *MS4A*, *CLU*, and *TREM2)* and endocytosis (*BIN1*, *PICALM CD2AP*, *EPHA1* and *SORL1*) [1]. Along with the genotypic and the phenotypic studies, AD brains have revealed the higher occurrence of adipose inclusions or lipoid granules suggesting aberrant lipid metabolism. These membrane lipids (glycerophospholipids and sphingolipids) modulate the protein-protein interactions, protein-lipid interactions and trafficking of the proteins involved in the pathogenesis of AD [11–13]. Studies have also shown the involvement of membrane lipid raft (rich in cholesterol and sphingolipids) in the processing of APP, production of Aβ and the clearance of Aβ from the intracellular spaces [14–16]. Post-mortem studies on the brain have demonstrated altered lipidome at the different stages of AD pathogenesis and these

changes could lead to parallel changes either in the content or composition or both of the lipid species in the plasma of the AD patients. The use of peripheral plasma markers has many obvious advantages over brain markers in terms of cost, risks, patient point of care and ability to monitor a patient over a long period. Over the past years, numerous studies have been reported on different matrices of AD using the lipidomics approach either using the targeted shotgun analysis [17,18] or the untargeted liquid chromatography-mass spectrometry (LC-MS) analysis [19–21]. However, these studies lack the appropriate classification/ staging of AD patients based on the genetic risk factor, cognitive deficit levels, other underlying vascular risk factors and existing pathophysiological conditions which could affect the plasma lipids. The shotgun lipidomic analysis is limited by the targeted lipid analysis, ion suppression, and isobaric peaks overlapping.

In our study, we employed liquid chromatography- quadrupole time of flight mass spectrometry (LC-QTOF-MS) based untargeted lipidomics analysis approach to search for the plausible biomarkers from plasma lipids, which could be differentially regulated between AD and normal cognitive controls (NCC) study subjects. Appropriate screening and staging of the patients were performed based on cognitive function (MoCA test), *ApoE* genotyping, cerebrospinal fluid (CSF)- Aβ 42, total tau, phospho tau and Aβ42/t-tau index. We applied solid-phase extraction (SPE) to fractionate the total lipids into two fractions to reduce the matrix interference and ion suppression in MS analysis and employed multiple internal standards representing each sub-class for normalization and semi quantitation of lipid species. Multivariate analysis was performed to obtain the potential lipid biomarkers which could be used for early diagnosis of AD.

2.2. Materials and Methods

2.2.1. Chemicals and Standard solutions

2.2.1.1. Chemicals

HPLC-grade acetonitrile, chloroform, isopropanol, methanol and water were purchased from Fisher Scientific (Hanover Park, IL, USA). Synthetic lipids including 1,2-dinonadecanoyl-*sn*-glycero-3-phosphocholine [PC(19:0/19:0)], 1,2-dipentadecanoyl-*sn*-glycero-3-phosphoethanolamine [PE(15:0/15:0)], 1,2-diheptadecanoyl-*sn*-glycero-3-phospho-(1'-*rac*-glycerol) (sodium salt) [PG(17:0/17:0)], 1,2-dimyristoyl-*sn*-glycero-3-phospho-L-serine (sodium salt) [PS(14:0/14:0)], 1-tridecanoyl-2-hydroxy-*sn*-glycero-3-phosphocholine [LPC(13:0/0:0)], 1-myristoyl-2-hydroxy-*sn*-glycero-3-phosphoethanolamine [LPE(14:0/0:0)], 1-myristoyl-2-hydroxy-*sn*-glycero-3-phospho-(1'-*rac*-glycerol) (sodium salt) [LPG(14:0/0:0)], 1-(10Z-heptadecenoyl)-2-hydroxy-*sn*-glycero-3-phospho-L-serine (sodium salt) [LPS(17:1/0:0)], 1-myristoyl-2-hydroxy-*sn*-glycero-3-phosphate (sodium salt) [LPA(14:0/0:0)], N-(heptadecanoyl)-sphing-4-enine [Cer(d18:1(4E)/17:0)] were purchased from Avanti Polar Lipids, Inc. (Alabaster, AL, USA). 1,2-dinonadecanoyl-*sn*-glycerol [DG(19:0/19:0/0:0) (Dinonadecanoin)] was purchased from Larodan Fine Chemicals AB (Solna, Stockholm, Sweden). 1,2,3-triheptadecanoyl-*sn*-glycerol [TG(17:0/17:0/17:0) (Glyceryl triheptadecanoate)], analytical grade ammonium acetate, glacial acetic acid and hydrochloric acid were purchased from Sigma-Aldrich (St. Louis, MO, USA).

2.2.1.2. Standard solutions

The standard stock solutions of PC(19:0/19:0), PE(15:0/15:0), PG(17:0/17:0), PS(14:0/14:0), LPC(13:0/0:0), LPE(14:0/0:0), LPG(14:0/0:0), LPS(17:1/0:0),

LPA(14:0/0:0) and Cer(d18:1(4E)/17:0) of 1.00×10^3 μM were prepared by dissolving in appropriate volumes of chloroform: methanol (2:1). Standard stock solutions of DG(19:0/19:0/0:0) and TG (17:0/17:0/17:0) of 1.00×10^3 μM was prepared by dissolving in appropriate volumes of chloroform. Stock solutions are stored in -20 ° C until further use.

Working internal standard mix (12 lipids) at a concentration of 5.00×10^4 nM was prepared by diluting the individual standard stock solutions with appropriate volumes of chloroform/methanol/300 mM ammonium acetate (30:66.5:3.5, v/v/v).

2.2.2. Study subjects and plasma collection

Caucasian subjects who were 60 years of age and above were recruited from the Lou Ruvo Center for Brain Health at Cleveland Clinic. The study group includes four age-matched normal cognitive control patients (n = 4) and three Alzheimer's disease patients (n = 3). Patients were diagnosed with AD using the National Institute of Aging (NIA) guidelines. Patients were interviewed, followed up with the medication history, cognitive screening, magnetic resonance imaging (MRI) scan, neurological and cerebrovascular examination, standard blood and cerebrospinal fluid chemistries were performed [5–7]. The patient medical histories were assessed for the presence of cardiovascular disease, dyslipidemia, and diabetes, any use of dietary supplements, medication and smoking habits. The Montreal Cognitive Assessment (MoCA) test was employed to assess the mental status of the patients to categorize AD patients as mild (MoCA score > 20) or moderate (MoCA score 10 - 20). Normal cognitive control subjects were participants who were determined to be free of cognition concerns and other significant neuropsychiatric disorders after reviewing their medical history, functional status, informant interviews and

MoCA score > 26 [22]. Clinical information of the study subjects were tabulated in Table 1.

Whole blood samples of volume 10 mL were collected into purple top vacutainer tube (Becton, Dickinson and Company, Franklin Lakes, NJ, USA) with potassium EDTA (~1.8 mg) by venipuncture procedure from each subject. Blood samples were mixed gently by inversion for 10 times and centrifuged at 2000 × g for 15 min at 4 °C using Sorvall Legend RT centrifuge (Thermo Scientific, Waltham, MA, USA). Upper plasma layer was aspirated with a transfer pipette and transferred into a 15-mL conical centrifuge tube (Corning Inc., Corning, NY, USA). Plasma samples were aliquoted into amber glass cryovials (Macherey-Nagel GmbH & Co., Bethlehem, PA, USA) after re-centrifugation at 2000 × g for 15 min at 4 °C and stored at -80 °C until extraction.

Table 2.1. Clinical information of the study subjects

Patient No.	Group	Age	Sex	Smoking	Cerebrovascular	*ApoE*[e]	MoCA[f]	Aβ[g]	Tau[h]	P Tau[i]	ATI[j]
1	AD[a]	60	F[c]	No	No	3.3	19	320.5	462.5	80.45	0.41
2	AD	65	F	No (Quit > 10 years)	No	4.4	10	ND	ND	ND	ND
3	AD	72	F	No	Yes	3.4	18	371.4	1031	105.8	0.25
4	NCC[b]	73	F	ND	ND	3.3	30	ND	ND	ND	ND
5	NCC	72	F	NDk	ND	3.3	30	ND	ND	ND	ND
6	NCC	60	M[d]	ND	ND	3.3	30	ND	ND	ND	ND
7	NCC	62	F	ND	ND	2.3	30	ND	ND	ND	ND

[a]AD = Alzheimer's disease; [b]NCC = normal cognitive control; [c]F = female; [d]M = male; [e]*ApoE* = apolipoprotein E genotyping; [f]MoCA = Montreal Cognitive Assessment; [g]Aβ = amyloid beta 42; [h]Tau = total tau; [i]P Tau = phospho tau; [j]ATI = Aβ42/t-tau index; [k]ND = not determined.

2.2.3. Plasma sample preparation

The samples were prepared by extracting the total lipids followed by fractionation using solid-phase extraction (SPE). The study samples (n = 7) includes 4 NCC and 3 AD subjects. For each patient plasma sample, three sample preparation replicates (same sample preparation was performed three times in parallel) and three technical replicates on one of the sample preparation replicate were performed (injected thrice from the same vial) making a total of five runs for each patient plasma sample.

2.2.3.1. Total lipid extraction

Total lipids were extracted using the modified Bligh-Dyer method [23]. 50 µL of plasma was diluted to 450 µL with 1 × phosphate buffer solution (PBS) in a borosilicate glass tube (13 x 100 mm) from Fisher Scientific (Hanover Park, IL, USA) and was spiked with 15µL of working internal standard mix (12 lipids) followed by acidification using 20 µL of 1 N hydrochloric acid (HCl). The sample was vortexed gently to mix the solutions. 3mL of chloroform: methanol (1:2) was added to the sample, vortexed for 5 min and left on ice for 10 min. Then, followed by addition of 1mL of chloroform and 1.3 mL of DI water which was vortexed for 5 min and centrifuged at 2671 × g (3500 rpm) for 20 min. Discard the upper phase and carefully pierce through the protein disc. The lower chloroform phase was collected into a new borosilicate glass tube (12 × 75 mm) and subjected to fractionation using solid-phase extraction.

2.2.3.2. Fractionation of lipids

The total lipid extracted were fractionated into phospho lipid (PL) and neutral lipid (NL) fractions using a solid-phase extraction method developed by Kaluzny et al [24] which reported highest recoveries for glycerolipids and glycerophospholipids. The total lipid extract in chloroform was loaded onto a 500 mg aminopropyl cartridge (Agilent Technologies, Wilmington, Delaware, USA) previously conditioned with 3 mL of hexane. The column was first eluted with 3 mL of chloroform: isopropanol (2:1) to collect the NL fraction. Followed by passing 3 mL of 2% acetic acid in diethyl ether through the column and the collected fraction was discarded. Another 6 mL of 2% acetic acid in diethyl ether was passed through the column to collect the free fatty acids fraction (FA). 4 mL methanol was passed to elute PL fraction. The collected NL and PL fractions were dried under nitrogen gas (TurboVap® LV evaporator, Biotage, Charlotte, NC, USA) at room temperature and reconstituted with 500 µL of chloroform: methanol: ammonium acetate (30:66.5:3.5). 5 µL of the reconstituted sample was subjected for further analysis using reverse-phase liquid chromatography- quadrupole time of flight mass spectrometry.

2.2.4. UHPLC-QTOF-MS/MS method for lipid profiling

Fractionated samples were subjected to reversed-phase chromatographic separation on Xterra® C_{18} (2.1 × 150 mm i.d.; 5 µm particle size) column (Waters, Milford, MA, USA) maintained at 40 ° C. The liquid chromatography system included an Agilent UHPLC system 1290 (Agilent Technologies, Santa Clara, CA, USA) composed of a solvent reservoir, a degasser, a binary pump (G4220A), a thermostat (G1330B), an autosampler (G4226A), and a thermostatted column compartment (G1316C). The gradient elution was performed using mobile phases: phase A (methanol: water (80:20) with 10mM

ammonium acetate and 0.1% acetic acid), and phase B (isopropyl alcohol: acetonitrile: water (70:29:1) with 10mM ammonium acetate and 0.1% acetic acid) at a flow rate of 0.2 mL/min with the following gradient program: 5% B at 0 min, 5–50% B from 0-19 min, 50-65% B from 19-24 min, 65% from 24-29 min, 65-60% B from 29-34 min, 80% B from 34-39 min, 80-100% B from 39-44 min, 100% B from 44- 47 min, 100-5% B from 47-50 min, 5% B from 50-60 min. Total run time was 60 min including column re-equilibration. Prior to sample analysis, the column was first equilibrated with at least 25 column volumes of the mobile phase at a flow rate of 0.2 mL/min.

Lipidomic analysis was performed using an Agilent 1290 Infinity series (UHPLC) system connected to an Agilent 6540 Quadrupole Time of Flight (Q-TOF) equipped with an orthogonal electrospray ionization (ESI) interface (Agilent Jet Stream, AJS) and was operated in both positive and negative ion modes. Data was acquired using Agilent MassHunter™ Acquisition software (version B.05.01). The MS operation parameters are as follows: Vcap- 4000 V; nebulizer pressure- 35 psig; drying gas flow rate-10 L/min; gas temperature- 300 °C; sheath gas flow- 11 L/min; sheath gas temperature- 300 °C; skimmer voltage- 65 V; fragmentor voltage- 100 V. Data was collected in both centroid and profile mode in extended dynamic range (2GHz). TOF MS accurate mass spectra were recorded at narrow isolation width of 1.3 m/z across the range of 100–1800 m/z at 5 spectra/s and MS/MS spectra were recorded across the range of 50 to 1800 m/z at 4 spectra/s. Collision energies (CE) of 10, 20 and 40 V were used. Data-dependent acquisition (DDA) was acquired using a maximum of 5 precursor ions per cycle with the absolute threshold of 5000 counts and charge states of 1, 2. Active exclusion of m/z after 3 spectral acquisitions for 0.4 min was used. TOF was calibrated daily and real-time calibration was performed

by continuous infusion of reference ions m/z 121. 050873 and 922.009798 (Catalog# G1969-85001) obtained from Agilent Technologies.

2.2.5. Data processing and multivariate data analysis

Data was evaluated for retention time (t_R) and mass shift by checking the extracted ion chromatograms (EIC) of spiked internal standards and reference ion m/z across the runs in Agilent MassHunter™ Qualitative Analysis software (Version B.06.00) to determine retention time and mass window. The acquired data was processed using Profinder software (Version B.06.00) which deconvolute the data into individual peaks and filters the features by performing batch recursive molecular feature extraction. Based on MS data, the algorithm extracts the features with at least 100 counts in intensity, align and bin the features based on isotopic pattern, dimers and adducts ($[H]^+$, $[M+NH_4]^+$, $[2M+H]^{+2}$, $[M-H_2O+H]^+$ in positive mode; ($[H]^-$, $[CH_3COO]^-$, $[2M-H]^{-2}$ in negative mode) with charge state of 1 or 2. Each extracted feature with calculated neutral mass have a corresponding unique retention time and abundance. Retention time window and mass windows were set at 0.5 min and 20.00 ppm respectively to perform retention time and mass corrections. The extracted features carrying MS data with relative standard deviation (%RSD) ≤ 20% were exported as compound exchange file (.cef) and comma-separated value (.csv) file for MSMS extraction and statistical analysis respectively. In Qualitative analysis software, each raw data (.d) and its corresponding processed .cef with MS data was used as a template to extract MSMS spectra using "Find by Formula" function. The extracted data with MS and summed MSMS spectra from different collision energies were exported as .cef for annotation in SimLipid®.

The .csv file carrying the details of mass, retention time and peak area of each feature was used for multivariate and statistical analysis in MetaboAnalyst (v4.0) [25]. The MS peak list data with mass, retention time and peak area as .csv files were compressed (.zip) and uploaded onto the server [26]. Mass tolerance of 0.005 Da and retention time tolerance of 15 s were used for feature alignment. Features with missing values in ≥ 90% of the samples were excluded for the downstream analysis. Normalization of the data was performed using the internal standard reference feature (Internal standard PC mass 817.6620 @ t_R 26.37 min) followed by transforming the data into logarithmic form using Pareto scaling (mean-centered and divided by the square root of the standard deviation of each feature). To compare and obtain statistically significant features between two study groups, a non-parametric, unpaired Wilcoxon rank-sum *t*-test was performed by applying the adjusted *p*-value (FDR) of ≤ 0.05 as the cut-off value. Unsupervised 2D PCA and supervised 2D PLS-DA score plots were plotted on data for the detection of the outliers and also to depict the inherent covariance between the study groups. VIP scores summarizes the significance of the individual feature contribution to the PLS-DA model. VIP scores are calculated as a weighted sum of the squared correlations between the PLS-DA components and the original variable.

2.2.6. Identification of lipids

Data acquired in +ESI and -ESI mode were used in complementary to each other for the identification of lipids against the database. The identification of the lipids was performed using SimLipid® software (version 5.0) using extracted data with MS and MSMS peak list (summed spectra from different CEs). SimLipid is an online database server with MS and MSMS spectral library. Data was searched against the database with

a relative threshold cut-off of 2%, mass tolerance of 20 ppm for MS and 30 ppm for MSMS data. The type of ions matched with the spectral database were annotated in the spectra. Annotation with the highest score was considered as the identity of lipid.

2.2.7. Pathway analysis

Joint network analysis was performed using the HMDB IDs of significant lipids and associated protein gene name list in MetaboAnalyst. For this Lipid Maps ID (LM ID), Human Metabolome Data Base ID (HMDB ID), and PubChem CID were sought from LIPID MAPS database (http://lipidmaps.org/) [27] which are listed in Table 2.2. Using the available HMDB IDs (http://www.hmdb.ca/metabolites) [28], proteins associations from each lipid were obtained and the duplicate proteins were deleted as listed in Table 2.3.

2.2.8. Method validation

The reproducibility of the sample preparation and the UPLC-Q-TOF-MS/MS method was evaluated by replicate analysis of study samples, which was further evaluated in 2D PCA and 2D PLS-DA score plots. The intra- and inter-assay precision was evaluated and expressed as relative standard deviation (%RSD). The intra-assay precision was determined by three-replicate measurements of 12 internal standards from one of the sample preparations of all the study subjects. Inter-assay precision was determined by three-replicate measurement of 12 internal standards from three-parallel sample preparations of all the study subjects.

2.2.9. Semi-quantitation

Semi quantitation of data was performed in Agilent MassHunter Quantitative analysis software (version: B.06, SP01) using the respective internal standard for each subclass of lipids (e.g. PC 817.6620 @ t_R 26.37 min was used to quantitate all PC lipids).

For unidentified features, internal standard closer in retention time to the feature was assigned for semi-quantitation. Raw data (.d file) and its corresponding compound exchange file (.cef) were used for this process and the results were calculated based on peak area ratio of the feature to the IS.

Table 2.2. Different unique IDs of 28 significant lipids from LipidMaps database

No.	Significant Lipid	LM ID[a]	HMDB ID[b]	PubChem CID[c]	KEGG ID[d]
1	LPC(16:0_0:0)	LMGP01050018; LMGP01050113	HMDB0010382	460602; 86544	C04230
2	LPC(18:2_0:0)	LMGP01050035; LMGP01050034	HMDB0010386	11005824; 24779467	C04230
3	LPC(18:1_0:0)	LMGP01050032; LMGP01050138; LMGP01050029; LMGP01050030; LMGP01050114	HMDB0002815; HMDB0010385	16081932; 53480465; 24779465; 24779466; 6449974	C04230
4	LPC(18:0_0:0)	LMGP01050026; LMGP01050076	HMDB0010384; HMDB0011128	497299; 24779491	C04230
5	LPC(20:4_0:0)	LMGP01050048 LMGP01050140	HMDB0010395 HMDB0010396	24779476 53480469	C04230
6	PC(O-14:0_18:1)	LMGP01020016	-	24779279	-
7	PC(15:0_16:0)	LMGP01010532 LMGP01010562	HMDB0007935 HMDB0007967	24778655	C00157
8	PC(O-16:0_20:5)	LMGP01020058	-	10485310	-
9	PC(18:4_18:3)	LMGP01011714; LMGP01011715	HMDB0008238; HMDB0008239	52922907; 52922909	C00157
10	PC(16:0_20:5)	LMGP01011932; LMGP01010633	HMDB0008495; HMDB0007984	52923341; 24778723	C00157
11	PC(16:0_20:4)	LMGP01011049; LMGP01011056; LMGP01010629; LMGP01012136	HMDB0008429; HMDB0007983; HMDB0007982	24779073; 24779079; 24778721; 53478669; 10747814	C00157
12	PC(18:3_20:5)	LMGP01011939; LMGP01011940; LMGP01011664; LMGP01011693	HMDB0008501; HMDB0008502; HMDB0008182; HMDB0008215	52923355; 52923357; 52922807; 52922865	C00157
13	PC(16:0_21:0)	LMGP01011958 LMGP01011470	-	52923393 52922422	-

14	PC(18:2_20:4)	LMGP01011909; LMGP01012212; LMGP01010943; LMGP01012171	HMDB0008434; HMDB0008467; HMDB0008147; HMDB0008148	52923295; 53479073; 24778979; 53478789	C00157
15	PC(16:0_22:6)	LMGP01011115; LMGP01011116; LMGP01010650; LMGP01012137	HMDB0008725; HMDB0007991	24779130; 24779131; 6506479; 6441886	C00157
16	PC(P-18:0_22:6)	LMGP01030014	HMDB0011262	42607430	-
17	PC(P-18:0_22:4)	LMGP01030073	HMDB0011259	52923974	-
18	PC(18:0_22:6)	LMGP01012107; LMGP01010821; LMGP01010823	HMDB0008727 ; HMDB0008057	52923691; 24778876; 24778878	C00157
19	PC(P-20:0_22:6)	LMGP01030104	-	52924036	-
20	PC(20:3_22:6)	LMGP01012118; LMGP01011896	HMDB0008738; HMDB0008419; HMDB0008387	52923713; 52923269; 53478995	C00157
21	SM(d18:2/18:0)	LMSP03010050	-	52931161	-
22	SM(d16:1/22:0)	LMSP03010061	-	52931183	-
23	SM(d16:1/23:0)	LMSP03010065	-	52931189	-
24	SM(d16:1/24:1)	LMSP03010071	-	52931201	-
25	GlcCer(d14:1/18:1)	LMSP0501AA41	-	70699222	-
26	TG(18:1/18:1/20:5)	LMGL03010748	HMDB0010464	9544709	-
27	TG(18:2/20:2/20:2)	LMGL03011005	-	9544966	-
28	TG(16:0/20:3/22:0)	LMGL03010963	-	9544924	-

[a]LM ID = Lipid Maps ID; [b]HMDB ID = Human Metabolome Database ID for metabolite; [c]PubChem CID = PubChem compound ID; [d]KEGG = Kyoto Encyclopedia of Genes and Genomes ID for compounds.

Table 2.3. Lipid-protein association list for the significant lipids with HMDB IDs.

No	Protein name	HMDBP ID[a]	UniProt ID[b]	Gene name	Protein associated lipids[c]
1	Sphingomyelin phosphodiesterase 2	HMDBP01090	O60906	SMPD2	3
2	Platelet-activating factor acetylhydrolase	HMDBP00523	Q13093	PLA2G7	1 - 5
3	Platelet-activating factor acetylhydrolase IB subunit gamma	HMDBP00528	Q15102	PAFAH1B3	1 - 5
4	Platelet-activating factor acetylhydrolase IB subunit beta	HMDBP00530	P68402	PAFAH1B2	1 - 5
5	Platelet-activating factor acetylhydrolase 2, cytoplasmic	HMDBP00534	Q99487	PAFAH2	1 - 5
6	60 kDa lysophospholipase	HMDBP07300	Q86U10	ASPG	1 - 5
7	Acyl-protein thioesterase 1	HMDBP00056	O75608	LYPLA1	1 - 5, 7, 9 - 12, 14, 15, 18, 20
8	Group XV phospholipase A2	HMDBP00057	Q8NCC3	PLA2G15	1 - 5, 7, 9 - 12, 14, 15, 18, 20
9	Calcium-dependent phospholipase A2	HMDBP00058	P39877	PLA2G5	1 - 5, 7, 9 - 12, 14, 15 - 18, 20
10	Group IIF secretory phospholipase A2	HMDBP00059	Q9BZM2	PLA2G2F	1 - 5, 7, 9 - 12, 14, 15 - 18, 20
11	Cytosolic phospholipase A2	HMDBP00060	P47712	PLA2G4A	1 - 5, 7, 9 - 12, 14, 15 - 18, 20
12	Phospholipase A2	HMDBP00061	P04054	PLA2G1B	1 - 5, 7, 9 - 12, 14, 15 - 18, 20
13	Group XIIB secretory phospholipase A2-like protein	HMDBP00062	Q9BX93	PLA2G12B	1 - 5, 7, 9 - 12, 14, 15, 18, 20
14	Group 10 secretory phospholipase A2	HMDBP00063	O15496	PLA2G10	1 - 5, 7, 9 - 12, 14, 15 - 18, 20
15	Group IIE secretory phospholipase A2	HMDBP00065	Q9NZK7	PLA2G2E	1 - 5, 7, 9 - 12, 14, 15 - 18, 20
16	Acyl-protein thioesterase 2	HMDBP00066	O95372	LYPLA2	1 - 5, 7, 9 - 12, 14, 15, 18, 20

17	Group XIIA secretory phospholipase A2	HMDBP00067	Q9BZM1	PLA2G12A	7, 9 - 12, 14, 15 - 18, 20
18	85/88 kDa calcium-independent phospholipase A2	HMDBP00068	O60733	PLA2G6	1 - 5, 7, 9 - 12, 14, 15 - 18, 20
19	Phosphatidylcholine-sterol acyltransferase	HMDBP00069	P04180	LCAT	1 - 5, 7, 9 - 12, 14, 15 - 18, 20
20	Eosinophil lysophospholipase	HMDBP00070	Q05315	CLC	1 - 5, 7, 9 - 12, 14, 15, 18, 20
21	Phospholipase A2, membrane associated	HMDBP00072	P14555	PLA2G2A	7, 9 - 12, 14, 15 - 18, 20
22	Group IID secretory phospholipase A2	HMDBP00073	Q9UNK4	PLA2G2D	1 - 5, 7, 9 - 12, 14, 15 - 18, 20
23	Phospholipase D2	HMDBP00080	O14939	PLD2	7, 9 - 12, 14, 15 - 18, 20
24	Phosphatidylethanolamine N-methyltransferase	HMDBP00081	Q9UBM1	PEMT	7, 9 - 12, 14, 15 - 18, 20
25	Phospholipase D1	HMDBP00082	Q13393	PLD1	7, 9 - 12, 14, 15 - 18, 20
26	Cytosolic phospholipase A2 gamma	HMDBP00529	Q9UP65	PLA2G4C	7, 9 - 12, 14, 15 - 18, 20
27	Group 3 secretory phospholipase A2	HMDBP00532	Q9NZ20	PLA2G3	1 - 5, 7, 9 - 12, 14, 15 - 18, 20
28	D-beta-hydroxybutyrate dehydrogenase, mitochondrial	HMDBP00540	Q02338	BDH1	7, 9 - 12, 14, 15 - 18, 20
29	Choline-phosphate cytidylyltransferase B	HMDBP00732	Q9Y5K3	PCYT1B	7, 9 - 12, 14, 15 - 18, 20
30	Choline-phosphate cytidylyltransferase A	HMDBP00755	P49585	PCYT1A	7, 9 - 12, 14, 15 - 18, 20
31	Phosphatidylcholine:ceramide cholinephosphotransferase 2	HMDBP00770	Q8NHU3	SGMS2	7, 9 - 12, 14, 15 - 18, 20
32	Phosphatidylcholine:ceramide cholinephosphotransferase 1	HMDBP00775	Q86VZ5	SGMS1	7, 9 - 12, 14, 15 - 18, 20
33	Choline kinase alpha	HMDBP00778	P35790	CHKA	7, 9 - 12, 14, 15 - 18, 20
34	Probable phospholipid-transporting ATPase IG	HMDBP01131	Q8NB49	ATP11C	7, 9 - 12, 14, 15 - 18, 20

35	Probable phospholipid-transporting ATPase IH	HMDBP01132	P98196	ATP11A	7, 9 - 12, 14, 15 - 18, 20
36	Probable phospholipid-transporting ATPase VA	HMDBP01169	O60312	ATP10A	7, 9 - 12, 14, 15 - 18, 20
37	Probable phospholipid-transporting ATPase IC	HMDBP01192	O43520	ATP8B1	7, 9 - 12, 14, 15 - 18, 20
38	Probable phospholipid-transporting ATPase IIA	HMDBP01220	O75110	ATP9A	7, 9 - 12, 14, 15 - 18, 20
39	Probable phospholipid-transporting ATPase VD	HMDBP01239	Q9P241	ATP10D	7, 9 - 12, 14, 15 - 18, 20
40	Probable phospholipid-transporting ATPase IB	HMDBP01247	Q9NTI2	ATP8A2	7, 9 - 12, 14, 15 - 18, 20
41	Probable phospholipid-transporting ATPase IA	HMDBP01359	Q9Y2Q0	ATP8A1	7, 9 - 12, 14, 15 - 18, 20
42	Probable phospholipid-transporting ATPase IM	HMDBP01463	Q8TF62	ATP8B4	7, 9 - 12, 14, 15 - 18, 20
43	Probable phospholipid-transporting ATPase IF	HMDBP01485	Q9Y2G3	ATP11B	7, 9 - 12, 14, 15 - 18, 20
44	Probable phospholipid-transporting ATPase IK	HMDBP01489	O60423	ATP8B3	7, 9 - 12, 14, 15 - 18, 20
45	Phosphatidylinositol transfer protein beta isoform	HMDBP01672	P48739	PITPNB	7, 9 - 12, 14, 15 - 18, 20
46	Multidrug resistance protein 3	HMDBP01901	P21439	ABCB4	7, 9 - 12, 14, 15 - 18, 20
47	Lecithin retinol acyltransferase	HMDBP01912	O95237	LRAT	7, 9 - 12, 14, 15 - 18, 20
48	Phospholipid scramblase 1	HMDBP01967	O15162	PLSCR1	7, 9 - 12, 14, 15 - 18, 20
49	Phosphatidylserine synthase 1	HMDBP02190	P48651	PTDSS1	7, 9 - 12, 14, 15 - 18, 20
50	Phosphatidylinositol transfer protein alpha isoform	HMDBP02524	Q00169	PITPNA	7, 9 - 12, 14, 15 - 18, 20
51	Phospholipid transfer protein	HMDBP02549	P55058	PLTP	7, 9 - 12, 14, 15 - 18, 20
52	Cholinephosphotransferase 1	HMDBP02855	Q8WUD6	CHPT1	7, 9 - 12, 14, 15 - 18, 20

53	2-acylglycerol O-acyltransferase 2	HMDBP03089	Q3SYC2	MOGAT2	7, 9 - 12, 14, 15 - 18, 20
54	Choline/ethanolaminephosphotransferase 1	HMDBP03349	Q9Y6K0	CEPT1	7, 9 - 12, 14, 15 - 18, 20
55	1-phosphatidylinositol 4,5-bisphosphate phosphodiesterase delta-3	HMDBP04457	Q8N3E9	PLCD3	7, 9 - 12, 14, 15 - 18, 20
56	Lysophospholipid acyltransferase 5	HMDBP07287	Q6P1A2	LPCAT3	1 - 5, 7, 9 - 12, 14, 15 - 18, 20
57	Putative inactive group IIC secretory phospholipase A2	HMDBP07288	Q5R387	PLA2G2C	7, 9 - 12, 14, 15 - 18, 20
58	Lysophosphatidylcholine acyltransferase 1	HMDBP07289	Q8NF37	LPCAT1	1 - 5, 7, 9 - 12, 14, 15 - 18, 20
59	Lysophosphatidylcholine acyltransferase 2	HMDBP07290	Q7L5N7	LPCAT2	1 - 5, 7, 9 - 12, 14, 15 - 18, 20
60	Phospholipase D3	HMDBP07291	Q8IV08	PLD3	7, 9 - 12, 14, 15 - 18, 20
61	Phospholipase D4	HMDBP07292	Q96BZ4	PLD4	7, 9 - 12, 14, 15 - 18, 20
62	Phosphatidylcholine transfer protein	HMDBP07293	Q9UKL6	PCTP	7, 9 - 12, 14, 15 - 18, 20
63	Phospholipid scramblase 2	HMDBP07294	Q9NRY7	PLSCR2	7, 9 - 12, 14, 15 - 18, 20
64	Phospholipid scramblase 3	HMDBP07295	Q9NRY6	PLSCR3	7, 9 - 12, 14, 15 - 18, 20
65	Phospholipid scramblase 4	HMDBP07296	Q9NRQ2	PLSCR4	7, 9 - 12, 14, 15 - 18, 20
66	Phospholipid scramblase family member 5	HMDBP07297	A0PG75	PLSCR5	7, 9 - 12, 14, 15 - 18, 20
67	Probable phospholipid-transporting ATPase VB	HMDBP07298	O94823	ATP10B	7, 9 - 12, 14, 15 - 18, 20
68	Probable phospholipid-transporting ATPase ID	HMDBP07299	P98198	ATP8B2	7, 9 - 12, 14, 15 - 18, 20
69	Phospholipase B1, membrane-associated	HMDBP07301	Q6P1J6	PLB1	7, 9 - 12, 14, 15 - 18, 20, 26
70	Phosphatidylethanolamine-binding protein 1	HMDBP07304	P30086	PEBP1	7, 9 - 12, 14, 15 - 18, 20

71	Phosphatidylethanolamine-binding protein 4	HMDBP07305	Q96S96	PEBP4	7, 9 - 12, 14, 15 - 18, 20
72	Membrane-associated phosphatidylinositol transfer protein 1	HMDBP07336	O00562	PITPNM1	7, 9 - 12, 14, 15 - 18, 20
73	Membrane-associated phosphatidylinositol transfer protein 2	HMDBP07337	Q9BZ72	PITPNM2	7, 9 - 12, 14, 15 - 18, 20
74	Membrane-associated phosphatidylinositol transfer protein 3	HMDBP07338	Q9BZ71	PITPNM3	7, 9 - 12, 14, 15 - 18, 20
75	Cytosolic phospholipase A2 delta	HMDBP07863	Q86XP0	PLA2G4D	7, 9 - 12, 14, 15 - 18, 20
76	Cytosolic phospholipase A2 epsilon	HMDBP07864	Q3MJ16	PLA2G4E	7, 9 - 12, 14, 15 - 18, 20
77	Cytosolic phospholipase A2 zeta	HMDBP07865	Q68DD2	PLA2G4F	7, 9 - 12, 14, 15 - 18, 20
78	ADP-ribosylation factor GTPase-activating protein 1	HMDBP08305	Q8N6T3	ARFGAP1	7, 9 - 12, 14, 15 - 18, 20
79	Cytosolic phospholipase A2 beta	HMDBP09120	P0C869	PLA2G4B	1 - 5, 7, 9 - 12, 14, 15 - 18, 20
80	Phospholipase D1 variant	HMDBP09354	Q59EA4		7, 9 - 12, 14, 15 - 18, 20
81	Phospholipase D6	HMDBP10645	Q8N2A8	PLD6	7, 9 - 12, 14, 15 - 18, 20
82	Neuropathy target esterase	HMDBP10677	Q8IY17	PNPLA6	7, 9 - 12, 14, 15 - 18, 20
83	Apolipoprotein A-V	HMDBP10986	Q6Q788	APOA5	7, 9 - 12, 14, 15 - 18, 20
84	Uteroglobin	HMDBP10987	P11684	SCGB1A1	7, 9 - 12, 14, 15 - 18, 20
88	Pancreatic triacylglycerol lipase	HMDBP00221	P16233	PNLIP	26
89	Hepatic triacylglycerol lipase	HMDBP00226	P11150	LIPC	26
90	Inactive pancreatic lipase-related protein 1	HMDBP00229	P54315	PNLIPRP1	26
91	Patatin-like phospholipase domain-containing protein 3	HMDBP00232	Q9NST1	PNPLA3	26

92	Gastric triacylglycerol lipase	HMDBP00236	P07098	LIPF	26
93	Endothelial lipase	HMDBP00239	Q9Y5X9	LIPG	26
94	Bile salt-activated lipase	HMDBP00241	P19835	CEL	26
95	Diacylglycerol O-acyltransferase 1	HMDBP00243	O75907	DGAT1	26
96	Pancreatic lipase-related protein 2	HMDBP00245	P54317	PNLIPRP2	26
97	Lipoprotein lipase	HMDBP00310	P06858	LPL	26
98	Monoglyceride lipase	HMDBP00314	Q99685	MGLL	26
99	Liver carboxylesterase 1	HMDBP00497	P23141	CES1	26
100	Hormone-sensitive lipase	HMDBP00531	Q05469	LIPE	26
101	Microsomal triglyceride transfer protein large subunit	HMDBP01619	P55157	MTTP	26
102	Protein disulfide-isomerase	HMDBP02802	P07237	P4HB	26
103	2-acylglycerol O-acyltransferase 2	HMDBP03089	Q3SYC2	MOGAT2	26
104	Patatin-like phospholipase domain-containing protein 4	HMDBP03160	P41247	PNPLA4	26
105	Diacylglycerol O-acyltransferase 2	HMDBP04483	Q96PD7	DGAT2	26
106	2-acylglycerol O-acyltransferase 1	HMDBP04645	Q96PD6	MOGAT1	26
107	2-acylglycerol O-acyltransferase 3	HMDBP07284	Q86VF5	MOGAT3	26
108	Phospholipase B1, membrane-associated	HMDBP07301	Q6P1J6	PLB1	1 - 5, 26
109	Glycerol-3-phosphate acyltransferase 3	HMDBP07314	Q53EU6	AGPAT9	26

110	Patatin-like phospholipase domain-containing protein 2	HMDBP07347	Q96AD5	PNPLA2	26
111	Pancreatic lipase-related protein 3	HMDBP10934	Q17RR3	PNLIPRP3	26
112	Perilipin-4	HMDBP10984	Q96Q06	PLIN4	26

[a]HMDBP ID = Human Metabolome Database Protein ID; [b]UniProt ID = Universal Protein resource ID; [c]Protein associated lipids = refer to Table S1 for lipid number designation.

2.3. Results

2.3.1. Lipid profiling and multivariate analysis

The lipids were profiled and processed as described in sections 2.2.4 and 2.2.5 respectively. A total of 35 samples were analyzed in each of +ESI and -ESI modes from PL and NL fractions which were further processed for identification, semi-quantitation, and multivariate analysis. Representative total ion chromatograms (TIC) for both fractions in both modes are shown in Fig. 2.1. Venn plots representing a total of 509 and 506 common features in AD and NCC study subjects respectively for PL fraction, and 341 and 340 common features in AD and NCC study subjects respectively for NL fraction as represented in Fig. 2.2. Of these features, only 498 were common between AD and NCC groups, 8 were unique to NCC and 11 were unique to AD in PL fraction, whereas 327 features were common between AD and NCC groups, 13 were unique to NCC and 14 were unique to AD in NL fraction (Fig. 2.2).

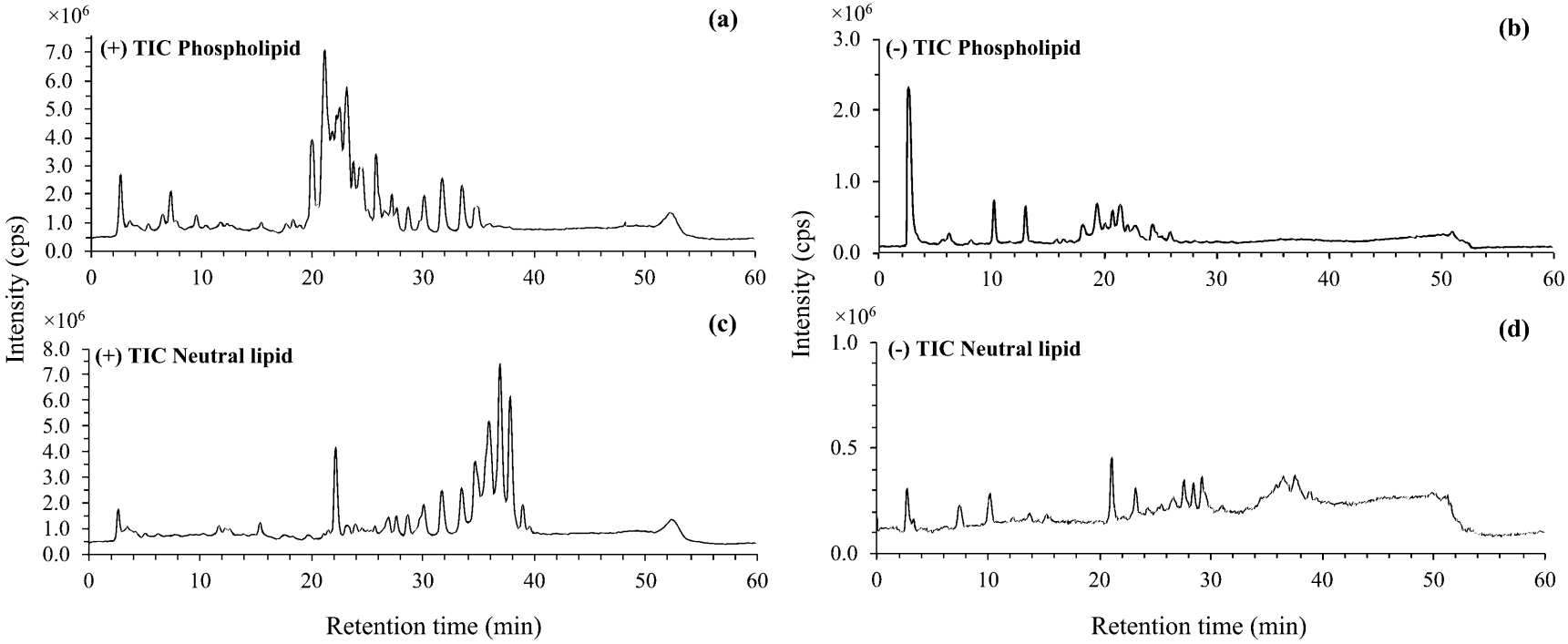

Figure 2.1. Representative total ion chromatograms (TICs) in positive and negative ionization modes of phospholipid fraction (a, b) and neutral lipid fraction (b, d) respectively.

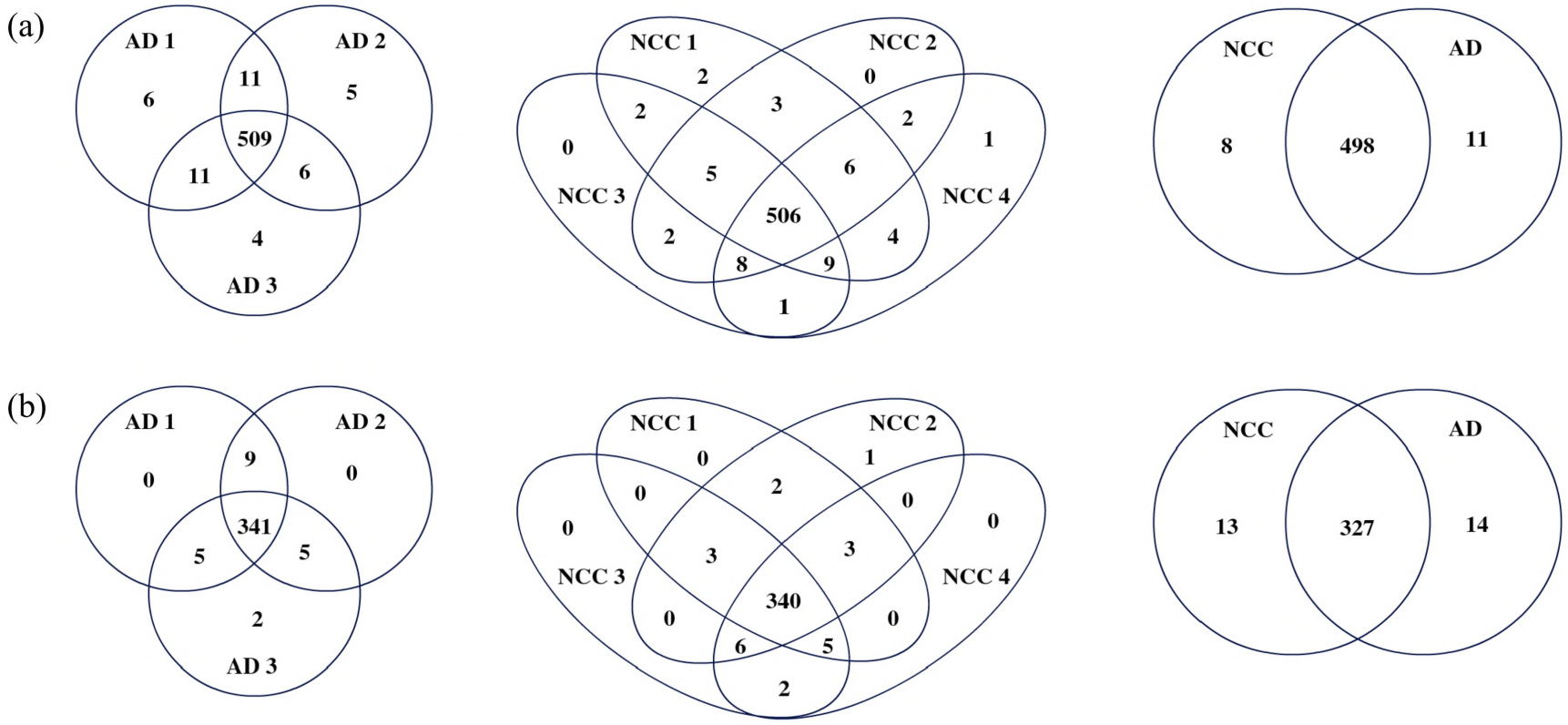

Figure 2.2. Venn plots representing the numbers of the common and unique features within AD, NCC and between AD and NCC study subjects in (a) phospholipid fraction, (b) neutral lipid fraction.

Unsupervised (PCA, without considering the correlation between the independent and dependent variables) and supervised (PLS-DA, considering a correlation between the independent and dependent variables) multivariate analysis performed on the common features between two groups (498 features from PL and 327 features from NL fractions respectively). As in Fig. 2.3, PCA score plots showed a total covariance of 56.4% for PL and 50.7% for NL fractions with a distinct covariance between the two groups for PL fraction. However, the model could not explain the covariance between groups for NL fraction. PLS-DA score plots for PL and NL showed a covariance of 54.1% and 42.2%, respectively, which indicate a distinct covariance between the two groups in both PL and NL fractions. Variable importance of the projections (VIP) scores were calculated for the features contributing the highest variability towards the PLS-DA components. The features with VIP scores of > 1.25 were considered significant (Table 2.4 and 2.5). Further statistical analysis was performed on these common features between two groups to obtain significant features. Though LC-MS data is a continuous gaussian distributed data, for the selection of significant feature a non-parametric, unpaired, Wilcoxon rank-sum *t*-test with false discovery rate (FDR) *p*-value of ≤ 0.05 was chosen due to less number of unpaired samples. A total of 59 significant features were obtained out of which 28 were identified as lipids (Table 2.4) and 31 were not annotated (Table 2.5).

Table 2.4. Measured concentration, fold change values and VIP scores of 28 common identified significant lipids with $p \leq 0.05$ (n = 5)

No	Category	Main Class	Lipid	Mass	t_R (min)	$[\bar{X}]_{NCC}$[a] ± SD (μM)	$[\bar{X}]_{AD}$[b] ± SD (μM)	Fold Change[c]	Regulation	p-value[d]	VIP score[e]
1	GP[f]	LPC[i]	PC (16:0_0:0)	495.3340	6.66	40 ± 1	104 ± 1	0.38	Up	2.53E-04	3.6799
2			PC (18:2_0:0)	519.3368	5.98	19 ± 1	47 ± 1	0.39	Up	1.69E-04	2.5948
3			PC (18:1_0:0)	521.3520	7.06	13.7 ± 0.6	36 ± 1	0.37	Up	1.69E-04	2.2989
4			PC (18:0_0:0)	523.3670	8.72	20.7 ± 0.9	48 ± 1	0.41	Up	2.96E-04	2.4356
5			PC (20:4_0:0)	543.3350	5.90	4.6 ± 0.5	11.9 ± 0.3	0.37	Up	5.59E-04	1.7504
6		PC[j]	PC (O-14:0_18:1)	717.5752	21.41	0.73 ± 0.03	0.43 ± 0.02	1.7	Down	6.48E-04	1.5189
7			PC (15:0_16:0)	719.5880	22.46	0.89 ± 0.02	0.59 ± 0.02	1.5	Down	1.21E-03	1.5176
8			PC(O-16:0_20:5)	765.5710	22.54	5.5 ± 0.2	4.1 ± 0.3	1.3	Down	2.53E-04	1.5632
9			PC (18:4_18:3)	775.5622	22.69	0.79 ± 0.03	0.43 ± 0.01	1.9	Down	1.69E-04	1.5069
10			PC(16:0_20:5)	779.5520	20.24	41.3 ± 0.5	30 ± 1	1.4	Down	1.69E-04	1.9478
11			PC(16:0_20:4)	781.5650	21.52	46.1 ± 0.8	37.4 ± 0.9	1.2	Down	7.56E-04	1.8206
12			PC(18:3_20:5)	801.5340	18.84	15.7 ± 0.7	4.2 ± 0.4	3.7	Down	1.91E-03	1.9305
13			PC (16:0_21:0)	803.5500	19.95	5.3 ± 0.2	4.1 ± 0.1	1.3	Down	2.57E-03	1.5609
14			PC (18:2_20:4)	805.5668	19.85	1.31 ± 0.02	1.0 ± 0.5	1.4	Down	2.98E-03	1.5306
15			PC (16:0_22:6)	805.5602	20.86	7.23 ± 0.08	5.6 ± 0.2	1.3	Down	2.71E-02	1.5589
16			PC (P-18:0_22:6)	817.6020	23.17	1.71 ± 0.08	1.2 ± 0.1	1.5	Down	1.69E-04	1.5409
17			PC(P-18:0/22:4)	821.5396	20.82	24 ± 1	16.0 ± 0.8	1.5	Down	1.57E-04	1.8109
18			PC (18:0_22:6)	833.5970	22.84	8.4 ± 0.2	3.4 ± 0.2	2.5	Down	5.59E-04	1.6891
19			PC (P-20:0/22:6)	845.5413	21.04	5.2 ± 0.2	2.0 ± 0.1	2.6	Down	1.91E-03	1.6378
20			PC(20:3_22:6)	855.5810	21.83	7.3 ± 0.2	3.6 ± 0.2	2.1	Down	1.69E-04	1.6508

21	SL[g]	SM[k]	SM (d18:2/18:0)	728.5880	19.53	9.6 ± 0.1	7.6 ± 0.2	1.3	Down	4.88E-03	1.5962
22			SM (d16:1/22:0)	758.6360	23.22	13.2 ± 0.3	9.8 ± 0.3	1.4	Down	2.66E-04	1.6489
23			SM(d16:1/23:0)	772.6510	24.16	9.0 ± 0.2	8.2 ± 0.2	1.1	Down	1.69E-04	1.5269
24			SM(d16:1/24:1)	784.6480	23.47	13.6 ± 0.3	13.0 ± 0.4	1.0	Down	3.48E-04	1.8203
25		NGSL[l]	GlcCer(d14:1/18:1)	669.5168	35.80	16.5 ± 0.5	11.7 ± 0.8	1.42	Down	9.62E-05	1.5182
26	GL[h]	TG[m]	TG(18:1_18:1_20:5)	904.7545	36.47	20.6 ± 0.8	29 ± 2	0.71	Up	9.62E-05	1.7089
27			TG(18:2_20:2_20:2)	934.7800	34.98	1.15 ± 0.04	3.1 ± 0.3	0.37	Up	8.38E-05	1.3522
28			TG(16:0_20:3_22:0)	940.8290	37.44	34 ± 1	49 ± 4	0.70	Up	9.28E-06	1.9914

[a]$[\bar{X}]_{NCC}$ = mean measured concentration in NCC subjects (n = 4); [b]$[\bar{X}]_{AD}$ = mean measured concentration in AD subjects (n = 3); [c]Fold Change = $[\bar{X}]_{NCC}/[\bar{X}]_{AD}$; [d]*p*-value = false discovery rate adjusted *p*-values; [e]VIP = Variable Importance in Projection score; [f]GP = glycerophospholipids; [g]SL = sphingolipids; [h]GL = glycerolipids; [i]LPC = lysophosphocholines; [j]PC = glycerophosphocholine; [k]SM = sphingomyelins; [l]NGSL = neutral glycosphingolipids; [m]TG = triacylglyceride.

Table 2.5. Measured concentration, fold change values and VIP scores of 31 common unidentified lipids with $p \leq 0.05$

No		Mass	t_R (min)	$[\bar{X}]_{NCC}$[a] ± SD (μM)	$[\bar{X}]_{AD}$[b] ± SD (μM)	Fold Change[c]	Regulation	p-value[d]	VIP score[e]
1	Phospholipid fraction [PL]	492.0114	2.62	3.0 ± 0.6	1.1 ± 0.2	2.9	Down	3.48E-04	1.5962
2		650.6503	26.32	1.2 ± 0.1	1.00 ± 0.05	1.3	Down	4.60E-03	1.5109
3		791.5910	21.24	31 ± 7	13 ± 10	2.4	Down	7.56E-04	2.1609
4		822.6165	23.71	9.5 ± 0.9	6 ± 1	1.5	Down	3.47E-03	1.6245
5		825.5674	23.48	26 ± 3	16 ± 1	1.6	Down	1.04E-03	1.8603
6		837.6048	18.86	31 ± 17	11 ± 1	2.7	Down	1.21E-03	2.2355
7		850.6426	25.14	17 ± 3	12 ± 1	1.4	Down	4.78E-04	1.6901
8		855.6241	26.44	1.3 ± 0.1	0.97 ± 0.08	1.3	Down	5.59E-04	1.5106
9		865.6337	21.05	13 ± 6	5.3 ± 0.2	2.3	Down	4.06E-04	1.7646
10		871.5533	21.87	9 ± 2	3.0 ± 0.5	3.1	Down	1.69E-04	1.7201
11		1027.6232	21.88	1.2 ± 0.3	0.6 ± 0.1	1.9	Down	1.69E-04	1.5397
12	Neutral lipid fraction [NL]	414.2066	3.72	36 ± 2	23 ±2	1.6	Down	2.82E-03	1.8201
13		430.3843	21.62	2.50 ± 0.06	3.3 ± 0.5	0.8	Up	1.41E-02	1.2962
14		487.4321	21.62	4.6 ± 0.1	6.6 ± 0.5	0.7	Up	9.46E-04	1.3607
15		521.5956	21.24	27 ± 2	35 ± 5	0.8	Up	1.79E-03	1.8593
16		535.4360	29.92	2.1 ± 0.1	5.0 ± 0.7	0.4	Up	6.93E-03	1.3991
17		602.5302	25.87	2.1 ± 0.1	1.3 ± 0.5	1.6	Down	5.16E-03	1.2898
18		634.5939	30.26	8.4 ± 0.2	6.6 ± 0.2	1.3	Down	3.18E-02	1.3406
19		687.6016	34.06	20.1 ± 0.7	53 ± 11	0.4	Up	1.06E-02	2.2963
20		688.5628	36.97	2.4 ± 0.1	4.0 ± 0.5	0.6	Up	9.21E-03	1.3412

21	690.5626	30.26	6.7 ± 0.2	16 ± 14	0.4	Up	6.93E-03	1.4201
22	708.5319	34.06	9.6 ± 0.5	24 ± 6	0.4	Up	1.82E-04	2.1723
23	710.5440	35.29	7.1 ± 0.5	11 ± 1	0.7	Up	4.14E-02	1.4682
24	833.6801	26.78	0.50 ± 0.07	2.6 ± 2.8	0.2	Up	1.22E-02	1.2814
25	886.7493	38.93	7.1 ± 0.1	8 ± 1	0.9	Up	5.82E-04	1.3592
26	907.3869	26.24	3.6 ± 0.2	4.0 ± 0.5	0.9	Up	4.14E-02	1.2816
27	927.8272	37.55	13.9 ± 0.5	7.1 ± 0.1	2.0	Down	2.13E-02	1.6094
28	1006.8341	41.14	1.4 ± 0.1	0.200 ± 0.007	6.9	Down	3.18E-02	1.3202
29	1096.3260	28.01	15.0 ± 0.9	23 ± 3	0.7	Up	2.13E-04	1.7889
30	1170.3461	29.26	35 ± 2	55 ± 7	0.6	Up	2.43E-03	2.6512
31	1688.4848	38.06	14 ± 1	5.4 ± 0.4	2.6	Down	1.82E-04	1.6976

[a]$[\bar{X}]_{NCC}$ = mean measured concentration in NCC subjects (n = 4); [b]$[\bar{X}]_{AD}$ = mean measured concentration in AD subjects (n = 3); [c]Fold Change = $[\bar{X}]_{NCC}/[\bar{X}]_{AD}$; [d]*p*-value = false discovery rate adjusted *p*-values; [e]VIP = Variable Importance in Projection score.

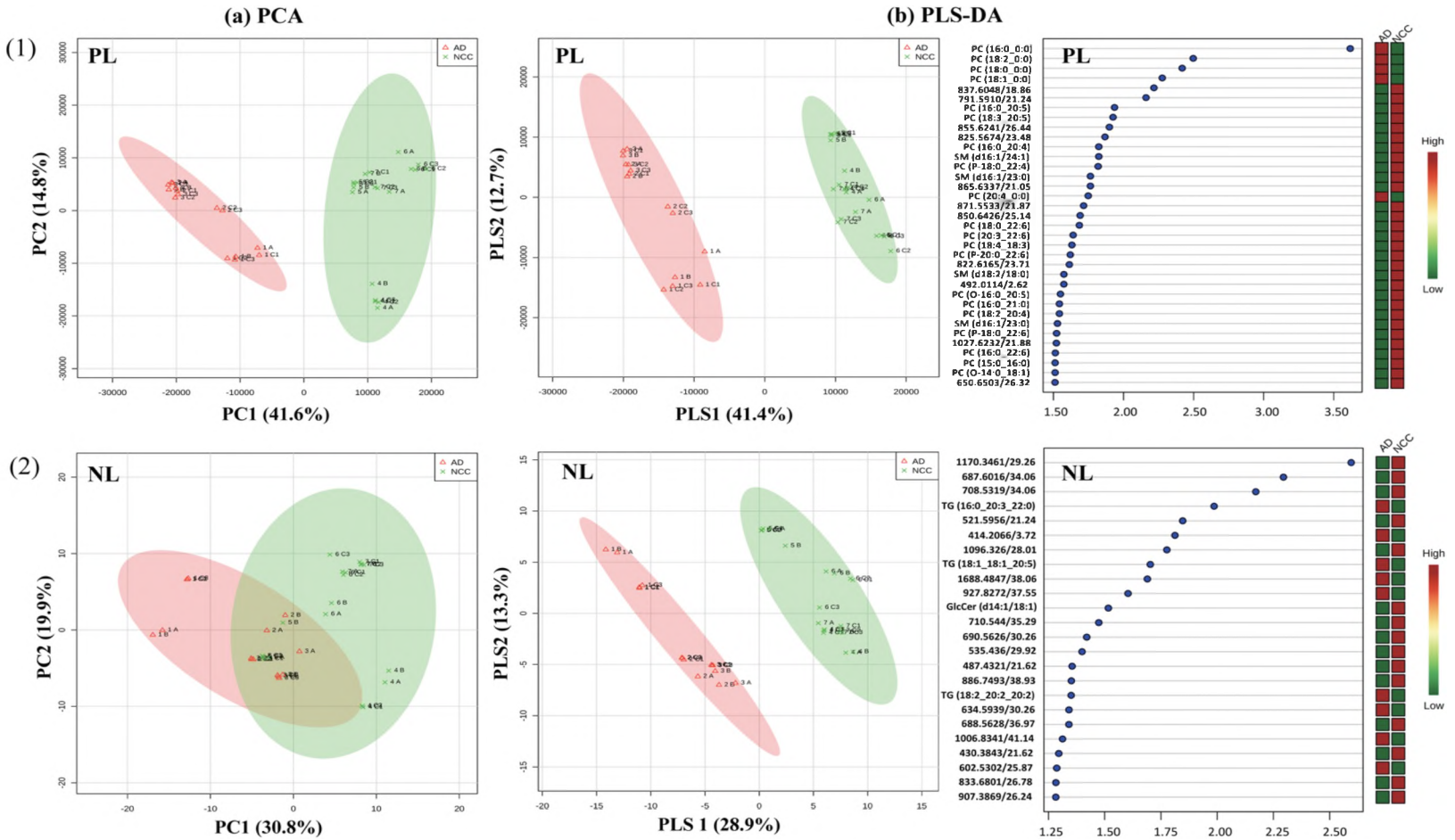

Figure 2.3. (a) PCA score plots and (b) PLS-DA score plots with VIP scores of AD and NCC study subjects. (1) phospholipid fraction, (2) neutral lipid fraction of the common features.

2.3.2. Identification of lipids

The identification of features was performed as per the procedure described in Section 2.2.6. A total of 148 and 108 lipid species were annotated in PL and NL fractions respectively (Table 2.6). In general, structural characterization of lipid requires identification of head group, *sn*-1 and *sn*-2 fatty acyl chains. In this study, the identification of the lipid against the database doesn't provide the information on position of the fatty acyl chain on glycerol backbone, and the location of the double bonds in the fatty acids. Therefore lipids are represented in the format PC(18:3_20:5) instead of PC(18:3/20:5). "_" indicates the uncertainty in the position of fatty acids on glycerol backbone.

Table 2.6. The total lipid identified from the phospho and neutral lipid fractions in AD and NCC study subjects.

No	Lipid Name	Observed Mass	t_R (min)	Precursor ion, m/z	ESI Mode	Category	Main Class
1	LacCer(d18:1_16:0)	861.6231	18.55	862.6283 $[M+H]^+$; 860.6156 $[M-H]^-$	P[h], N[i]	Sphingolipids [SP]	Neutral glycosphingolipids
2	(3'-sulfo)Galbeta-Cer(d18:1_24:0)	891.6520	21.83	892.6585 $[M+H]^+$	P	Sphingolipids [SP]	Acidic glycosphingolipids
3	CL(1'-[18:1_20:4],3'-[20:0_20:0])	1539.1330	20.11	1540.1379 $[M+H]^+$	P	Glycerophospholipids [GP]	Cardiolipin
4	CL(1'-[20:0_20:0],3'-[20:4_20:4])	1561.0936	20.04	1562.1198 $[M+H]^+$	P	Glycerophospholipids [GP]	Cardiolipin
5	PA(14:0/0:0) (IS)	382. 1089	4.42	383. 3467 $[M+H]^+$; 404.1946 $[M+Na]^+$	P	Glycerophospholipids [GP]	PA[a]
6	PC(13:0/0:0) (IS)	453.2887	4.45	454.2841 $[M+H]^+$; 452.1989 $[M-H]^-$	P, N	Glycerophospholipids [GP]	PC[b]
7	PC(16:1_0:0)	493.3170	5.42	494.3265 $[M+H]^+$; 492.2998 $[M-H]^-$	P, N	Glycerophospholipids [GP]	PC
8	PC(16:0_0:0)	495.3340	6.66	496.3425 $[M+H]^+$	P	Glycerophospholipids [GP]	PC
9	PC(18:3_0:0)	517.3215	6.66	518.3245 $[M+H]^+$; 516.3102 $[M-H]^-$	P, N	Glycerophospholipids [GP]	PC
10	PC(18:2_0:0)	519.3368	5.98	520.3328 $[M+H]^+$	P	Glycerophospholipids [GP]	PC
11	PC(18:1_0:0)	521.3520	7.06	522.3585 $[M+H]^+$	P	Glycerophospholipids [GP]	PC
12	PC(O-16:0_2:0)	523.3646	8.22	524.3747 $[M+H]^+$	P	Glycerophospholipids [GP]	PC

13	PC(0:0_18:0)	523.3670	8.72	524.3743 $[M+H]^+$; 522.3240 $[M-H]^-$	P, N	Glycerophospholipids [GP]	PC
14	PC(20:5_0:0)	541.3200	5.15	542.3250 $[M+H]^+$	P	Glycerophospholipids [GP]	PC
15	PC(20:4_0:0)	543.3350	5.90	544.3402 $[M+H]^+$; 542.3019 $[M-H]^-$	P, N	Glycerophospholipids [GP]	PC
16	PC(20:3_0:0)	545.3510	6.64	546.3564 $[M+H]^+$	P	Glycerophospholipids [GP]	PC
17	PC(12:0_18:0)	705.5360	19.07	706.5416 $[M+H]^+$	P	Glycerophospholipids [GP]	PC
18	PC (O-14:0_18:1)	717.5752	21.41	718.5816 $[M+H]^+$; 716.5545 $[M-H]^-$	P, N	Glycerophospholipids [GP]	PC
19	PC(O-14:0_18:0)	719.5880	22.46	720.5930 $[M+H]^+$	P	Glycerophospholipids [GP]	PC
20	PC(14:0_18:2)	729.5360	18.02	730.5425 $[M+H]^+$	P	Glycerophospholipids [GP]	PC
21	PC(16:0_16:1)	731.5510	19.48	732.5574 $[M+H]^+$	P	Glycerophospholipids [GP]	PC
22	PC(10:0_22:0)	733.5670	21.16	734.5732 $[M+H]^+$	P	Glycerophospholipids [GP]	PC
23	PC(O-16:0_18:3)	741.5720	21.21	742.5778 $[M+H]^+$; 740. 5536 $[M-H]^-$	P, N	Glycerophospholipids [GP]	PC
24	PC(15:0_18:2)	743.5510	19.16	744.5568 $[M+H]^+$	P	Glycerophospholipids [GP]	PC
25	PC(15:0_18:1)	745.5670	20.54	746.5728 $[M+H]^+$	P	Glycerophospholipids [GP]	PC
26	PC(O-16:1_18:0)	745.6040	22.68	746.6096 $[M+H]^+$; 744.5816 $[M-H]^-$	P, N	Glycerophospholipids [GP]	PC

27	PC(14:0_20:5)	751.5180	18.02	752.5242 $[M+H]^+$	P	Glycerophospholipids [GP]	PC
28	PC(14:0_20:4)	753.5340	19.48	754.5396 $[M+H]^+$	P	Glycerophospholipids [GP]	PC
29	PC(16:0_18:3)	755.5480	21.21	756.5577 $[M+H]^+$	P	Glycerophospholipids [GP]	PC
30	PC(16:1_18:2)	755.5510	19.11	756.5582 $[M+H]^+$	P	Glycerophospholipids [GP]	PC
31	PC(16:0_18:2)	757.5670	20.19	758.5728 $[M+H]^+$	P	Glycerophospholipids [GP]	PC
32	PC(16:0_18:1)	759.5820	21.52	760.5800 $[M+H]^+$	P	Glycerophospholipids [GP]	PC
33	PC(16:0_18:0)	761.6000	23.17	762.6053 $[M+H]^+$; 760.5897 $[M-H]^-$	P, N	Glycerophospholipids [GP]	PC
34	PC(O-16:0_20:5)	765.5710	22.54	766.5782 $[M+H]^+$; 764.5620 $[M-H]^-$	P, N	Glycerophospholipids [GP]	PC
35	PC(18:2_17:2)	767.5470	19.53	768.5572 $[M+H]^+$	P	Glycerophospholipids [GP]	PC
36	PC(15:0_20:4)	767.5510	18.98	768.5572 $[M+H]^+$	P	Glycerophospholipids [GP]	PC
37	PC(O-16:0_20:4)	767.5530	22.46	768.5939 $[M+H]^+$; 766.5432 $[M-H]^-$	P, N	Glycerophospholipids [GP]	PC
38	PC(P-16:0_20:3)	767.5880	21.79	768.5939 $[M+H]^+$; 766.5699 $[M-H]^-$	P, N	Glycerophospholipids [GP]	PC
39	PC(O-16:0_20:3)	769.6070	23.17	770.6091 $[M+H]^+$; 768.5964 $[M-H]^-$	P, N	Glycerophospholipids [GP]	PC
40	PC(17:0_18:2)	771.5228	21.23	772.5898 $[M+H]^+$	P	Glycerophospholipids [GP]	PC

41	PC(13:0_22:2)	771.5230	21.21	772.5891 $[M+H]^+$	P	Glycerophospholipids [GP]	PC
42	PC(O-18:0_18:2)	771.6187	24.45	772.6254 $[M+H]^+$, 770.6002 $[M-H]^-$	P, N	Glycerophospholipids [GP]	PC
43	PC(O-16:0_20:2)	771.6200	23.30	772.6255 $[M+H]^+$	P	Glycerophospholipids [GP]	PC
44	PC(17:0_18:1)	773.5990	22.50	774.6043 $[M+H]^+$	P	Glycerophospholipids [GP]	PC
45	PC(16:1_20:5)	777.5330	18.60	778.5392 $[M+H]^+$	P	Glycerophospholipids [GP]	PC
46	PC(18:3_18:3)	777.5330	19.11	778.5394 $[M+H]^+$	P	Glycerophospholipids [GP]	PC
47	PC(18:2_18:3)	779.5490	20.24	780.5552 $[M+H]^+$; 778.5209 $[M-H]^-$	P, N	Glycerophospholipids [GP]	PC
48	PC(16:0_20:5)	779.5520	18.84	780.5552 $[M+H]^+$	P	Glycerophospholipids [GP]	PC
49	PC(16:0_20:4)	781.5650	21.52	782.5711 $[M+H]^+$	P	Glycerophospholipids [GP]	PC
50	PC(18:2_18:2)	781.5650	19.16	782.5727 $[M+H]^+$	P	Glycerophospholipids [GP]	PC
51	PC(18:1_18:3)	781.5670	19.99	782.5726 $[M+H]^+$; 780.5478 $[M-H]^-$	P, N	Glycerophospholipids [GP]	PC
52	PC(18:1_18:2)	783.5820	20.80	784.5800 $[M+H]^+$	P	Glycerophospholipids [GP]	PC
53	PC(18:0_18:2)	785.5990	22.18	786.6049 $[M+H]^+$	P	Glycerophospholipids [GP]	PC
54	PC(18:0_18:1)	787.6150	23.43	788.6208 $[M+H]^+$	P	Glycerophospholipids [GP]	PC
55	PC(O-16:0_22:5)	793.6040	22.97	794.6097 $[M+H]^+$; 792.5986 $[M-H]^-$	P, N	Glycerophospholipids [GP]	PC

56	PC(17:0_20:4)	795.5850	21.06	796.5892 $[M+H]^+$	P	Glycerophospholipids [GP]	PC
57	PC(O-18:0_20:4)	795.6190	23.17	796.6247 $[M+H]^+$; 800.5674 $[M-H]^-$	P, N	Glycerophospholipids [GP]	PC
58	PC(18:3_20:5)	801.5340	18.84	802.5403 $[M+H]^+$	P	Glycerophospholipids [GP]	PC
59	PC(18:4_20:4)	801.6030	19.16	802.5403 $[M+H]^+$	P	Glycerophospholipids [GP]	PC
60	PC(16:1_22:5)	803.5500	19.95	804.5551 $[M+H]^+$	P	Glycerophospholipids [GP]	PC
61	PC(16:0_22:6)	805.5602	20.86	806.5709 $[M+H]^+$	P	Glycerophospholipids [GP]	PC
62	PC(18:2_20:4)	805.5668	19.85	806.5715 $[M+H]^+$	P	Glycerophospholipids [GP]	PC
63	PC(16:1_22:5)	805.5679	19.22	806.5734 $[M+H]^+$	P	Glycerophospholipids [GP]	PC
64	PC(16:0_22:5)	807.5810	22.24	808.5868 $[M+H]^+$, 806.5629 $[M-H]^-$	P, N	Glycerophospholipids [GP]	PC
65	PC(18:1_20:4)	807.5820	20.54	808.5882 $[M+H]^+$	P	Glycerophospholipids [GP]	PC
66	PC(18:0_20:5)	807.5830	22.33	808.5869 $[M+H]^+$	P	Glycerophospholipids [GP]	PC
67	PC(18:0_20:4)	809.5970	23.43	810.6028 $[M+H]^+$	P	Glycerophospholipids [GP]	PC
68	PC(16:0_22:4)	809.5990	22.00	810.6031 $[M+H]^+$; 808.5790 $[M-H]^-$	P, N	Glycerophospholipids [GP]	PC
69	PC(18:2_20:1)	811.5536	22.56	812.6118 $[M+H]^+$	P	Glycerophospholipids [GP]	PC
70	PC(18:0_20:3)	811.6096	22.87	812.6118 $[M+H]^+$	P	Glycerophospholipids [GP]	PC

71	PC(18:0_20:2)	813.6310	23.85	814.6273 $[M+H]^+$	P	Glycerophospholipids [GP]	PC
72	PC(P-18:0_22:6)	817.6020	23.17	818.6079 $[M+H]^+$; 816.5904 $[M-H]^-$	P, N	Glycerophospholipids [GP]	PC
73	PC(19:0/19:0) (IS)	817.6615	26.42	818.6674 [M+H]+; 816.6430 [M-H]-	P, N	Glycerophospholipids [GP]	PC
74	PC(P-18:0_22:4)	821.6350	20.82	822.6414 [M+H]+; 820.6230 [M-H]-	P, N	Glycerophospholipids [GP]	PC
75	PC(17:0_22:4)	823.6599	25.81	824.6210 $[M+H]^+$	P	Glycerophospholipids [GP]	PC
76	PC(18:3_22:6)	827.5500	19.78	828.5558 $[M+H]^+$	P	Glycerophospholipids [GP]	PC
77	PC(18:2_22:6)	829.5650	20.54	830.5717 $[M+H]^+$	P	Glycerophospholipids [GP]	PC
78	PC(20:4_20:4)	829.5660	18.72	830.5709 $[M+H]^+$	P	Glycerophospholipids [GP]	PC
79	PC(18:1_22:6)	831.5810	22.00	832.5872 $[M+H]^+$	P	Glycerophospholipids [GP]	PC
80	PC(18:2_22:5)	831.5820	20.50	832.5884 $[M+H]^+$; 830.5640 $[M-H]^-$	P, N	Glycerophospholipids [GP]	PC
81	PC(18:3_22:4)	831.6480	22.54	832.5866 $[M+H]^+$	P	Glycerophospholipids [GP]	PC
82	PC(18:0_22:6)	833.5970	22.84	834.6023 $[M+H]^+$	P	Glycerophospholipids [GP]	PC
83	PC(18:0_22:5)	835.6069	22.46	836.6182 $[M+H]^+$	P	Glycerophospholipids [GP]	PC
84	PC(20:2_20:3)	835.6132	23.90	836.6182 $[M+H]^+$; 834.5924 $[M-H]^-$	P, N	Glycerophospholipids [GP]	PC

85	PC(18:0_22:3)	839.6430	26.37	840.6499 $[M+H]^+$	P	Glycerophospholipids [GP]	PC
86	PC(20:3_22:6)	855.5810	21.83	856.5865 $[M+H]^+$	P	Glycerophospholipids [GP]	PC
87	PC(20:2_22:6)	857.5980	22.50	858.6026 $[M+H]^+$	P	Glycerophospholipids [GP]	PC
88	PC(20:1_22:6)	859.6074	23.45	860.6168 $[M+H]^+$	P	Glycerophospholipids [GP]	PC
89	PC(O-22:2_22:3)	877.7010	26.42	878.7051 $[M+H]^+$; 876.6932 $[M-H]^-$	P, N	Glycerophospholipids [GP]	PC
90	PE(14:0/0:0) (IS)	425.2579	6.74	426. 2627 $[M+H]^+$; 424.3098 $[M-H]^-$	P, N	Glycerophospholipids [GP]	PE[c]
91	PE(16:0_0:0)	453.2862	6.83	545.3256 $[M+H]^+$	P	Glycerophospholipids [GP]	PE
92	PE(18:2_0:0)	477.2850	6.17	478.3001 $[M+H]^+$	P	Glycerophospholipids [GP]	PE
93	PE(18:1_0:0)	479.3379	7.54	480.4586 $[M+H]^+$	P	Glycerophospholipids [GP]	PE
94	PE(24:6_0:0)	553.3896	6.66	554.3900 $[M+H]^+$	P	Glycerophospholipids [GP]	PE
95	PE(15:0/15:0) (IS)	663.4881	19.45	664.4939 $[M+H]^+$; 662.4532 $[M-H]^-$	P, N	Glycerophospholipids [GP]	PE
96	PE (p-16:0_20:5)	721.5051	21.19	722.5162 $[M+H]^+$	P	Glycerophospholipids [GP]	PE
97	PE (p-16:0_20:4)	723.5199	21.44	724.5269 $[M+H]^+$; 722.5258 $[M-H]^-$	P, N	Glycerophospholipids [GP]	PE
98	PE (p-18:1_18:2)	725.5385	22.01	726.5432 $[M+H]^+$	P	Glycerophospholipids [GP]	PE

99	PE (p-18:1_18:1)	727.5519	23.63	728.5634 $[M+H]^+$	P	Glycerophospholipids [GP]	PE
100	PE (16:0_20:5)	737.5004	20.82	738.5130 [M+H]+; 736.4986 [M-H]-	P, N	Glycerophospholipids [GP]	PE
101	PE(16:0_20:4)	739.5223	21.14	738.5178 [M-H]-	P	Glycerophospholipids [GP]	PE
102	PE(18:0_18:2)	743.5476	19.17	742.5482 [M-H]-	P, N	Glycerophospholipids [GP]	PE
103	PE (p-16:0_22:6)	747.5234	20.67	748.5426 $[M+H]^+$; 746.5134 $[M-H]^-$	P, N	Glycerophospholipids [GP]	PE
104	PE(O-38:6) OR PE(P-38:5)	749.5359	21.82	750.5569 $[M+H]^+$	P	Glycerophospholipids [GP]	PE
105	PE(P-18:0_20:4)	751.5575	23.41	752.5627 $[M+H]^+$; 750.5541 $[M-H]^-$	P, N	Glycerophospholipids [GP]	PE
106	PE(16:0_22:6)	763.5872	19.15	762.5175 $[M-H]^-$	P, N	Glycerophospholipids [GP]	PE
107	PE(18:0_20:4)	767.5559	21.59	766.5491 $[M-H]^-$	N	Glycerophospholipids [GP]	PE
108	PE (p-18:1_22:6)	773.5315	23.41	774.5430 {$M+H]^+$	P	Glycerophospholipids [GP]	PE
109	PE (p-18:0_22:6)	775.5518	23.22	776.5701 $[M+H]^+$	P	Glycerophospholipids [GP]	PE
110	PE (18:2_22:6)	787.5213	18.20	788.5421 $[M+H]^+$	P	Glycerophospholipids [GP]	PE
111	PE(18:0_22:6)	791.5468	21.43	790.5536 $[M-H]^-$	N	Glycerophospholipids [GP]	PE
112	PE(19:0_22:6)	805.5537	17.86	806.5729 $[M+H]^+$	P	Glycerophospholipids [GP]	PE

113	PE(19:0_22:6)	805.5537	17.86	806.5704 $[M+H]^+$	P	Glycerophospholipids [GP]	PE
114	PG(14:0/0:0) (IS)	456.2727	4.46	457.2488 $[M+H]^+$; 478.2310 $[M+Na]^+$; 455.2016 $[M-H]^-$	P, N	Glycerophospholipids [GP]	PG[d]
115	PG(17:0/17:0) (IS)	750.9856	20.50	749.5643 $[M-H]^-$; 773.6026 $[M+Na]^+$	P, N	Glycerophospholipids [GP]	PG
116	PG(17:0_22:0)	820.621	20.73	819.6072 $[M-H]^-$	N	Glycerophospholipids [GP]	PG
117	PG(21:0_20:3)	842.6098	18.35	841.5879 $[M-H]^-$	N	Glycerophospholipids [GP]	PG
118	PG(19:0_22:2)	844.6209	20.05	843.6060 $[M-H]^-$	N	Glycerophospholipids [GP]	PG
119	PS(17:1/0:0) (IS)	509.3494	7.64	508.3126 $[M-H]^-$	N	Glycerophospholipids [GP]	PG
120	PS(22:1_0:0)	579.3545	5.57	578.354 $[M-H]^-$	N	Glycerophospholipids [GP]	PS[e]
121	PS(22:0_0:0)	581.3709	6.64	580.3688 $[M-H]^-$	N	Glycerophospholipids [GP]	PS
122	PS(14:0/14:0) (IS)	679.3678	18.08	678.4424 $[M-H]^-$			
123	PS(16:0_20:0)	791.5863	18.73	790.5674 $[M-H]^-$	N	Glycerophospholipids [GP]	PS
124	PS(16:1_22:1)	815.5684	17.73	814.5684 $[M-H]^-$	N	Glycerophospholipids [GP]	PS
125	PS(22:1_16:0)	817.5839	19.39	816.5903 $[M-H]^-$	N	Glycerophospholipids [GP]	PS
126	PS(22:0_16:0)	819.6134	20.73	818.6038 $[M-H]^-$	N	Glycerophospholipids [GP]	PS
127	PS(20:0_20:3)	841.5860	18.35	840.5849 $[M-H]^-$	N	Glycerophospholipids [GP]	PS

128	PS(18:2_22:1)	841.58345	19.21	840.5868 $[M-H]^-$	N	Glycerophospholipids [GP]	PS
129	PS(18:1_22:2)	841.6001	19.23	840.5905 $[M-H]^-$	N	Glycerophospholipids [GP]	PS
130	PS(18:1_22:1)	843.6017	20.05	842.6036 $[M-H]^-$	N	Glycerophospholipids [GP]	PS
131	PS(18:2_22:0)	843.5989	19.76	842.6058 $[M-H]^-$	N	Glycerophospholipids [GP]	PS
132	PS(18:0_22:1)	845.6378	21.43	844.6227 $[M-H]^-$	N	Glycerophospholipids [GP]	PS
133	PS(22:0_18:0)	847.6315	22.76	846.6368 $[M-H]^-$	N	Glycerophospholipids [GP]	PS
134	PS(20:5_22:0)	865.5840	19.07	864.5900 $[M-H]^-$	N	Glycerophospholipids [GP]	PS
135	PS(20:4_22:0)	867.6009	19.81	866.6028 $[M-H]^-$	N	Glycerophospholipids [GP]	PS
136	PS(20:1_22:2)	869.6257	21.26	868.6227 $[M-H]^-$	N	Glycerophospholipids [GP]	PS
137	PS(20:1_22:1)	871.6403	22.12	870.6337 $[M-H]^-$	N	Glycerophospholipids [GP]	PS
138	PS(22:2_22:2)	895.6419	21.73	894.6337 $[M-H]^-$	N	Glycerophospholipids [GP]	PS
139	SM(d18:1_14:0)	674.5420	16.57	675.5476 $[M+H]^+$	P	Sphingolipids [SP]	Phosphosphingolipids
140	SM(d16:1_17:0)	688.5570	17.81	689.5628 $[M+H]^+$	P	Sphingolipids [SP]	Phosphosphingolipids
141	SM(d18:2_16:0)	700.4060	21.16	701.5633 $[M+H]^+$	P	Sphingolipids [SP]	Phosphosphingolipids
142	SM(d18:1_16:0)	702.5720	18.93	703.5784 $[M+H]^+$	P	Sphingolipids [SP]	Phosphosphingolipids
143	SM(d18:0_16:0)	704.5880	19.82	705.5942 $[M+H]^+$	P	Sphingolipids [SP]	Phosphosphingolipids

144	SM(d18:1_18:1)	728.5880	19.53	729.5943 $[M+H]^+$	P	Sphingolipids [SP]	Phosphosphingolipids
145	SM(d18:1_18:0)	730.6030	21.16	731.6096 $[M+H]^+$	P	Sphingolipids [SP]	Phosphosphingolipids
146	SM(d18:2_20:0)	756.6190	21.76	757.626 $[M+H]^+$	P	Sphingolipids [SP]	Phosphosphingolipids
147	SM(d16:1_22:1)	756.6470	22.88	757.6255 $[M+H]^+$	P	Sphingolipids [SP]	Phosphosphingolipids
148	SM(d16:1_22:0)	758.6360	23.22	759.6417 $[M+H]^+$	P	Sphingolipids [SP]	Phosphosphingolipids
149	SM(d16:1_23:0)	772.6510	24.16	773.657 $[M+H]^+$	P	Sphingolipids [SP]	Phosphosphingolipids
150	SM(d18:1_22:1)	784.6480	23.47	785.6572 $[M+H]^+$	P	Sphingolipids [SP]	Phosphosphingolipids
151	SM(d18:1_22:0)	786.6660	24.97	787.6730 $[M+H]^+$	P	Sphingolipids [SP]	Phosphosphingolipids
152	SM(d18:0_22:0)	788.6812	25.69	789.6811 $[M+H]^+$	P	Sphingolipids [SP]	Phosphosphingolipids
153	SM(d17:1_24:1)	798.6670	24.47	799.6729 $[M+H]^+$	P	Sphingolipids [SP]	Phosphosphingolipids
154	SM(d16:1_25:0)	800.6820	25.74	801.6882 $[M+H]^+$	P	Sphingolipids [SP]	Phosphosphingolipids
155	SM(d18:2_24:1)	810.6060	24.11	811.6725 $[M+H]^+$	P	Sphingolipids [SP]	Phosphosphingolipids
156	SM(d18:1_24:1)	812.6820	25.01	813.6893 $[M+H]^+$	P	Sphingolipids [SP]	Phosphosphingolipids
157	SM(d18:1_24:0)	814.6979	26.55	815.7043 $[M+H]^+$	P	Sphingolipids [SP]	Phosphosphingolipids
158	SM(d17:1_26:1)	826.6911	25.51	827.7037 $[M+H]^+$	P	Sphingolipids [SP]	Phosphosphingolipids
159	SM(d18:1_25:0)	828.7061	27.02	829.7194 $[M+H]^+$	P	Sphingolipids [SP]	Phosphosphingolipids

160	Cer(d18:1/17:0) (IS)	551.5320	23.76	552.5381 $[M+H]^+$	P	Sphingolipids [SP]	Ceramides
161	Cer(d18:1/24:0)	649.6420	29.65	650.6535 $[M+H]^+$	P	Sphingolipids [SP]	Ceramides
162	GlcCer(d14:1/18:1)	669.5168	35.80	670.5294 $[M+H]^+$, 687.5567 $[M+NH4]^+$	P	Sphingolipids [SP]	Neutral glycosphingolipids
163	DG(16:0_18:2_0:0)	592.5099	23.76	593.5165 $[M+H]^+$, 610.5438 $[M+NH4]^+$	P	Glycerolipids [GL]	DG[f]
164	DG(18:1_16:0_0:0)	594.5285	26.63	595.5329 $[M+H]^+$, 612.5594 $[M+NH4]^+$	P	Glycerolipids [GL]	DG
165	DG(18:1_18:1_0:0)	620.5412	26.87	621.5482 $[M+H]^+$, 638.5755 $[M+NH4]^+$	P	Glycerolipids [GL]	DG
166	DG(18:1_18:2_0:0)	618.5299	25.77	619.5324 $[M+H]^+$, 636.5597 $[M+NH4]^+$	P	Glycerolipids [GL]	DG
167	DG(18:1_20:5_0:0)	640.5090	25.77	641.5209 $[M+H]^+$	P	Glycerolipids [GL]	DG
168	DG(19:0/19:0/0:0) (IS)	652.6090	31.61	653.6104 $[M+H]^+$, 670.6377 $[M+NH4]^+$	P	Glycerolipids [GL]	DG
169	TG(12:0_16:1_18:1)	774.6744	34.40	775.6891 $[M+H]^+$, 792.7164 $[M+NH4]^+$	P	Glycerolipids [GL]	TG[g]
170	TG(13:0_19:0_19:1)	846.7695	34.84	847.7630 $[M+H]^+$	P	Glycerolipids [GL]	TG
171	TG(14:0_14:0_18:1)	776.6915	35.67	777.7054 $[M+H]^+$, 794.7327 $[M+NH4]^+$	P	Glycerolipids [GL]	TG
172	TG(14:0_16:0_16:0)	778.7096	36.87	779.7215 $[M+H]^+$, 796.7488 $[M+NH4]^+$	P	Glycerolipids [GL]	TG

173	TG(14:0_16:0_18:1)	804.7289	36.12	805.7377 $[M+H]^+$, 822.7650 $[M+NH4]^+$	P	Glycerolipids [GL]	TG
174	TG(14:0_16:0_19:0)	820.7540	36.95	821.7477 $[M+H]^+$	P	Glycerolipids [GL]	TG
175	TG(14:0_16:1_18:2)	800.6920	34.59	801.7055 $[M+H]^+$, 818.7328 $[M+NH4]^+$	P	Glycerolipids [GL]	TG
176	TG(14:0_17:0_22:1)	874.7993	35.33	875.7923 $[M+H]^+$	P	Glycerolipids [GL]	TG
177	TG(14:0_18:1_18:2)	828.7211	35.99	829.7378 [M+H]+, 846.7651 [M+NH4]+	P	Glycerolipids [GL]	TG
178	TG(14:0_18:2_20:5)	848.6930	34.94	849.7046 $[M+H]^+$	P	Glycerolipids [GL]	TG
179	TG(14:0_20:0_20:0)	890.8140	38.09	891.8223 $[M+H]^+$	P	Glycerolipids [GL]	TG
180	TG(14:0_21:0_22:6)	920.7898	34.43	921.7842 [M+H]+, 938.8115 $[M+NH4]^+$	P	Glycerolipids [GL]	TG
181	TG(14:0_22:0_22:4)	938.8302	35.51	939.8253 $[M+H]^+$	P	Glycerolipids [GL]	TG
182	TG(14:1_20:1_22:1)	912.7970	36.19	913.809 $[M+H]^+$	P	Glycerolipids [GL]	TG
183	TG(15:0_15:0_18:2)	802.7091	35.84	803.7165 $[M+H]^+$, 820.7438 $[M+NH4]^+$	P	Glycerolipids [GL]	TG
184	TG(15:0_15:0_20:5)	824.6940	35.80	825.6992 $[M+H]^+$	P	Glycerolipids [GL]	TG
185	TG(15:0_16:0_18:1)	818.7389	37.49	819.7524 $[M+H]^+$, 836.7797 $[M+NH4]^+$	P	Glycerolipids [GL]	TG

186	TG(15:0_17:1_17:1)	816.7218	36.48	817.7321 $[M+H]^+$, 834.7594 $[M+NH4]^+$	P	Glycerolipids [GL]	TG
187	TG(15:0_18:1_18:2)	842.7389	36.62	843.7541 $[M+H]^+$, 860.7814 $[M+NH4]^+$	P	Glycerolipids [GL]	TG
188	TG(15:1_17:0_19:1)	844.7589	33.61	845.7476 $[M+H]^+$	P	Glycerolipids [GL]	TG
189	TG(15:1_18:0_19:0)	860.7876	35.55	861.7787 $[M+H]^+$	P	Glycerolipids [GL]	TG
190	TG(15:1_18:1_20:3)	866.7325	38.41	867.7597 $[M+H]^+$, 884.787 $[M+NH4]^+$	P	Glycerolipids [GL]	TG
191	TG(15:1_18:1_20:4)	864.7239	37.34	865.7432 $[M+H]^+$, 882.7705 $[M+NH4]^+$	P	Glycerolipids [GL]	TG
192	TG(15:1_19:1_21:0)	900.8192	36.38	901.8099 $[M+H]^+$	P	Glycerolipids [GL]	TG
193	TG(16:0_16:0_18:0)	834.7490	35.63	835.759 $[M+H]^+$	P	Glycerolipids [GL]	TG
194	TG(16:0_16:0_18:1)	832.7571	38.05	833.7677 $[M+H]^+$, 850.795 $[M+NH4]^+$	P	Glycerolipids [GL]	TG
195	TG(16:0_16:0_20:0)	862.7800	36.95	863.7988 $[M+H]^+$	P	Glycerolipids [GL]	TG
196	TG(16:0_16:0_20:1)	860.7878	39.24	861.7865 $[M+H]^+$, 878.8138 $[M+NH4]^+$	P	Glycerolipids [GL]	TG
197	TG(16:0_16:0_20:5)	852.7217	36.01	853.7304 $[M+H]^+$	P	Glycerolipids [GL]	TG
198	TG(16:0_16:0_21:0)	876.8193	37.33	877.8151 $[M+H]^+$	P	Glycerolipids [GL]	TG
199	TG(16:0_16:1_18:1)	830.7398	37.03	831.7531 $[M+H]^+$, 848.7804 $[M+NH4]^+$	P	Glycerolipids [GL]	TG

200	TG(16:0_16:1_20:0)	860.7650	35.80	861.7757 $[M+H]^+$	P	Glycerolipids [GL]	TG
201	TG(16:0_17:0_18:1)	846.7639	38.51	847.7842 $[M+H]^+$, 864.8115 $[M+NH4]^+$	P	Glycerolipids [GL]	TG
202	TG(16:0_17:0_19:0)	862.7923	36.66	863.7944 $[M+H]^+$	P	Glycerolipids [GL]	TG
203	TG(16:0_17:1_18:1)	844.7511	37.57	845.7688 $[M+H]^+$, 862.7961 $[M+NH4]^+$	P	Glycerolipids [GL]	TG
204	TG(16:0_17:2_19:0)	858.7692	36.22	859.7699 $[M+H]^+$, 876.7972 $[M+NH4]^+$	P	Glycerolipids [GL]	TG
205	TG(16:0_18:0_18:1)	860.7833	37.19	861.7865 $[M+H]^+$, 878.8138 $[M+NH4]^+$	P	Glycerolipids [GL]	TG
206	TG(16:0_18:0_18:2)	858.7626	33.42	859.7596 $[M+H]^+$	P	Glycerolipids [GL]	TG
207	TG(16:0_18:0_19:0)	876.8111	36.38	877.8064 $[M+H]^+$	P	Glycerolipids [GL]	TG
208	TG(16:0_18:1_18:1)	858.7677	36.38	859.7753 $[M+H]^+$, 876.8026 $[M+NH4]^+$	P	Glycerolipids [GL]	TG
209	TG(16:0_18:1_18:2)	856.7237	37.17	857.7629 $[M+H]^+$, 874.7902 $[M+NH4]^+$	P	Glycerolipids [GL]	TG
210	TG(16:0_18:1_18:3)	854.7410	38.01	855.7506 $[M+H]^+$	P	Glycerolipids [GL]	TG
211	TG(16:0_18:1_19:0)	874.7090	35.40	875.7938 $[M+H]^+$	P	Glycerolipids [GL]	TG
212	TG(16:0_18:1_20:4)	880.7535	36.38	881.7697 $[M+H]^+$, 898.797 $[M+NH4]^+$	P	Glycerolipids [GL]	TG

213	TG(16:0_18:1_21:0)	902.8397	37.45	903.8307 $[M+H]^+$	P	Glycerolipids [GL]	TG
214	TG(16:0_18:1_22:5)	906.7685	36.99	907.7853 $[M+H]^+$, 924.8126 $[M+NH4]^+$	P	Glycerolipids [GL]	TG
215	TG(16:0_18:2_19:0)	872.7898	35.15	873.7786 $[M+H]^+$	P	Glycerolipids [GL]	TG
216	TG(16:0_20:1_20:3)	910.7992	36.19	911.7924 $[M+H]^+$	P	Glycerolipids [GL]	TG
217	TG(16:0_20:1_20:5)	906.7627	37.42	907.7791 $[M+H]^+$	P	Glycerolipids [GL]	TG
218	TG(16:0_20:3_20:4)	904.7598	36.53	905.7642 $[M+H]^+$, 922.7915 $[M+NH4]^+$	P	Glycerolipids [GL]	TG
219	TG(16:0_20:3_22:0)	940.8290	37.44	941.8389 $[M+H]^+$	P	Glycerolipids [GL]	TG
220	TG(16:1_16:1_18:2)	826.7050	34.98	827.7170 $[M+H]^+$, 844.7443 $[M+NH4]^+$	P	Glycerolipids [GL]	TG
221	TG(16:1_18:0_18:1)	858.7612	38.09	859.7797 $[M+H]^+$, 876.807 $[M+NH4]^+$	P	Glycerolipids [GL]	TG
222	TG(16:1_18:1_18:2)	854.7364	36.26	855.7544 $[M+H]^+$, 872.7817 $[M+NH4]^+$	P	Glycerolipids [GL]	TG
223	TG(16:1_18:1_18:3)	852.7250	34.31	853.7386 $[M+H]^+$, 870.7659 $[M+NH4]^+$	P	Glycerolipids [GL]	TG
224	TG(16:1_18:1_18:3)	852.7250	36.99	853.7359 $[M+H]^+$	P	Glycerolipids [GL]	TG
225	TG(16:1_18:1_18:4)	850.7100	35.99	851.7212 $[M+H]^+$	P	Glycerolipids [GL]	TG
226	TG(16:1_18:1_19:0)	872.7828	38.56	873.8002 $[M+H]^+$, 890.8275 $[M+NH4]^+$	P	Glycerolipids [GL]	TG

227	TG(16:1_18:1_20:4)	878.7477	37.17	879.7518 $[M+H]^+$	P	Glycerolipids [GL]	TG
228	TG(16:1_18:1_21:0)	900.7260	35.99	901.8149 $[M+H]^+$	P	Glycerolipids [GL]	TG
229	TG(16:1_18:2_19:0)	870.7655	33.94	871.7684 $[M+H]^+$	P	Glycerolipids [GL]	TG
230	TG(16:1_20:0_20:0)	916.6990	35.99	917.8383 [M+H]+	P	Glycerolipids [GL]	TG
231	TG(17:0/17:0/17:0) (IS)	848.7859	39.90	849.8004 $[M+H]^+$, 866.8277 $[M+NH4]^+$	P	Glycerolipids [GL]	TG
232	TG(17:0_17:1_17:1)	844.7571	36.66	845.7641 $[M+H]^+$, 862.7914 $[M+NH4]^+$	P	Glycerolipids [GL]	TG
233	TG(17:0_18:0_22:4)	924.8378	36.61	925.8149 $[M+H]^+$, 942.8422 $[M+NH4]^+$	P	Glycerolipids [GL]	TG
234	TG(17:0_18:1_19:0)	888.7970	37.06	889.8091 $[M+H]^+$	P	Glycerolipids [GL]	TG
235	TG(17:0_20:1_20:2)	926.8346	36.53	927.8312 $[M+H]^+$, 944.8585 $[M+NH4]^+$	P	Glycerolipids [GL]	TG
236	TG(17:1_18:0_18:1)	872.7867	37.68	873.7953 $[M+H]^+$, 890.8226 $[M+NH4]^+$	P	Glycerolipids [GL]	TG
237	TG(17:1_18:1_18:1)	870.7627	37.66	871.7842 $[M+H]^+$, 888.8115 $[M+NH4]^+$	P	Glycerolipids [GL]	TG
238	TG(17:1_18:1_19:0)	886.7810	35.99	887.7927 $[M+H]^+$	P	Glycerolipids [GL]	TG
239	TG(17:2_18:1_18:1)	868.7559	36.66	869.7522 $[M+H]^+$, 886.7795 $[M+NH4]^+$	P	Glycerolipids [GL]	TG

240	TG(17:2_19:0_19:1)	898.7972	35.34	899.7947 $[M+H]^+$	P	Glycerolipids [GL]	TG
241	TG(18:0_18:0_18:2)	886.7934	39.28	887.8106 $[M+H]^+$, 904.8379 $[M+NH4]^+$	P	Glycerolipids [GL]	TG
242	TG(18:0_18:0_20:2)	914.8398	37.72	915.8251 $[M+H]^+$, 932.8524 $[M+NH4]^+$	P	Glycerolipids [GL]	TG
243	TG(18:0_18:1_19:0)	902.8389	36.75	903.8223 $[M+H]^+$	P	Glycerolipids [GL]	TG
244	TG(18:0_18:1_20:4)	908.7842	35.45	909.7992 $[M+H]^+$	P	Glycerolipids [GL]	TG
245	TG(18:0_18:2_19:0)	900.8172	36.38	901.8099 $[M+H]^+$	P	Glycerolipids [GL]	TG
246	TG(18:0_18:3_19:0)	898.7989	35.34	899.7947 $[M+H]^+$	P	Glycerolipids [GL]	TG
247	TG(18:0_18:4_19:0)	896.7629	35.27	897.7856 $[M+H]^+$, 914.8129 $[M+NH4]^+$	P	Glycerolipids [GL]	TG
248	TG(18:1_18:1_18:1)	884.7876	38.22	885.7913 $[M+H]^+$, 902.8186 $[M+NH4]^+$	P	Glycerolipids [GL]	TG
249	TG(18:1_18:1_18:2)	882.7626	37.30	883.7789 $[M+H]^+$, 900.8062 $[M+NH4]^+$	P	Glycerolipids [GL]	TG
250	TG(18:1_18:1_18:3)	880.7570	38.09	881.7669 $[M+H]^+$	P	Glycerolipids [GL]	TG
251	TG(18:1_18:1_19:0)	900.8165	36.38	901.8099 $[M+H]^+$	P	Glycerolipids [GL]	TG
252	TG(18:1_18:1_19:0)	900.8237	34.52	901.8147 $[M+H]^+$, 918.842 $[M+NH4]^+$	P	Glycerolipids [GL]	TG
253	TG(18:1_18:1_20:4)	906.7689	39.24	907.7834 $[M+H]^+$	P	Glycerolipids [GL]	TG

254	TG(18:1_18:1_20:5)	904.7545	36.47	905.7621 $[M+H]^+$	P	Glycerolipids [GL]	TG
255	TG(18:1_18:2_18:2)	880.7519	35.49	881.7709 $[M+H]^+$, 898.7982 $[M+NH4]^+$	P	Glycerolipids [GL]	TG
256	TG(18:1_18:2_19:0)	898.7470	39.24	899.7947 $[M+H]^+$	P	Glycerolipids [GL]	TG
257	TG(18:1_18:2_20:4)	904.7290	38.31	905.767 $[M+H]^+$	P	Glycerolipids [GL]	TG
258	TG(18:1_18:2_21:0)	926.7410	36.53	927.8306 $[M+H]^+$	P	Glycerolipids [GL]	TG
259	TG(18:1_18:3_18:3)	876.7298	35.33	877.738 $[M+H]^+$	P	Glycerolipids [GL]	TG
260	TG(18:1_19:0_20:4)	922.7986	34.87	923.7946 $[M+H]^+$	P	Glycerolipids [GL]	TG
261	TG(18:2_18:2_18:3)	876.7278	35.07	877.7377 $[M+H]^+$, 894.765 $[M+NH4]^+$	P	Glycerolipids [GL]	TG
262	TG(18:2_18:2_20:4)	902.7410	36.43	903.7538 $[M+H]^+$	P	Glycerolipids [GL]	TG
263	TG(18:2_18:2_20:5)	900.7227	34.40	901.7367 $[M+H]^+$	P	Glycerolipids [GL]	TG
264	TG(18:2_19:0_19:0)	914.8130	37.20	915.8227 $[M+H]^+$	P	Glycerolipids [GL]	TG
265	TG(18:2_19:0_20:3)	922.7470	38.31	923.8011 $[M+H]^+$	P	Glycerolipids [GL]	TG
266	TG(18:2_20:2_20:2)	934.7800	34.98	935.7914 $[M+H]^+$	P	Glycerolipids [GL]	TG
267	TG(20:1_20:1_20:4)	962.8130	36.03	963.8246 $[M+H]^+$	P	Glycerolipids [GL]	TG

[a]PA= phosphatidic acid; [b]PC= glycerophosphocholine; [c]PE= glycerophosphorylethanolamines; [d]PG= phosphatidylglycerol; [e]PS= phosphatidylserine; [f]DG= diacylglycerol; [g]TG= triacylglycerol; [h]P = positive; [i]N = negative.

2.3.3. Joint pathway analysis

The results from the lipid-gene centric pathway analysis suggested that the key genes and metabolites were involved in 13 metabolic pathways. The pathways with raw $p \leq 0.05$ were listed in the Table 2.7 and as shown in Fig. 2.4, glycerophospholipid metabolism pathway was the top-ranking enriched pathway.

2.3.4. Method validation

The intra- and inter-assay precision calculated using 12 spiked internal standards are shown in Table 2.8. The intra- and inter-assay precision of the method from 7 study subjects plasma sample by three replicate measurements from one of the sample preparation and three replicate measurements from three-parallel sample preparations were $\leq 5\%$ and $\leq 8\%$ respectively. The results indicate the coefficient of variation of internal standards are within limits set for fit-for-purpose biomarker research by US Food and Drug Administration ($\leq 30\%$) [29] and the method is reliable to quantitate the lipids using internal standards.

Table 2.7. Lipid-gene centric pathways with raw $p \leq 0.05$ of significant lipids with HMDB ID's

No	Pathway	-log$_e$(p)[a]	Impact score[b]	KEGG pathway	AD relevant genes	AD relevant lipids[c]
1	Glycerophospholipid metabolism	55.598	0.733	map00564	LPLAT1; LPCAT3; LYPLA1; PNPLA6; PLA2G4B; CEPT1; PLD1; PEMT; PTDSSA; PCYT1A; CHKA; AGPAT6; LYPLA1; LPCAT3; LCAT	1 – 5, 7, 9 – 12, 14, 15 – 18, 20
2	Ether lipid metabolism	54.231	0.759	map00565	CEPT1; PAFAH1B1; LPCAT4; LPCAT2; PLA2G4B; PLD1; CEPT1	1 – 5, 7, 9 – 12, 14, 15 – 18, 20
3	alpha-Linolenic acid metabolism	34.120	0.150	map00592	PLA2G4B	1 – 5, 7, 9 – 12, 14, 15 – 18, 20
4	Linoleic acid metabolism	34.120	0.375	map00591	PLA2G4B	1 – 5, 7, 9 – 12, 14, 15 – 18, 20
5	Glycerolipid metabolism	15.591	0.486	map00561	AGPAT6; MGLL; CEL; LPL; MOGAT3	26
6	Arachidonic acid metabolism	14.492	0.077	map00590	PLA2G4B	1 – 5, 7, 9 – 12, 14, 15 – 18, 20

[a]-log$_e$(p) = natural log of (p) value calculated from the enrichment analysis (Fisher' Exact test); [b]Impact score = pathway impact value calculated from topology analysis (degree centrality); [c]AD relevant lipids = refer to Table S1 for significant lipid number designation.

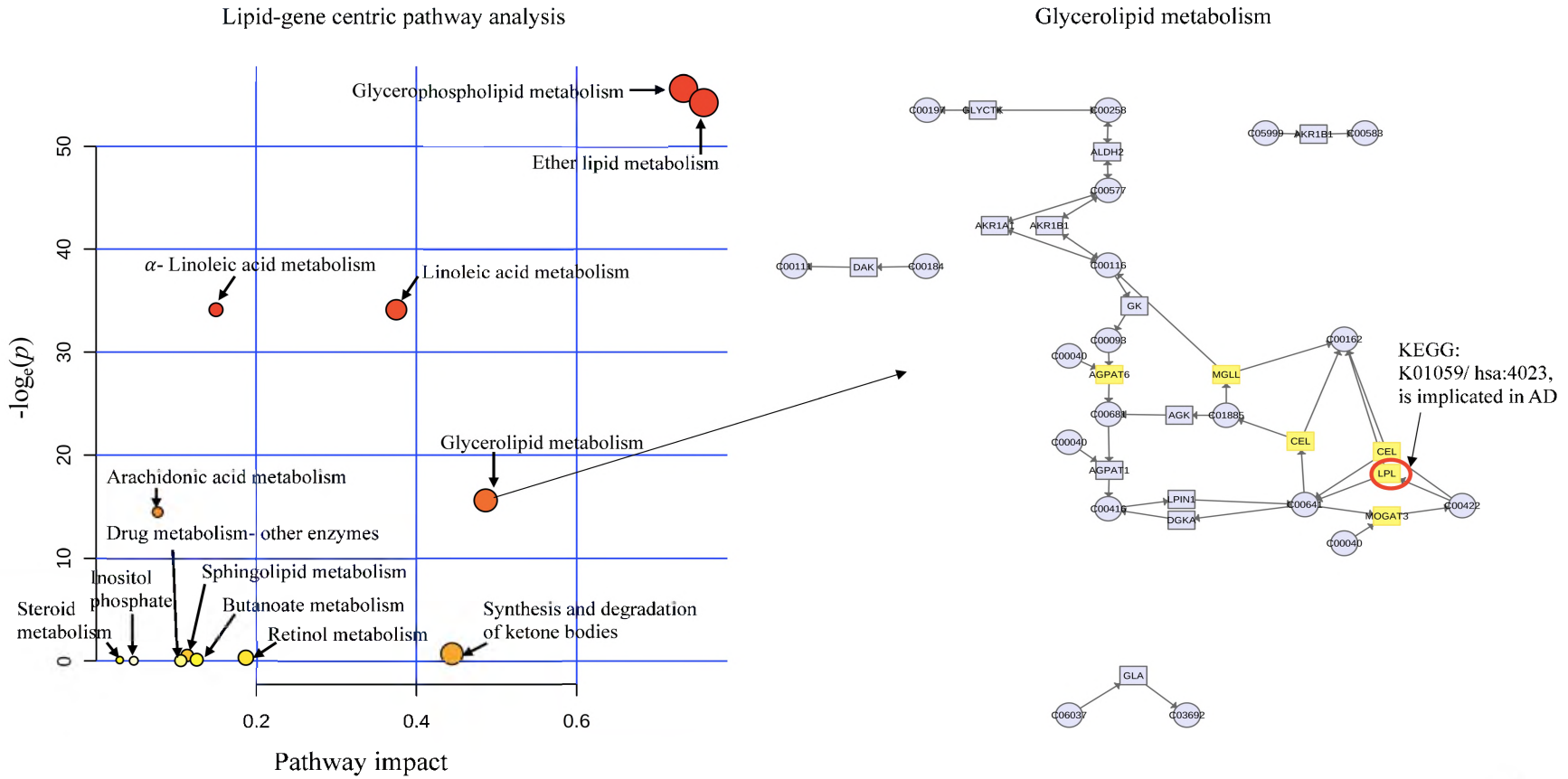

Figure 2.4. Lipid-gene centric pathway analysis on significant lipids. All matched pathways are plotted according to *p*-value from pathway enrichment analysis (Red: higher *p*-value and yellow: lower *p*-value) and pathway impact score from pathway topology analysis (larger the circle higher the impact score) respectively. By selecting the circle displays the overall pathway with matched genes from the data set.

Table 2.8. Intra- and inter-assay precision of the internal standards spiked in four AD and three NCC study subjects (n = 21)

	Lipid			Intra assay		Inter assay	
No.	Internal standard[a]	Mass	t_R (min)	(PA_{avg}[b] ± SD) × 10^5	%RSD[c]	(PA_{avg} ± SD) × 10^5	%RSD
1	PA(14:0/0:0)	382.1089	4.42	6.30 ± 0.02	0.3	6.4 ± 0.2	3
2	PE(14:0/0:0)	425.2579	6.74	2.20 ± 0.04	2	2.13 ± 0.04	2
3	PC(13:0/0:0)	453.2887	4.45	16.2 ± 0.2	1	16.0 ± 0.4	3
4	PG(14:0/0:0)	456.2727	4.46	6.6 ± 0.3	5	6.4 ± 0.5	8
5	PS(17:1/0:0)	509.3494	7.64	4.0 ± 0.1	3	4.0 ± 0.1	3
6	Cer(d18:1/17:0)	551.5320	23.76	11.0 ± 0.2	2	11.3 ± 0.4	4
7	DG(19:0/19:0/0:0)	652.6090	31.61	4.6 ± 0.1	2	5.0 ± 0.2	4
8	PE(15:0/15:0)	663.4881	19.45	11.0 ± 0.1	1	11.0 ± 0.3	3
9	PS(14:0/14:0)	679.3678	18.08	117 ± 1	1	118 ± 1	1
10	PG(17:0/17:0)	750.9856	20.50	2.50 ± 0.01	0.4	2.52 ± 0.04	2
11	PC(19:0/19:0)	817.6615	26.42	23.0 ± 0.3	1	22.6 ± 0.7	3
12	TG(17:0/17:0/17:0)	848.7859	39.90	13.0 ± 0.2	2	13.6 ± 0.5	4

[a] The concentration of each lipid in final sample for analysis was 1.5 μM.

[b] PA_{avg}= average of peak areas of each internal standard across all the study subjects.

[c] %RSD = (SD/PA_{avg})×100, relative standard deviation of peak areas of each internal standard in all study subjects .

2.3.5. Quantitative lipidomics

Quantitation of the identified and unidentified lipids was performed by assigning the respective class of spiked internal standards as described in Section 2.2.9. The concentrations obtained were multiplied with the dilution factor of 10 to calculate the final concentrations, expressed in μM. Table 2.3 and Table 2.4 represents the mean measured micromolar (μM) concentrations of identified and unidentified significant features in NCC and AD study subjects. Fold changes were calculated by the ratio between the mean measured micromolar concentrations in NCC to AD. The list of internal standards and their retention times were listed in Table 2.8.

2.3.6. Unique lipids in AD and NCC

In our study, we found the features unique to each group. A total of 21 features are unique to NCC whereas 25 features are unique to AD. Table 2.9 and 2.10 summarizes the unique features in AD and NCC respectively with mean measured micromolar concentrations (μM).

Table 2.9. Unique unidentified features common in four AD study subjects (n = 20)

Phospholipid					Neutral lipid			
No.	Mass	t_R (min)	$[\bar{X}]_{PL}$[a] ± SD	Precursor ion, m/z	Mass	t_R (min)	$[\bar{X}]_{NL}$[b] ± SD	Precursor ion, m/z
1	162.0791	3.29	1.4 ± 0.3	161.0718 [M-H]-	125.0872	2.77	6.0 ± 0.5	126.0945 $[M+H]^+$
2	162.0867	3.56	1.0 ± 0.2	161.0794 [M-H]-	153.0810	2.77	7.1 ± 0.6	154.0883 $[M+H]^+$
3	220.1129	4.30	1.6 ± 0.4	221.1206 $[M+H]^+$	290.0477	2.92	8 ± 1	291.0550 $[M+H]^+$; 289.0404 $[M-H]^-$
4	375.2932	14.41	4 ± 1	376.3010 $[M+H]^+$	292.0859	2.82	8.5 ± 0.6	293.0932 $[M+H]^+$
5	519.3318	2.70	2.5 ± 0.4	520.3387 $[M+H]^+$	310.1456	2.96	8.0 ± 0.6	311.1529 $[M+H]^+$; 309.1383 $[M-H]^-$
6	579.4016	7.09	8 ± 4	580.4096 $[M+H]^+$	436.1887	3.72	10 ± 1	437.1960 $[M+H]^+$; 454.2225 $[M+NH4]^+$
7	721.5114	19.80	1.3 ± 0.7	722.5187 $[M+H]^+$; 720.5041 $[M-H]^-$	488.1890	3.06	4.0 ± 0.3	489.1963 $[M+H]^+$
8	800.6723	24.56	2.7 ± 0.3	801.6802 $[M+H\}^+$	722.6408	29.22	8 ± 3	723.6481 $[M+H]^+$; 740.6746 $[M+NH4]^+$
9	817.5965	21.44	1.0 ± 0.5	818.6037 $[M+H]^+$; 816.5899 $[M-H]^-$	936.8206	39.49	4 ± 0	937.8279 $[M+H\}^+$
10	833.0848	21.92	1.3 ± 0.3	834.0921 $[M+H]^+$	938.8335	40.76	1.7 ± 0.1	939.8408 $[M+H]^+$
11	1055.2989	28.01	1.8 ± 0.3	1056.3062 $[M+H]^+$	954.8065	40.95	1 ± 2	955.8138 $[M+H]^+$
12					962.8310	39.78	1 ± 2	963.8385 $[M+H]^+$
13					964.8523	40.76	4.1 ± 0.1	965.8603 $[M+H]^+$
14					1026.9411	40.97	3.4 ± 0.1	1027.9484 $[M+H]^+$

[a] $[\bar{X}]_{PL}$ = mean measure concentration in phospholipid fraction.

[b] $[\bar{X}]_{NL}$ = mean measured concentration in neutral lipid fraction.

Table 2.10. Unique unidentified features common in three NCC study subjects (n = 15)

Phospholipid					Neutral lipid			
No.	Mass	t_R (min)	$[\bar{X}]_{PL}$[a] ± SD	Precursor ion, m/z	Mass	t_R (min)	$[\bar{X}]_{NL}$[b] ± SD	Precursor ion, m/z
1	227.1918	10.33	45± 15	226.9089 $[M-H]^-$	152.1214	3.41	11.0 ± 0.4	153.1923 $[M+H]^+$; 151.0956 $[M-H]^-$
2	260.1260	2.73	1.0 ± 0.1	261.2087 $[M+H]^+$	258.0520	3.15	11 ± 1	259.1024 $[M+H]^+$; 257.0023 $[M-H]^-$
3	298.1579	4.15	1.2 ± 0.6	297.0089 $[M-H]^-$	270.1110	2.86	12 ± 5	271.1206 $[M+H]^+$; 269.0975 $[M-H]^-$
4	334.2273	4.15	0.8 ± 0.2	335.3561 $[M+H]^+$	276.0997	2.71	2.3 ± 0.4	277.1078 $[M+H]^+$; 275.0924 $[M-H]^-$
5	676.5499	17.58	2.0 ± 0.3	677. 6904 $[M+H]^+$; 675.5326 $[M-H]^-$	368.3486	29.19	1.7 ± 0.3	369.2398 $[M+H]^+$; 367.4927 $[M-H]^-$
6	732.6146	22.04	2.3 ± 0.2	733.7290 $[M+H]^+$	658.5014	25.84	4 ± 2	659.5123 $[M+H]^+$; 657.4901 $[M-H]^-$
7	827.5530	18.58	22 ± 14	828.6006 $[M+H]^+$; 826.4603 $[M-H]^-$	716.3846	24.25	2 ± 1	717.4001 $[M+H]^+$
8	993.7218	23.58	4.4 ± 0.5	994.7986 $[M+H]^+$	720.5062	21.21	7 ± 1	721.5135 $[M+H]^+$
9					757.5707	20.30	56 ± 5	758.5780 $[M+H]^+$
10					783.5852	20.91	20 ± 3	784.5925 $[M+H]^+$; 801.6190 $[M+NH4]^+$
11					832.6487	23.20	3.2 ± 0.3	833.6560 $[M+H]^+$
12					834.6629	24.33	4.4 ± 0.2	835.6702 $[M+H]^+$; 852.6967 $[M+NH4]^+$
13					836.6786	25.70	2.4 ± 0.5	837.6859 $[M+H]^+$

[a] $[\bar{X}]_{PL}$ = mean measure concentration in phospholipid fraction.

[b] $[\bar{X}]_{NL}$ = mean measured concentration in neutral lipid fraction.

2.4. Discussion

2.4.1. Optimization of sample preparation and UHPLC-QTOF-MS/MS

Total lipids extracted and fractionated from plasma samples were analyzed as described in sections 2.2.3 and 2.2.4. The Bligh-Dyer method was modified by acidifying the samples with 1 N HCl for higher recoveries of the acidic lipids. Two-step sample separation was performed on the extracted total lipids. In the first step, the total lipids were fractionated using aminopropyl SPE, to separate the interfering analytes and thus reducing the matrix interference and ion suppression in MS analysis for the detection of low abundant lipids. Secondly, liquid chromatography was performed on each fraction for the separation of the analytes and to eliminate the isobaric overlap. Different percent compositions of isopropyl alcohol in mobile phase B were tested to minimize the column carry over in the gradient profile. Based on the analyte structure, they require different collision energies to generate adequate MSMS fragments. So, collision energies of 10, 20 and 40 eV were used to get MS/MS spectra which were summed and used for the unambiguous identification of the analyte against the database.

2.4.2. Comparison of Up- and Down regulated lipids in AD

In the current study, our results indicate an overall trend in abundance for LPC (NCC < AD), PC (NCC >AD), SM (NCC > AD), GlcCer (NCC >AD) and TG (NCC < AD). These lipid species belong to three major categories *i.e.*, glycerophospholipids, sphingolipids and glycerolipids. The pathways referenced in this section are from Kyoto Encyclopedia of Genes and Genomes (KEGG) database for human (https://www.genome.jp/kegg/pathway.html) [30]

2.4.2.1 Glycerophospholipids (GP)

In AD (map05010, Fig. 2.7), the Wnt signaling pathway (map04310, Fig. 2.8) is affected which in turn affects the MAPK signaling (map04010) and Ras signaling (map04014) pathways leading to increased activation or levels of PLA_2 (entry: K01047). The elevated levels of PLA_2 cause the dysregulation in the glycerophospholipid metabolism pathway (map00564, Fig. 2.5, 2.6 and 2.9). To maintain the neuronal membrane integrity and normal cellular events, LPC is generated transiently during the deacylation and reacylation cycle. LPCs are generated by the action of phospholipase A_2 (PLA_2, 3.1.1.4 in map00564, Fig. 2.9) on PCs, releasing the fatty acid from its *sn*-2 position. Studies have reported the increased levels of PLA_2 in AD plasma [31–33]. From our results, we report the increased levels of LPCs (LPC 16:0; LPC 18:0; LPC 18:1; LPC 20:4) (Table 3) along with the LPC 18:2 reported in previous study [19]. LPCs are not only the intermediate products in the metabolism of glycerophospholipids but also serve as mediators in many pathways involved in AD [34]. LPC 16:0 is a precursor for the platelet-activating factor (PAF), an important mediator in inflammation-related processes [35]. LPC 20:4 serves as a precursor for the mediators involved in the immune response via arachidonic acid metabolism pathway. Further investigation is required to validate whether the catabolic or the anabolic stimulation leads to the elevated levels of these lipids in AD plasma [20]. PLA2 is also involved in ether lipid, arachidonic acid, linoleic acid, alpha-linolenic acid metabolism pathways. Fatty acid composition in membrane glycerophosphocholine lipids influences their biophysical properties like permeability, charge, and fluidity [14]. In AD plasma, decreased concentrations of PCs with polyunsaturated fatty acid (PUFA)

tails were observed (Table 3) [21,36]. Decreased levels of alpha-linolenic acid (18:3, n-3), eicosapentaenoic acid (EPA) (20:5, n-3) and docosahexaenoic acid (DHA) (22:6, n-3) containing PCs were observed [37]. These fatty acids are utilized in the generation of anti-inflammatory and neuroprotective metabolites like docosanoids [38]. In neurons at cell junction, lipid raft contains a high concentration of lipids with docosahexaenoic acid (DHA) fatty acid tail. Disruption to the lipid raft leads to loss of communication between the neurons, causing a decline in cognition. Randomized trial of DHA administration showed an increase in cognition in AD, relating DHA to cognition in AD [39,40]. Studies have reported the release of arachidonic acid (AA) (20:4 n-6) implicates the activation of the immune system, which is common in AD pathophysiology. AA generates a wide variety of eicosanoids mediators which cause neuroinflammation [14].

2.4.2.2. Sphingolipids (SL)

Sphingolipids play an important role in many biological functions like cell growth, differentiation, senescence and apoptosis [41,42]. In our study, we found the decreased levels of sphingomyelins (SM) and neutral glycosphingolipids in AD plasma. Our results from the lipid-gene centric pathway analysis suggested that the associated genes and lipids were involved in sphingolipid metabolism, however it did not meet the criteria of $p \leq 0.05$. In AD, it is evident that the sphingolipid signaling pathway (map04071, Fig. 2.10) is affected via phosphatidylinositol phospholipase C (PLC, entry: K05858). Previous studies have reported that amyloid-β induces the increased activity of neutral sphingomyelinase (N-SMase) in oligodendrocytes of the brain in AD patients [43].

The post-mortem on brain from AD patients showed decreased sphingomyelins (SM) and increased ceramide (Cer) accumulation. Mediators (AA, eicosanoids, PAF)

generated by the PLA_2 also stimulates sphingolipid signaling pathway by activating SMase [41].

2.4.2.3. Glycerolipids (GL)

In our study, we found the increased levels of triacylglycerols (TG) in AD plasma suggesting the changes in the glycerolipid metabolism pathway (map00561, Fig. 2.11). These changes were related to lipoprotein lipase (LPL, entry: K01059) which is associated with the *ApoE* gene in AD [44]

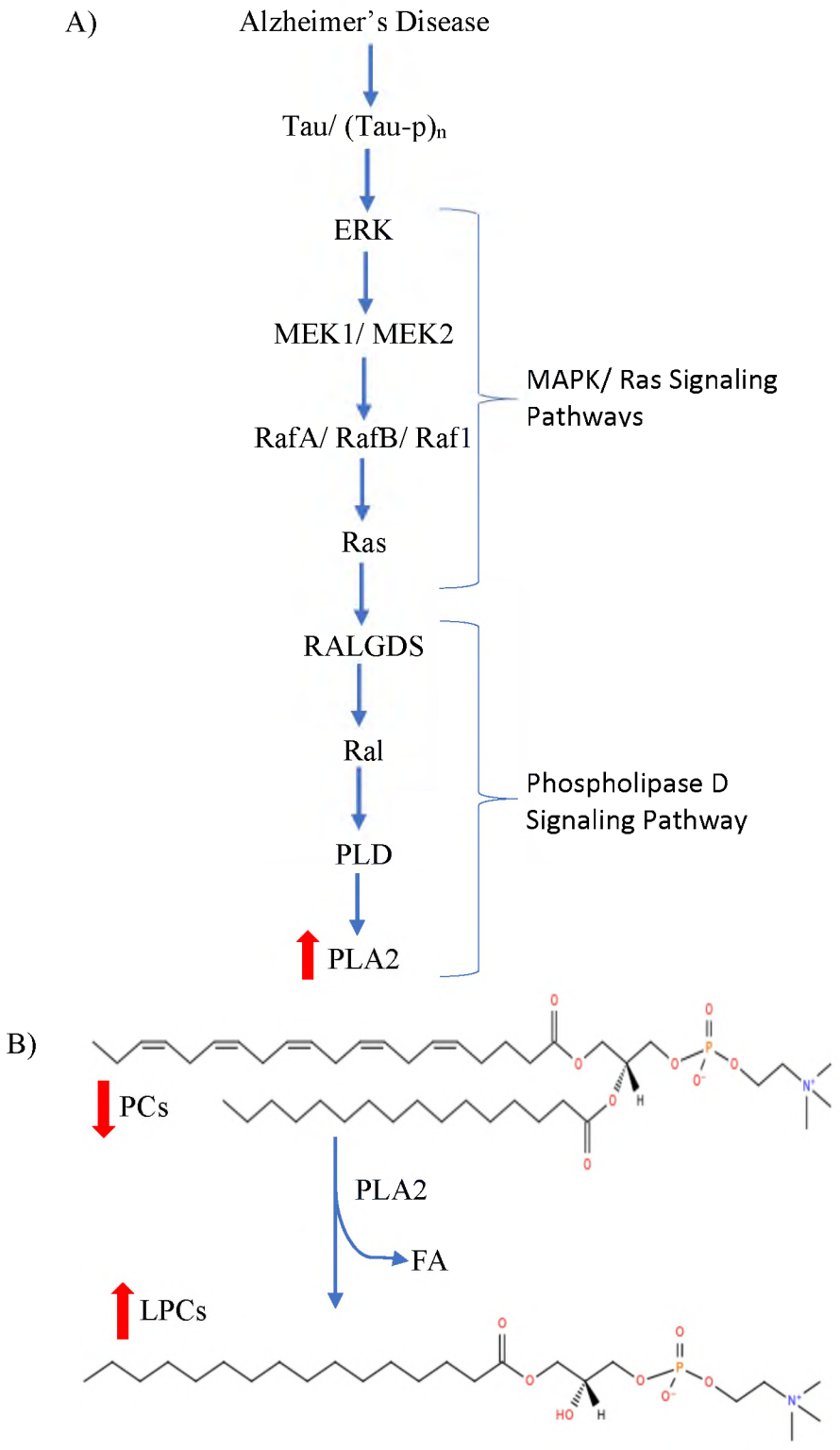

Fig 2.5. A) Increased activity or expression of PLA2 in Alzheimer's disease via MAPK/Ras signaling pathways. B) Conversion of phosphocholine to lysophosphocholine by the action of PLA2

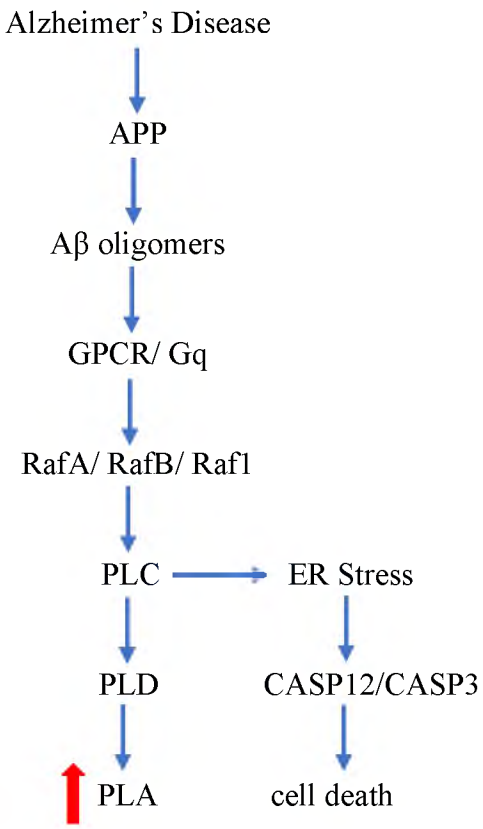

Fig 2.6. Increased activity or expression of PLA2 in AD via Ras signaling pathway.

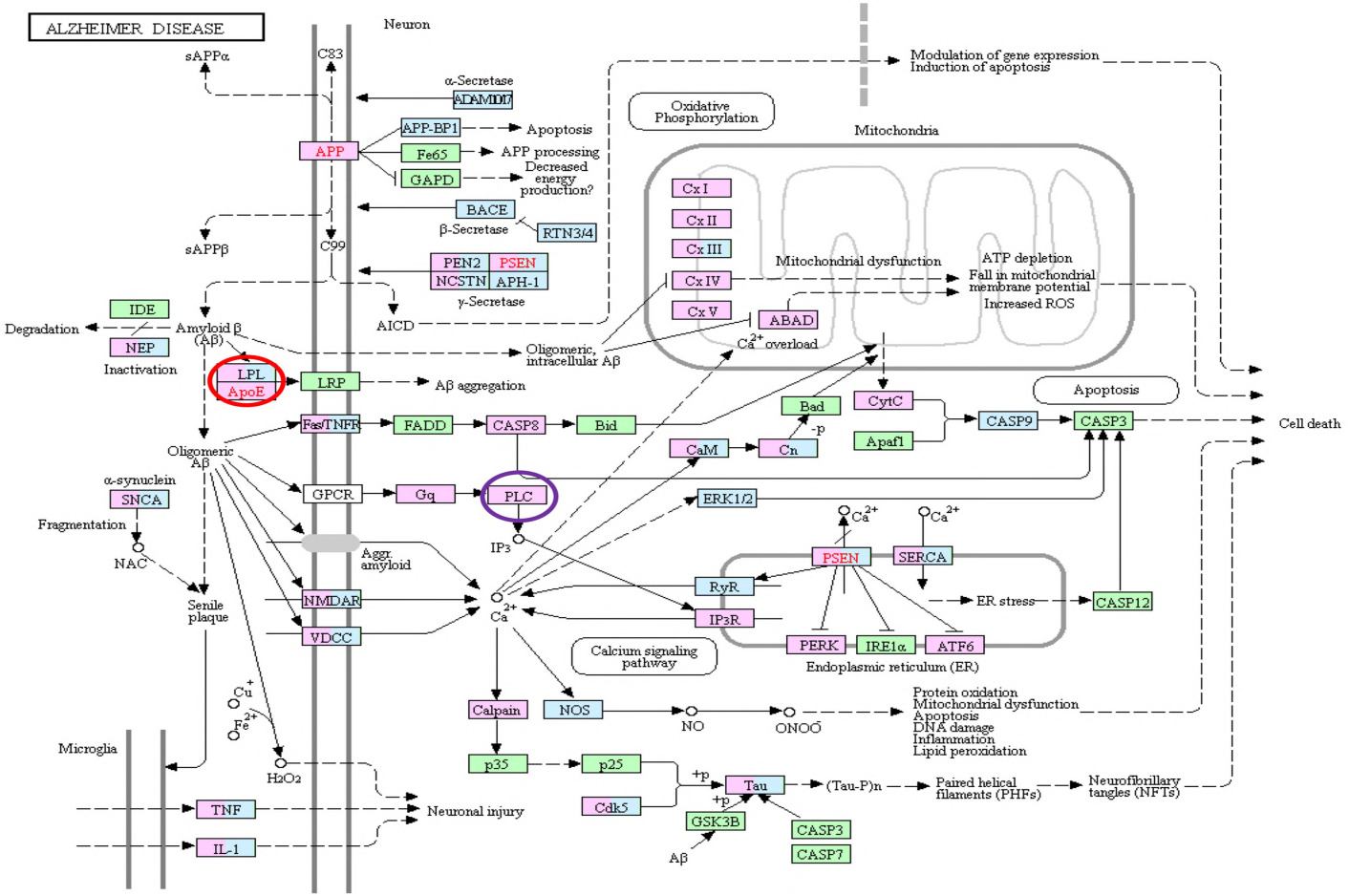

Figure 2.7. Alzheimer's disease pathway (map05010) from the KEGG database indicating the implicated disease genes (pink), drug targets (blue), disease gene-drug target (pink | blue) and organism specific pathways (green). The red text genes indicates the perturbed and implicated genes in the AD. Circled genes implicate the glycerolipid metabolism (red), Ras signaling pathway and sphingolipid signaling pathway (purple) [30].

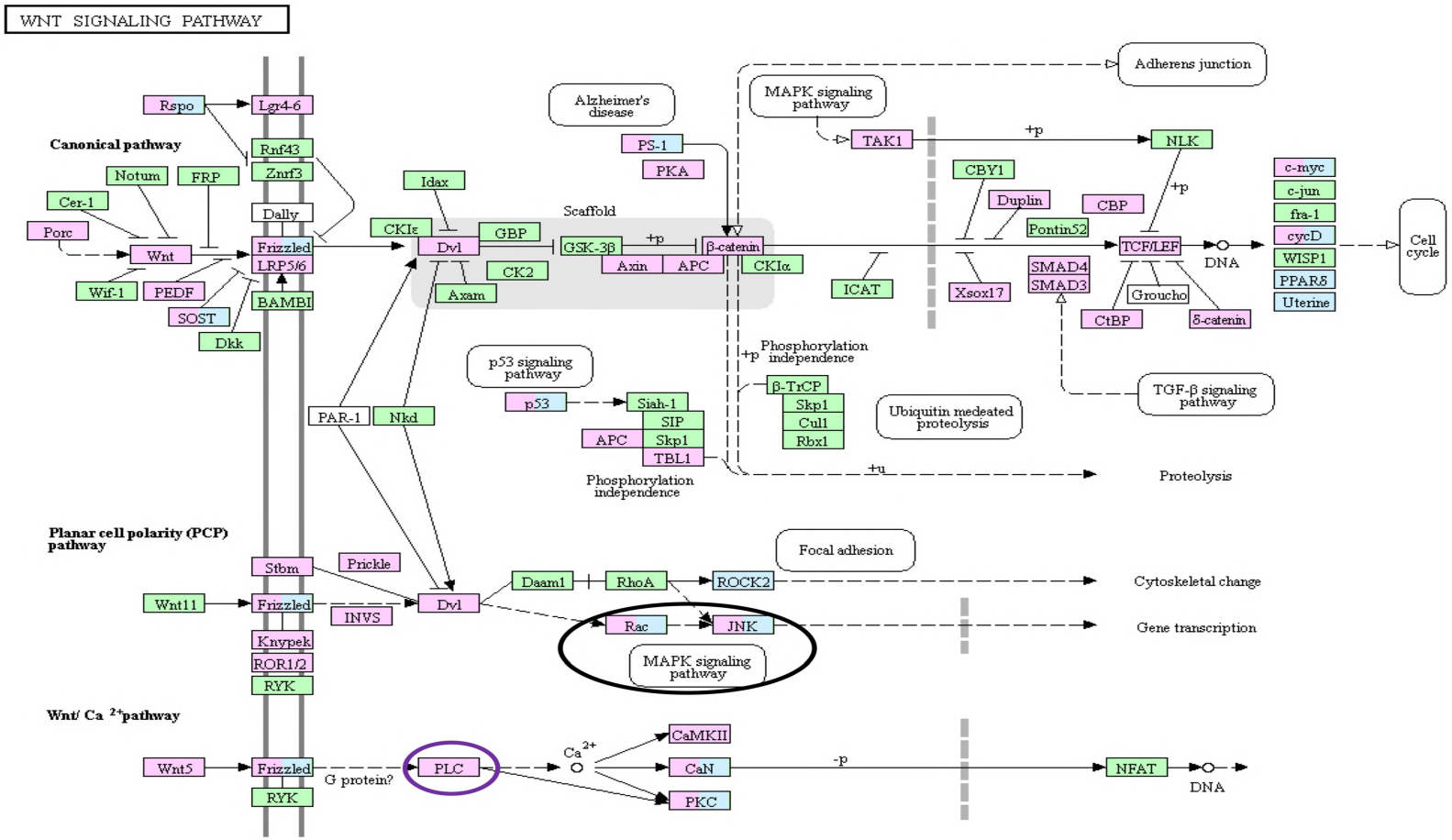

Figure 2.8. Implication of Wnt Signaling pathway (map04310) in AD. Circled genes activates the MAPK and Ras signaling (black) and sphingolipid signaling pathway (purple) which in-turn implicate glycerophospholipid metabolism [30].

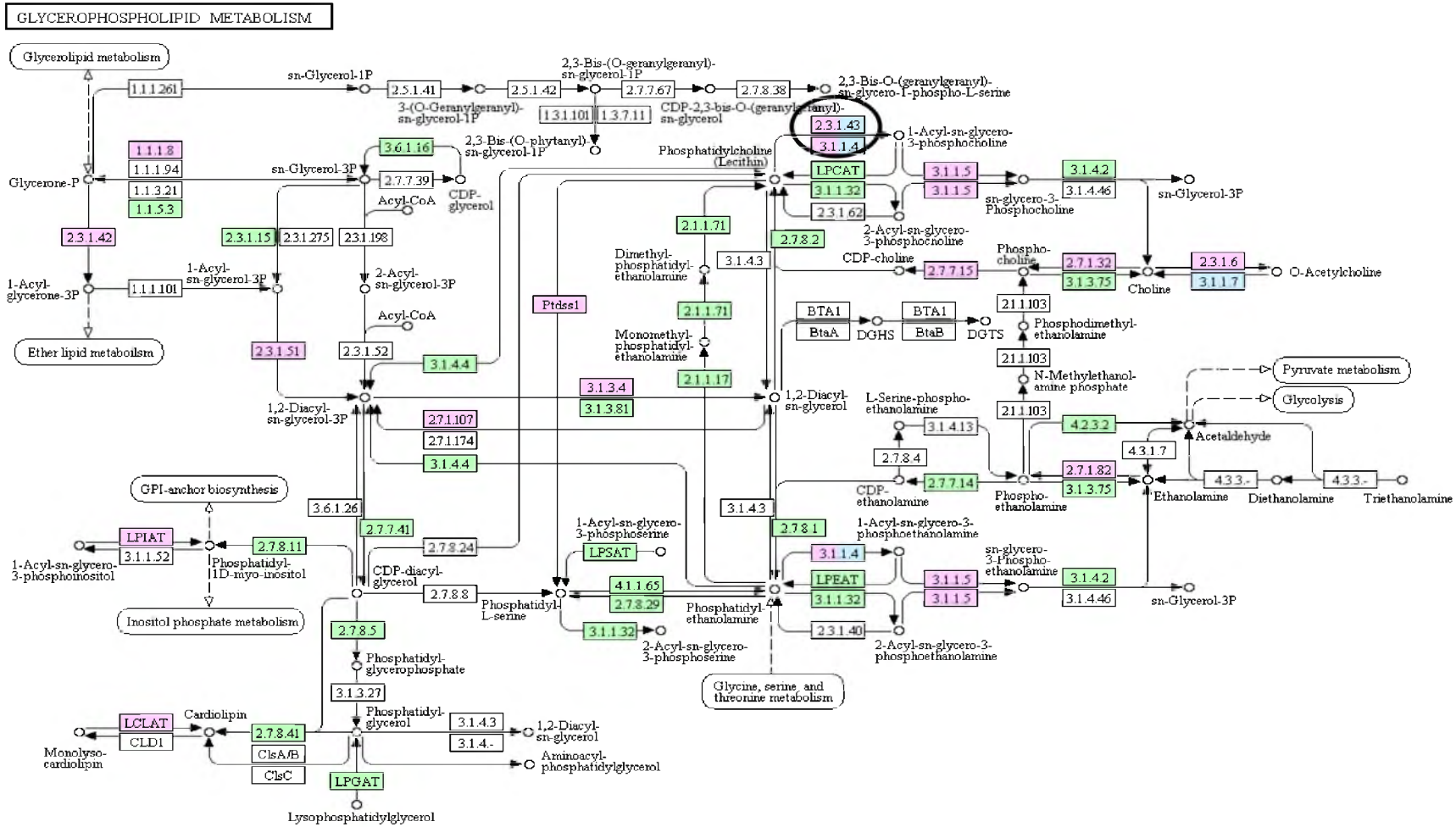

Figure 2.9. PLA2G/ SPLA2 enzyme (gene circled in black) implicated in AD plays role in glycerophospholipid , ether lipid, arachidonic acid, linoleic acid, alpha-linolenic acid metabolisms. Our results from gene- lipid centric pathway analysis also indicate the same as represented in Table 2.7 [30].

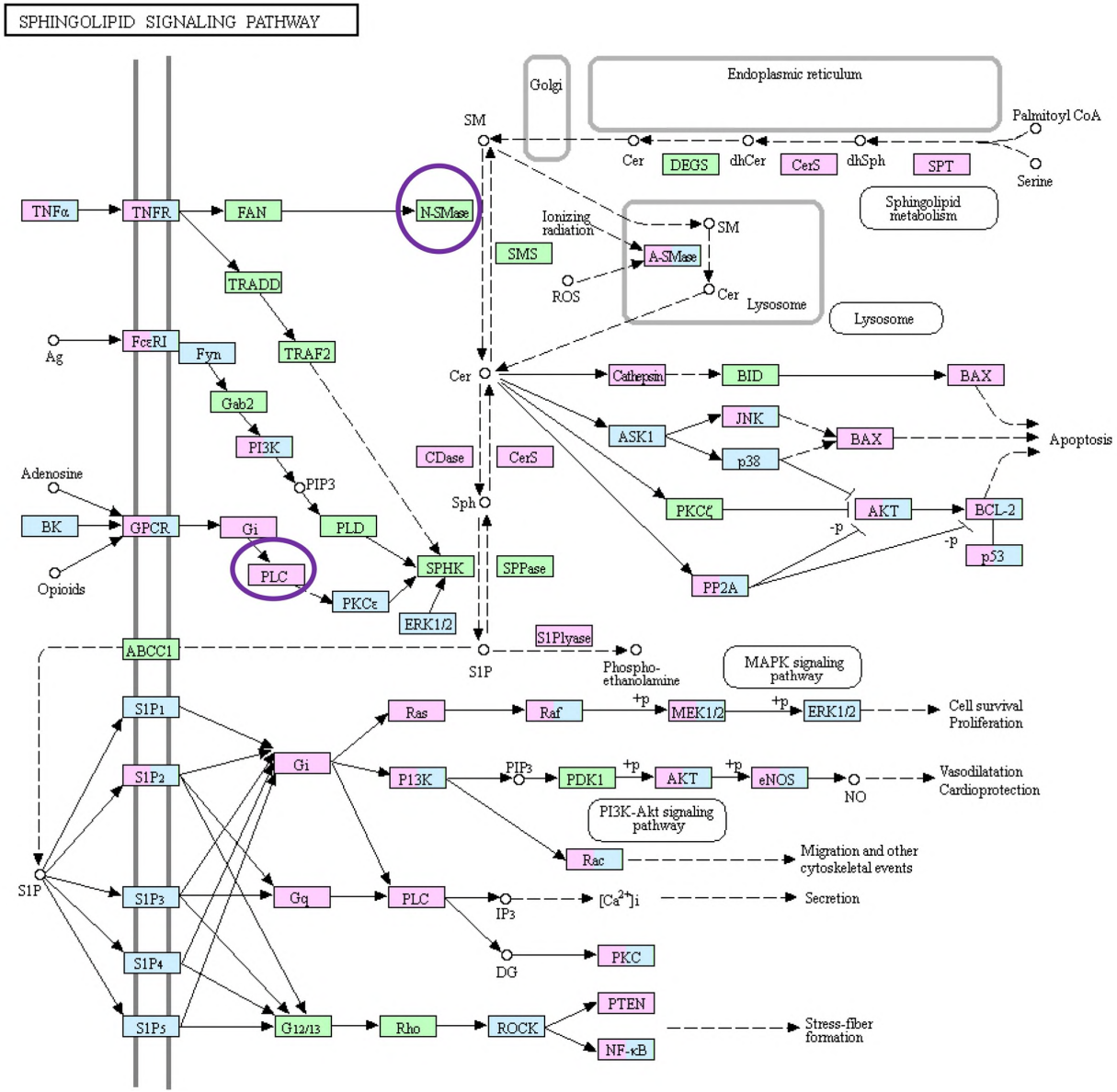

Figure 2.10. Circled genes implicate the sphingolipid signaling pathway. Increased activity of N-SMase in AD leads to decreased concentration of sphingomyelins impacting sphingolipid signaling pathway [30].

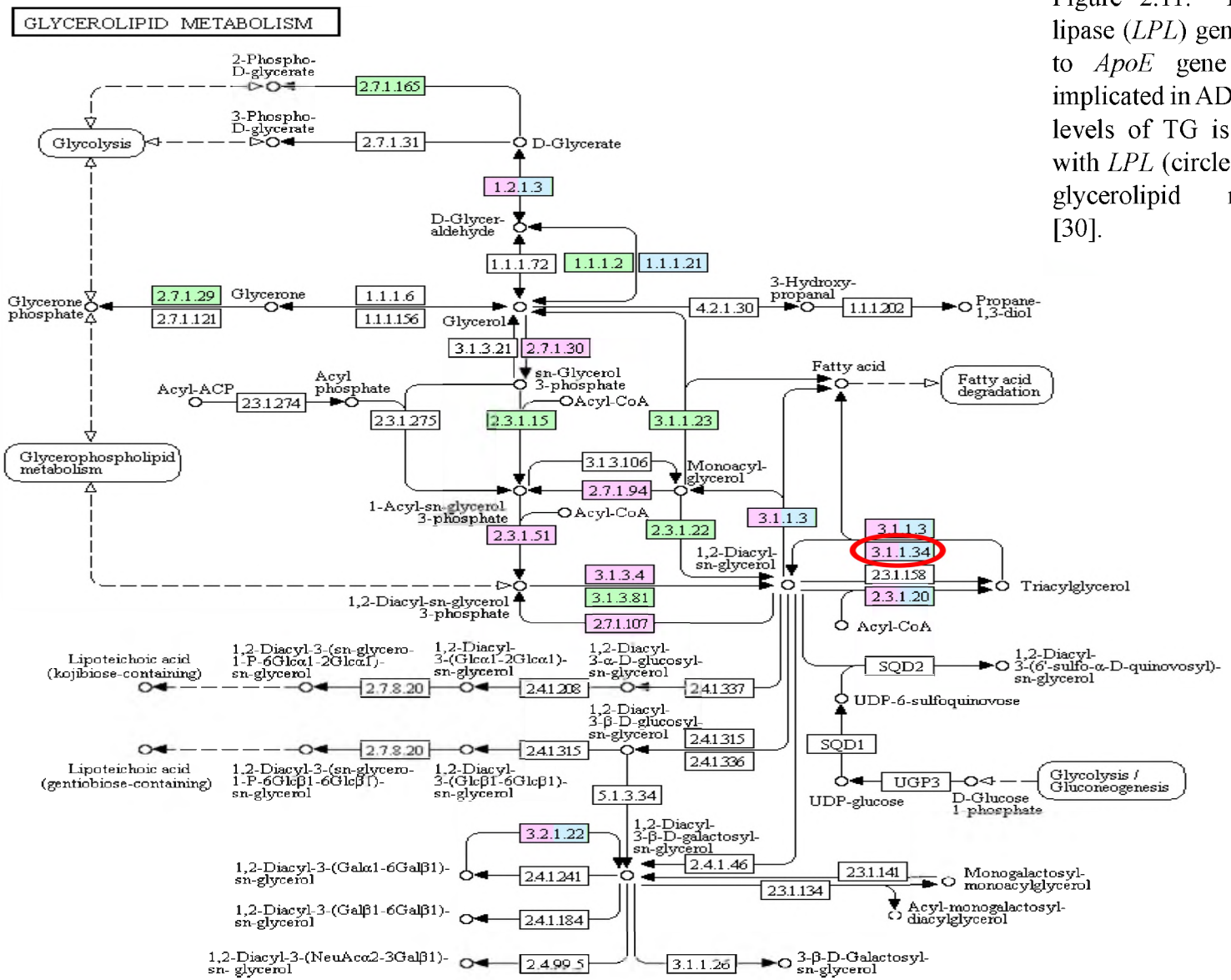

Figure 2.11. Lipoprotein lipase (*LPL*) gene is related to *ApoE* gene which is implicated in AD. Increased levels of TG is associated with *LPL* (circled in red) in glycerolipid metabolism [30].

2.5. Conclusion

In our study, we detailed the workflow for UHPLC-QTOF-MS based lipidomics to identify the lipid biomarkers in human plasma. We employed 12 lipid internal standards representing major sub-classes of plasma lipidome for data normalization and semi-quantitation. We found greater variation in the PL fraction between NCC and AD, suggesting perturbations in phospho lipidome. Our study showed 28 potential lipid biomarkers related to phosphocholines, sphingomyelins, neutral glycosphingolipids, and triacylglycerols. Lipid-gene centric pathway analysis suggested the implicated pathways are either directly or indirectly related to AD.

Limitations to our study also warrant consideration. The small sample size limited this study to account for the interference from systemic metabolism and the stage of disease development. Further investigation is required to validate the results in a larger cohort of samples. However, this pilot study was intended to investigate AD plasma lipidome and stimulate further studies in AD.

2.6. REFERENCES

1. Karch, C.M.; Goate, A.M. Alzheimer's disease risk genes and mechanisms of disease pathogenesis. *Biol. Psychiatry* **2015**, *77*, 43–51.
2. Kumar, A.; Singh, A.; Ekavali, null A review on Alzheimer's disease pathophysiology and its management: an update. *Pharmacol Rep* **2015**, *67*, 195–203.
3. Viola, K.L.; Klein, W.L. Amyloid β oligomers in Alzheimer's disease pathogenesis, treatment, and diagnosis. *Acta Neuropathol.* **2015**, *129*, 183–206.
4. Pooler, A.M.; Noble, W.; Hanger, D.P. A role for tau at the synapse in Alzheimer's disease pathogenesis. *Neuropharmacology* **2014**, *76 Pt A*, 1–8.
5. McKhann, G.M.; Knopman, D.S.; Chertkow, H.; Hyman, B.T.; Jack, C.R.; Kawas, C.H.; Klunk, W.E.; Koroshetz, W.J.; Manly, J.J.; Mayeux, R.; et al. The diagnosis of dementia due to Alzheimer's disease: recommendations from the National Institute on Aging-Alzheimer's Association workgroups on diagnostic guidelines for Alzheimer's disease. *Alzheimers Dement* **2011**, *7*, 263–269.
6. Albert, M.S.; DeKosky, S.T.; Dickson, D.; Dubois, B.; Feldman, H.H.; Fox, N.C.; Gamst, A.; Holtzman, D.M.; Jagust, W.J.; Petersen, R.C.; et al. The diagnosis of mild cognitive impairment due to Alzheimer's disease: recommendations from the National Institute on Aging-Alzheimer's Association workgroups on diagnostic guidelines for Alzheimer's disease. *Alzheimers Dement* **2011**, *7*, 270–279.
7. Sperling, R.A.; Aisen, P.S.; Beckett, L.A.; Bennett, D.A.; Craft, S.; Fagan, A.M.; Iwatsubo, T.; Jack, C.R.; Kaye, J.; Montine, T.J.; et al. Toward defining the

preclinical stages of Alzheimer's disease: recommendations from the National Institute on Aging-Alzheimer's Association workgroups on diagnostic guidelines for Alzheimer's disease. *Alzheimers Dement* **2011**, *7*, 280–292.

8. Long, J.; Pan, G.; Ifeachor, E.; Belshaw, R.; Li, X. Discovery of Novel Biomarkers for Alzheimer's Disease from Blood. *Dis. Markers* **2016**, *2016*, 4250480.
9. Olsson, B.; Lautner, R.; Andreasson, U.; Öhrfelt, A.; Portelius, E.; Bjerke, M.; Hölttä, M.; Rosén, C.; Olsson, C.; Strobel, G.; et al. CSF and blood biomarkers for the diagnosis of Alzheimer's disease: a systematic review and meta-analysis. *Lancet Neurol* **2016**, *15*, 673–684.
10. Florent-Béchard, S.; Desbène, C.; Garcia, P.; Allouche, A.; Youssef, I.; Escanyé, M.-C.; Koziel, V.; Hanse, M.; Malaplate-Armand, C.; Stenger, C.; et al. The essential role of lipids in Alzheimer's disease. *Biochimie* **2009**, *91*, 804–809.
11. Di Paolo, G.; Kim, T.-W. Linking lipids to Alzheimer's disease: cholesterol and beyond. *Nat. Rev. Neurosci.* **2011**, *12*, 284–296.
12. Rebeck, G.W. The role of APOE on lipid homeostasis and inflammation in normal brains. *J. Lipid Res.* **2017**, *58*, 1493–1499.
13. Fantini, J.; Garmy, N.; Mahfoud, R.; Yahi, N. Lipid rafts: structure, function and role in HIV, Alzheimer's and prion diseases. *Expert Rev Mol Med* **2002**, *4*, 1–22.
14. Torres, M.; Price, S.L.; Fiol-Deroque, M.A.; Marcilla-Etxenike, A.; Ahyayauch, H.; Barceló-Coblijn, G.; Terés, S.; Katsouri, L.; Ordinas, M.; López, D.J.; et al. Membrane lipid modifications and therapeutic effects mediated by hydroxydocosahexaenoic acid on Alzheimer's disease. *Biochim. Biophys. Acta* **2014**, *1838*, 1680–1692.

15. Zhu, L.; Zhong, M.; Elder, G.A.; Sano, M.; Holtzman, D.M.; Gandy, S.; Cardozo, C.; Haroutunian, V.; Robakis, N.K.; Cai, D. Phospholipid dysregulation contributes to ApoE4-associated cognitive deficits in Alzheimer's disease pathogenesis. *Proc. Natl. Acad. Sci. U.S.A.* **2015**, *112*, 11965–11970.

16. Wood, P.L. Lipidomics of Alzheimer's disease: current status. *Alzheimers Res Ther* **2012**, *4*, 5.

17. Han, X.; Yang, K.; Cheng, H.; Fikes, K.N.; Gross, R.W. Shotgun lipidomics of phosphoethanolamine-containing lipids in biological samples after one-step in situ derivatization. *J. Lipid Res.* **2005**, *46*, 1548–1560.

18. Han, X.; Gross, R.W. Shotgun lipidomics: electrospray ionization mass spectrometric analysis and quantitation of cellular lipidomes directly from crude extracts of biological samples. *Mass Spectrom Rev* **2005**, *24*, 367–412.

19. Li, N.; Liu, W.; Li, W.; Li, S.; Chen, X.; Bi, K.; He, P. Plasma metabolic profiling of Alzheimer's disease by liquid chromatography/mass spectrometry. *Clin. Biochem.* **2010**, *43*, 992–997.

20. González-Domínguez, R.; García-Barrera, T.; Gómez-Ariza, J.L. Combination of metabolomic and phospholipid-profiling approaches for the study of Alzheimer's disease. *J Proteomics* **2014**, *104*, 37–47.

21. Mapstone, M.; Cheema, A.K.; Fiandaca, M.S.; Zhong, X.; Mhyre, T.R.; MacArthur, L.H.; Hall, W.J.; Fisher, S.G.; Peterson, D.R.; Haley, J.M.; et al. Plasma phospholipids identify antecedent memory impairment in older adults. *Nat. Med.* **2014**, *20*, 415–418.

22. Nasreddine, Z.S.; Phillips, N.A.; Bédirian, V.; Charbonneau, S.; Whitehead, V.; Collin, I.; Cummings, J.L.; Chertkow, H. The Montreal Cognitive Assessment, MoCA: a brief screening tool for mild cognitive impairment. *J Am Geriatr Soc* **2005**, *53*, 695–699.
23. Bligh, E.G.; Dyer, W.J. A rapid method of total lipid extraction and purification. *Can J Biochem Physiol* **1959**, *37*, 911–917.
24. Kaluzny, M.A.; Duncan, L.A.; Merritt, M.V.; Epps, D.E. Rapid separation of lipid classes in high yield and purity using bonded phase columns. *J. Lipid Res.* **1985**, *26*, 135–140.
25. Chong, J.; Soufan, O.; Li, C.; Caraus, I.; Li, S.; Bourque, G.; Wishart, D.S.; Xia, J. MetaboAnalyst 4.0: towards more transparent and integrative metabolomics analysis. *Nucleic Acids Res.* **2018**, *46*, W486–W494.
26. MetaboAnalyst Available online: https://www.metaboanalyst.ca/ (accessed on Oct 2, 2019).
27. LIPID MAPS Lipidomics Gateway Available online: http://lipidmaps.org/ (accessed on Oct 27, 2019).
28. Human Metabolome Database Available online: http://www.hmdb.ca/ (accessed on Oct 27, 2019).
29. Bioanalytical Method Validation Guidance for Industry. **2018**, 44.
30. KEGG PATHWAY Database Available online: https://www.genome.jp/kegg/pathway.html (accessed on Oct 1, 2019).

31. van Oijen, M.; van der Meer, I.M.; Hofman, A.; Witteman, J.C.M.; Koudstaal, P.J.; Breteler, M.M.B. Lipoprotein-associated phospholipase A2 is associated with risk of dementia. *Ann. Neurol.* **2006**, *59*, 139–144.

32. Fitzpatrick, A.L.; Irizarry, M.C.; Cushman, M.; Jenny, N.S.; Chi, G.C.; Koro, C. Lipoprotein-associated phospholipase A2 and risk of dementia in the Cardiovascular Health Study. *Atherosclerosis* **2014**, *235*, 384–391.

33. Davidson, J.E.; Lockhart, A.; Amos, L.; Stirnadel-Farrant, H.A.; Mooser, V.; Sollberger, M.; Regeniter, A.; Monsch, A.U.; Irizarry, M.C. Plasma lipoprotein-associated phospholipase A2 activity in Alzheimer's disease, amnestic mild cognitive impairment, and cognitively healthy elderly subjects: a cross-sectional study. *Alzheimers Res Ther* **2012**, *4*, 51.

34. Frisardi, V.; Panza, F.; Seripa, D.; Farooqui, T.; Farooqui, A.A. Glycerophospholipids and glycerophospholipid-derived lipid mediators: a complex meshwork in Alzheimer's disease pathology. *Prog. Lipid Res.* **2011**, *50*, 313–330.

35. Ryan, S.D.; Whitehead, S.N.; Swayne, L.A.; Moffat, T.C.; Hou, W.; Ethier, M.; Bourgeois, A.J.G.; Rashidian, J.; Blanchard, A.P.; Fraser, P.E.; et al. Amyloid-beta42 signals tau hyperphosphorylation and compromises neuronal viability by disrupting alkylacylglycerophosphocholine metabolism. *Proc. Natl. Acad. Sci. U.S.A.* **2009**, *106*, 20936–20941.

36. Whiley, L.; Sen, A.; Heaton, J.; Proitsi, P.; García-Gómez, D.; Leung, R.; Smith, N.; Thambisetty, M.; Kloszewska, I.; Mecocci, P.; et al. Evidence of altered

phosphatidylcholine metabolism in Alzheimer's disease. *Neurobiol. Aging* **2014**, *35*, 271–278.

37. Conquer, J.A.; Tierney, M.C.; Zecevic, J.; Bettger, W.J.; Fisher, R.H. Fatty acid analysis of blood plasma of patients with Alzheimer's disease, other types of dementia, and cognitive impairment. *Lipids* **2000**, *35*, 1305–1312.
38. Niemoller, T.D.; Bazan, N.G. Docosahexaenoic acid neurolipidomics. *Prostaglandins Other Lipid Mediat.* **2010**, *91*, 85–89.
39. Cole, G.M.; Frautschy, S.A. Docosahexaenoic acid protects from amyloid and dendritic pathology in an Alzheimer's disease mouse model. *Nutr Health* **2006**, *18*, 249–259.
40. Quinn, J.F.; Raman, R.; Thomas, R.G.; Yurko-Mauro, K.; Nelson, E.B.; Van Dyck, C.; Galvin, J.E.; Emond, J.; Jack, C.R.; Weiner, M.; et al. Docosahexaenoic acid supplementation and cognitive decline in Alzheimer disease: a randomized trial. *JAMA* **2010**, *304*, 1903–1911.
41. Farooqui, A.A.; Horrocks, L.A.; Farooqui, T. Interactions between neural membrane glycerophospholipid and sphingolipid mediators: a recipe for neural cell survival or suicide. *J. Neurosci. Res.* **2007**, *85*, 1834–1850.
42. Mielke, M.M.; Haughey, N.J.; Bandaru, V.V.R.; Weinberg, D.D.; Darby, E.; Zaidi, N.; Pavlik, V.; Doody, R.S.; Lyketsos, C.G. Plasma sphingomyelins are associated with cognitive progression in Alzheimer's disease. *J. Alzheimers Dis.* **2011**, *27*, 259–269.

43. Lee, J.-T.; Xu, J.; Lee, J.-M.; Ku, G.; Han, X.; Yang, D.-I.; Chen, S.; Hsu, C.Y. Amyloid-beta peptide induces oligodendrocyte death by activating the neutral sphingomyelinase-ceramide pathway. *J. Cell Biol.* **2004**, *164*, 123–131.

44. Altman, R.; Rutledge, J.C. The vascular contribution to Alzheimer's disease. *Clin Sci (Lond)* **2010**, *119*, 407–421.

CHAPTER III

AN LC-MS/MS METHOD FOR DETERMINATION OF O^6-BENZYLGUANINE AND ITS METABOLITE O^6-BENZYL-8-OXOGUANINE IN HUMAN PLASMA

3.1 Introduction

The resistance mechanisms developed by the tumor cells pose a major challenge in the clinical treatment of various types of tumors such as malignant melanoma, malignant glioma, and lymphomas [1,2]. The most important resistance mechanism is mediated by the DNA-repair enzyme O^6-alkylguanine-DNA alkyltransferase (AGT) which plays an important role in the protection of tumor cells from the cytotoxicity of alkylnitrosoureas and methylating agents [3–6]. Increased AGT activity was reported in human solid tumors such as colon cancer, melanoma, lung cancer, etc. Studies have shown that the inactivation of AGT leads to the enhancement of the cytotoxic effects of chloroethyl nitrosoureas (e.g., carmustine) and methylating agents (e.g., dacarbazine and temozolomide) [7–9].

O^6-benzylguanine (O^6BG) is known to irreversibly inhibit cellular AGT activity; thus, it helps to increase the cytotoxic sensitivity of tumor cells to alkylating agents and halts the repair of the damaged DNA bases as shown in Fig. 3.1A. In vivo, O^6BG is rapidly metabolized into O^6-benzyl-8-oxoguanine (8-oxo-O^6BG) (Fig. 3.1B) which is equally potent inhibitors of AGT [10–14]. Therefore, to evaluate the efficacy of O^6BG, both O^6BG and 8-oxo-O^6BG must be measured simultaneously. Up to date, 34 clinical trials of O^6BG have been reported for various cancer treatments across the world at various phases of studies (https://clinicaltrials.gov/ct2/results?cond=&term=O6-benzylguanine&cntry=&state=&city=&dist=, accessed 25 July 2019). The goal of this work is to develop and validate an LC-MS/MS method for the measurement of O^6BG and 8-oxo-O^6BG in clinical samples. Although there were previously developed LC-DAD methods available, these methods suffered interference from endogenous components and other interfering drugs in plasma samples [15–17]. Furthermore, these LC-DAD methods used 500 µL aliquot of plasma and required 12.5 times of pre-concentration prior to sample analysis [15–17]. Since mass spectrometric detector possesses the unparalleled selectivity and specificity over those of diode array detector, the aforementioned problems of LC-DAD methods can be easily overcome.

In this work, we described the development and validation of a rapid and sensitive LC-MS/MS method for the quantitation of O^6BG and 8-oxo-O^6BG in human plasma. It uses 10.0 µL aliquot of human plasma, which is well-suited for pediatric studies with compared to the previously reported studies where 500 µL of pediatric plasma were used [18]. The developed method was applied for the measurement of O^6BG and 8-oxo-O^6BG

in human plasma samples from the prior phase I clinical trial. This method is the first fully validated LC-MS/MS method for the determination of O6BG and 8-oxo-O6BG.

3.2 Experimental

3.2.1. Chemicals and materials

The reference materials of O^6BG and 8-oxo-O^6BG in powder form were purchased from Sigma-Aldrich (St. Louis, MO, USA) and Toronto Chemical Research (North York, ON, Canada), respectively. O^6-(p-chlorobenzyl)guanine (pCl-O^6BG) used as internal standard (IS) was supplied by Dr. Robert Moschel, Frederick Cancer Research, and Development Center (Frederick, MD, USA). ACS-reagent-grade formic acid, sodium hydroxide, and ethyl acetate were purchased from Sigma-Aldrich. LC/MS-grade acetonitrile and LC/MS-grade methanol were purchased from Fischer Scientific (Pittsburgh, PA, USA). The pooled and six individual lots (Lot No.: 1M2070-02, 1M2070-04, 1M2070-06, 1M2070-05, 1M2070-03, 1M2070-01) of blank human plasmas were purchased from Innovative Research (Novi, MI, USA).

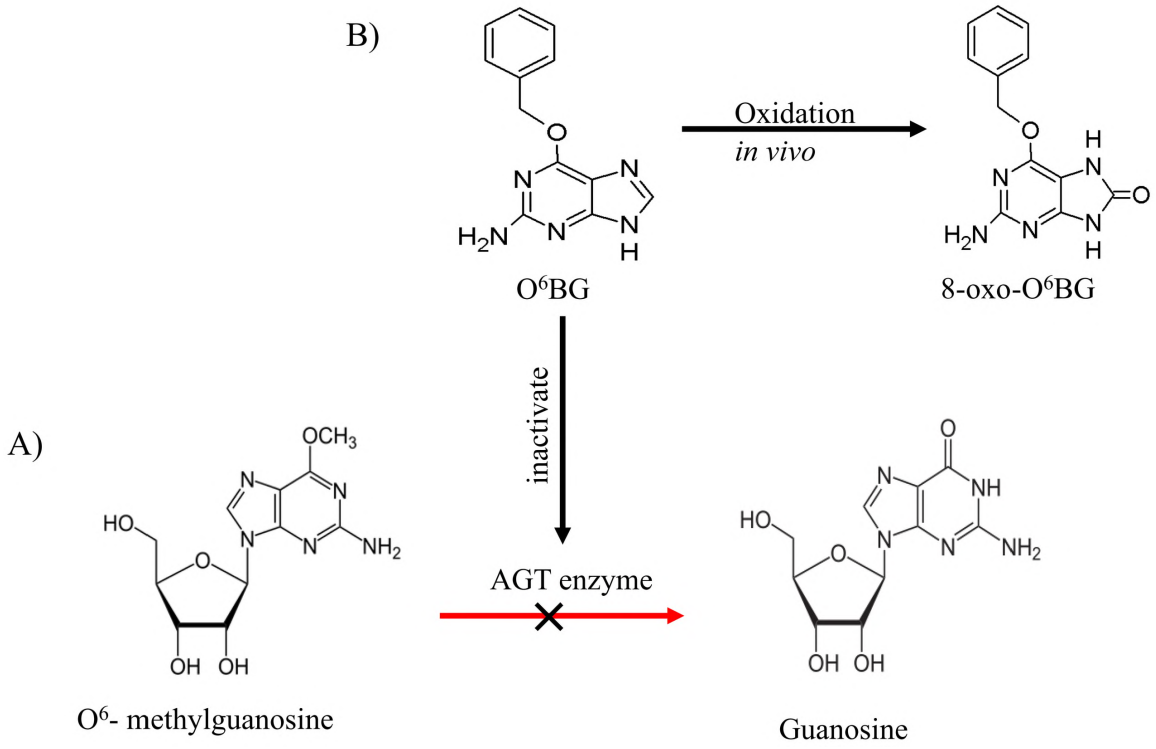

Figure 3.1. (A) Inhibition of DNA repair enzyme O6-alkylguanine-DNA alkyltransferase (AGT) by O^6BG , and (B) metabolism of O^6BG to 8-oxo-O^6BG.

3.2.2. Solutions

The stock standard solutions of O^6BG, 8-oxo-O^6BG, and pCl-O^6BG (IS) were prepared at 1.00 mg/mL by dissolving the appropriate amount of each compound in a known volume of methanol. The working stock standard solutions of O^6BG, 8-oxo-O^6BG, and pCl-O^6BG (IS) were prepared at the concentrations of 200, 250 and 10.0 µg/mL respectively by the serial dilution of each stock with methanol. All the stock and the working stock standard solutions were stored at -70° C in glass vials before use.

The solvent-mixed working standard solutions containing O^6BG/8-oxo-O^6BG at the concentrations of $4.00 \times 10^4/1.60 \times 10^5$, $5.00 \times 10^3/2.00 \times 10^4$, $3.75 \times 10^3/1.50 \times 10^4$, $2.50 \times 10^3/1.00 \times 10^4$, $1.25 \times 10^3/5.00 \times 10^3$, $5.00 \times 10^2/2.00 \times 10^3$, $250/1.00 \times 10^3$, 125/500, 75.0/300, 50.0/200, and 25.0/100 ng/mL were prepared by mixing the appropriate volumes of the working stock solutions in a known volume of methanol. The IS working solution of pCl-O^6BG was prepared at a concentration of 2.00×10^3 ng/mL by diluting the IS stock solution with a known volume of methanol. The mobile phase was prepared by mixing 80% acetonitrile and 0.05% formic acid in water (v/v). The solvent-mixed QCs (low, mid, high, and dilution) of O^6BG/8-oxo-O^6BG at the concentration of 3.75/15.0, 25.0/100, 188/750, $2.00 \times 10^3/8.00 \times 10^3$ ng/mL were prepared at room temperature by adding 5.00 µL each of the respective solvent-mixed working standard solution to 95.0 µL of the mobile phase in individual borosilicate glass tubes (13.0 × 100 mm), then vortexed for 5 s using MaxiMix II vortex mixer from Thermo Scientific.

3.2.3. Preparation of plasma calibrators and quality controls (QCs)

Plasma calibrators of O^6BG/8-oxo-O^6BG at the concentrations of 1.25/5.00, 2.50/10.0, 6.25/25.0, 12.5/50.0, 25.0/100, 62.5/250, 125/500, 250/1.00 × 10^3 ng/mL and the plasma QCs (low, mid, high and dilution) at the concentrations of 3.75/15.0, 25.0/100, 188/750, 2.00 × 10^3/8.00 × 10^3 ng/mL were prepared at room temperature by adding 5.00 µL each of the respective solvent-mixed working standard solution to 95.0 µL of the pooled blank human plasma in individual borosilicate glass tubes (13.0 × 100 mm), then vortexed for 5 s using MaxiMix II vortex mixer from Thermo Scientific. The calibrators and QCs were stored at -70° C before use. It is worth noting that the solvent-mixed working standard solutions for calibrators and QCs were prepared from two sets of independently prepared stock solutions of O^6BG and 8-oxo-O^6BG.

3.2.4. Sample preparation

Prior to extraction, patient samples, calibrators, and QCs stored at -70°C were thawed unassisted on ice. After vortexing, 10.0 µL aliquot of each patient plasma was mixed with 90.0 µL of the pooled human plasma to prepare 100 µL of a diluted patient sample in individual borosilicate glass tubes (13.0 × 100 mm). Then, 5.00 µL of the IS working solution was added to each 100 µL aliquot of the diluted patient samples, calibrators, and QCs in borosilicate glass tubes. All these glass tubes were vortexed for 5 s using a Multi-Tube Vortex Mixer from Troemner Precision Weights and Laboratory Equipment (Thorofare, NJ, USA) followed by the addition of 50.0 µL of 0.100 M sodium hydroxide solution and vortexed for another 5 s. These samples were subjected to liquid-

liquid extraction with ethyl acetate (1.50 mL to each tube) and vortexing for 5 min, followed by centrifugation at 1800 x g to facilitate phase separation. The top layer of organic content was transferred to another borosilicate glass tube and dried under nitrogen (15 psi) in a TurboVap LV evaporator from Caliper Life Sciences (Hopkinton, MA, USA) at 30°C for 15 min. The residue was reconstituted in 100 µL of the mobile phase and subjected to LC-MS/MS analyses.

3.2.5. LC-MS/MS system

The LC-MS system used for this work consisted of an LC-20AD HPLC unit with SIL-20AC autosampler from Shimadzu Scientific Instruments (Columbia, MD, USA) in conjunction with a Symmetry Shield RP18 column (2.1 mm x 100 mm, 3.5 µm) from Waters Corporation (Milford, MA, USA), and an API 3200 turbo-ion-spray triple quadrupole tandem mass spectrometer from AB Sciex (Foster City, CA, USA). The LC-MS system was controlled by AB Sciex Analyst software (version 1.5.1) which was used for both data acquisition and processing. The autosampler was maintained at 4°C with an injection volume of 5.00 µL of the reconstituted sample. Prior to sample analysis, the column was equilibrated with the mobile phase at a flow rate of 0.600 mL/min for 10 min. The analytes were then separated by the column and detected by the mass spectrometer with a total run time of 5 min per sample.

The mass spectrometer was operated in the positive turbo-ion-spray ionization mode. The molecular ions and its fragmentation pattern of O^6BG, 8-oxo-O^6BG and for pCl-O^6BG were determined using a solvent mixed standard solution at each concentration of 500 ng/mL. Flow injection analysis was used for the optimization of the compound-

dependent (i.e., declustering potential, entrance potential, collision energy, collision exit potential) and the source-dependent (i.e., curtain gas, collision assisted dissociation gas, ionization voltage, source temperature, sheath gas, desolvation gas). The mass transitions used for multiple-reaction-monitoring (MRM) mode were m/z 242.2 > 91.1 for O^6BG, m/z 258.2 > 91.1 for 8-oxo-O^6BG, and m/z 276.1 > 125.1 for pCl-O^6BG. The optimized parameters of the mass spectrometer were as follows: declustering potential at 50 V; entrance potential at 10 V, collision energy at 30 psi, collision exit potential at 13 V, curtain gas at 45 psi, collision assisted dissociation gas at 5 psi, ionization voltage at 5500 V, source temperature at 600°C, sheath gas at 35 psi, desolvation gas at 45 psi, and the quadrupole resolutions (Q1 and Q2) were set at unit. The LC column eluate was diverted to waste at 3.20 min and returned to mass spectrometer at the beginning of each run using a program-controlled switching valve of the instrument.

3.2.6. Method validation

3.2.6.1. Selectivity and lower limits of quantitation (LLOQs)

The experiments were performed to determine the selectivity and LLOQs of the method at the retention times and mass transitions of O^6BG, 8-oxo-O^6BG, and pCl-O^6BG. Six lots of blank human plasmas and corresponding plasma calibrators at LLOQ were used, which were prepared by the sample extraction procedure described in Section 3.2.4 and analyzed by five replicates per sample

3.2.6.2. Recovery and matrix factor (MF)

The absolute recovery of O^6BG or 8-oxo-O^6BG (or the IS) was determined by the mean peak area of O^6BG or 8-oxo-O^6BG (or the IS) at a specific concentration in human plasma over the mean peak area of O^6BG or 8-oxo-O^6BG (or the IS) at the same concentration in the extracted human plasma multiplying 100%. The IS normalized recovery was determined by the absolute recovery of O^6BG or 8-oxo-O^6BG over that of the IS multiplying 100%. For this study, O^6BG/8-oxo-O^6BG QCs at three concentrations (3.75/15.0, 25.0/100, 188/750 ng/mL) with a fixed concentration of the IS (100 ng/mL) were prepared in the pooled blank human plasma and the corresponding matrices of extracted pooled blank human plasma.

The absolute MF of O^6BG or 8-oxo-O^6BG (or the IS) was determined by the mean peak area of O^6BG or 8-oxo-O^6BG (or the IS) at a specified concentration in the extracted blank human plasma over that of O^6BG or 8-oxo-O^6BG (or the IS) at the same concentration in the mobile phase. The IS normalized MF was determined by the absolute MF of O^6BG or 8-oxo-O^6BG over that of the IS. For this study, O^6BG/8-oxo-O^6BG QCs at three concentrations (3.75/15.0, 25.0/100, 188/750 ng/mL) with a fixed concentration of the IS (100 ng/mL) were prepared in the six individual lots of blank human plasma and the mobile phase.

3.2.6.3. Calibration curve

The calibration curves of O^6BG and 8-oxo-O^6BG were obtained using a double blank human plasma (contains neither the analytes nor the IS), a single blank human plasma

(contains only the IS) and eight non-zero human plasma calibrators (with the IS) for O^6BG/8-oxo-O^6BG at the concentrations of 1.25/5.00, 2.50/10.0, 6.25/25.0, 12.5/50.0, 25.0/100, 62.5/250, 125/500, 250/1.00 × 10^3 ng/mL. These calibration curves were constructed by plotting the corresponding peak area ratios of O^6BG or 8-oxo-O^6BG to that of the IS as y-axis versus the respective concentrations of O6BG or 8-oxo-O6BG as x-axis by linear regression with $1/x^2$ weighting.

3.2.6.4. Accuracy, precision and dilution study

The intra-assay accuracy and precision were assessed by five replicate analyses of each QC sample of O^6BG/8-oxo-O^6BG at three different concentrations (3.75/15.0, 25.0/100, 188/750 ng/mL) in the same validation batch. The inter-assay accuracy and precision were evaluated by five parallel analyses of five identical QC samples of O^6BG/8-oxo-O^6BG at the three QC concentrations over five validation batches. Accuracy and precision were expressed as percent error (%RE) and coefficient of variation (CV). These studies were also conducted on the dilution QCs (O^6BG/8-oxo-O^6BG; 2.00 × 10^3/8.00 × 10^3 ng/mL), where they were prepared after 10-fold dilution using the pooled blank human plasma.

3.2.6.5. Stability studies

The stabilities of O^6BG and 8-oxo-O^6BG were investigated using the stock standard solutions of O^6BG and 8-oxo-O^6BG (1.00 mg/mL each), and the low and high plasma QCs of O^6BG and 8-oxo-O^6BG (3.75/15.0 and 188/750 ng/mL). The stock standard solutions were diluted according to the procedure described in Section 3.2.2 and

used to prepare the low and high solvent-mixed QCs of O^6BG/8-oxo-O^6BG (3.75/15.0 and 188/750 ng/mL) in the mobile phase prior to the instrumental analyses.

The stabilities of the stock standard solutions and the plasma QCs were assessed for short-term placement (6 and 24 h) on bench-top at 23°C and in the autosampler at 4°C (post preparative); three freeze-thaw cycles (where the samples were frozen at -20°C for at least 24 h and thawed at room temperature, 23°C, unassisted); and long-term storage (65 days) at -70°C. The stabilities of O^6BG and 8-oxo-O^6BG were determined with five replicates by comparing the mean-peak-area ratios of analytes to IS in the test sample to those of freshly prepared samples and expressed as percent recoveries.

3.2.7. Method application

The method developed was tested using the leftover patient samples from a previous phase I clinical trial of O^6BG (Stefan et al., 1996, 1997). Based on the clinical trial protocol, each patient received a 1-h bolus IV infusion of O^6BG at a dose of 23.5 mg/m^2. Blood samples were drawn from each patient prior to the infusion, and at intervals of 15 min during the 1-h infusion; then, blood samples were drawn post-infusion at 5 min intervals for 20 min, and at 30, 45, 60, 90 and 120 min, and subsequently at 4, 6, 8 12 and 24 h. Plasma samples were harvested from whole blood by a refrigerated centrifuge, and then stored at -80°C until analysis.

In clinical sample analysis, patient samples together with 10 calibrators (i.e. double- and single-blank, and eight nonzero) and a set of QCs at low, medium and high concentrations were prepared according to the procedures described in the Section 3.2.4, then analyzed by the procedure in the Section 3.2.5. The concentrations of patient samples

were back-calculated based on the dilution factor applied to the samples which was 10 in this work.

3.3. Results and Discussion

3.3.1. Method development

3.3.1.1. Sample preparation and extraction

In this work, plasma samples were thawed on ice to maintain the endogenous enzymatic activity at a minimal rate and to avoid interconversion between O^6BG and 8-oxo-O^6BG. Due to the relatively high concentrations of O^6BG and 8-oxo-O^6BG in patient samples in the O^6BG clinical trial (Stefan et al., 1997), only 10 μL of patient plasma was needed for instrumental analysis, which was subsequently diluted by 10 folds using the pooled blank plasma. This feature of the method would be advantageous for pediatric patients in comparison to the reported pediatric study of O^6BG (Neville et al., 2004b), where 500 μL of each plasma sample was used.

Prior to extraction, alkalinization of the plasma sample in 0.100 M sodium hydroxide was performed to deprotonate the analytes and to improve extraction efficiency. Ethyl acetate was chosen as the organic solvent for extraction of O^6BG, 8-oxo-O^6BG, and pCl-O^6BG, which had been proven to be effective in the previous studies (Stefan et al., 1996, 1997).

3.3.1.2. Mass spectrometric detection

Since O^6BG, 8-oxo-O^6BG and pCl-O^6BG can be protonated more easily than be deprotonated in mass spectrometry under acidic condition; therefore, positive ionization spectra were acquired in this work. As shown in Fig. 3.2 (A, C and E), the predominated molecular ions of O^6BG, 8-oxo-O^6BG and pCl-O^6BG were at m/z 242.2, m/z 258.2, m/z 276.1, respectively. These protonated molecular ions could be further fragmented in the collision cell of the triple quadrupole mass spectrometer by nitrogen gas and produced the predominant product ions at m/z 91.1 (tropylium cation, a fragment often found in aromatic compounds containing a benzyl unit) for both O^6BG and 8-oxo-O^6BG, and m/z 125.1 for pCl-O^6BG (Fig. 3.2.B, D and F). Hence, the mass transitions at m/z 242.2 > 91.1 for O^6BG, m/z 258.2 > 91.1 for 8-oxo-O^6BG, and m/z 276.1 > 125.1 for pCl-O^6BG were used for quantitation of O^6BG and 8-oxo-O^6BG using MRM mode

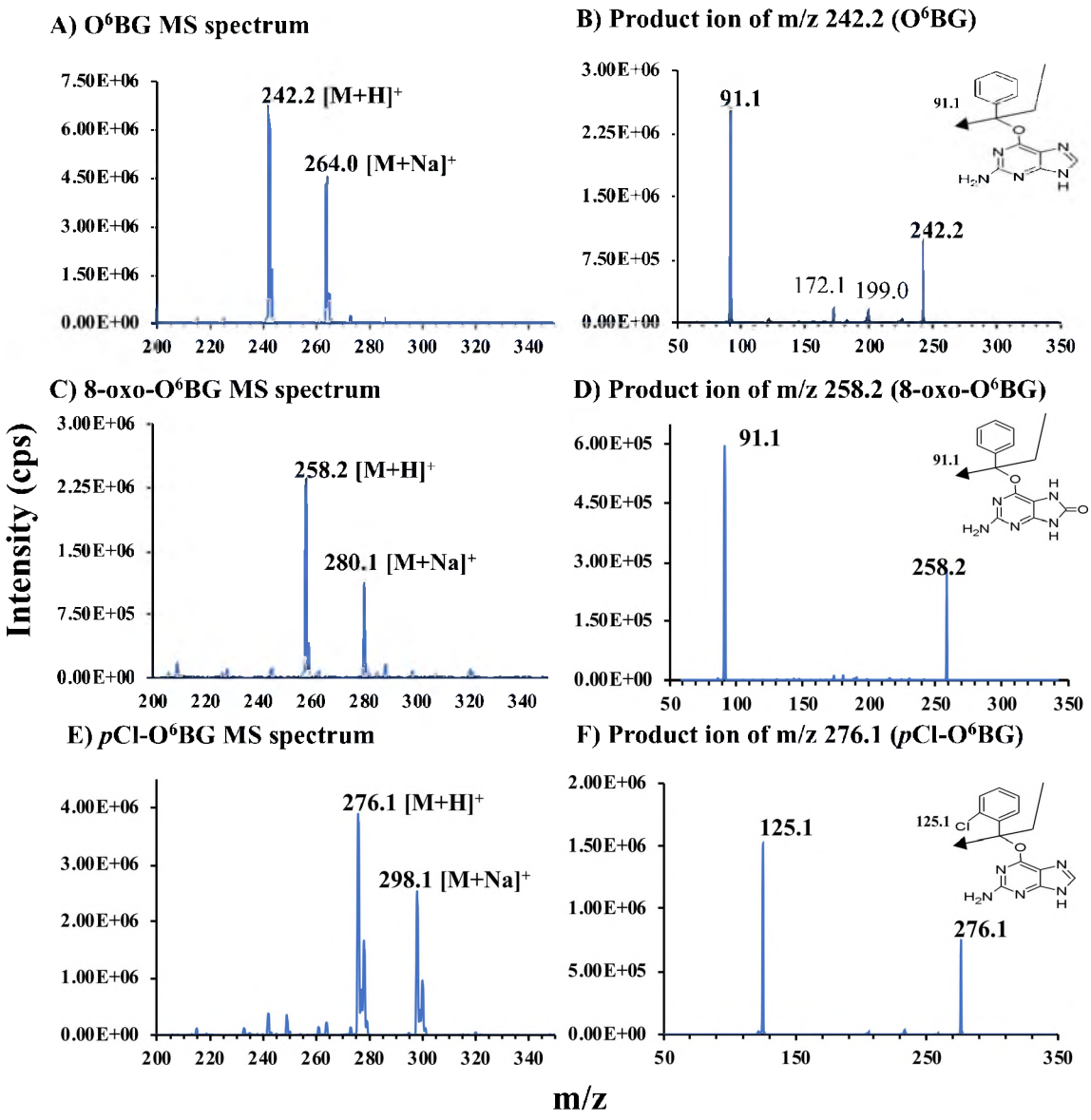

Figure. 3.2. The representative MS and MS/MS spectra of O^6BG (A and B), 8-oxo-O^6BG (C and D) and *p*Cl-O^6BG (E and F).

3.3.1.3. Liquid chromatographic separation

To achieve baseline resolution of the analytes and IS, different column chemistries and mobile phase compositions were investigated. Most of the columns tested resulted in broad and tailing peaks. The desirable peak shape with baseline separation of O^6BG, 8-oxo-O^6BG and pCl-O^6BG were achieved by isocratic elution on Waters Symmetry Shield RP18 column (2.1 mm x 100 mm, 3.5 μm) using the mobile phase consisting of 80% acetonitrile and 0.05% formic acid in water. As shown in Fig. 3.3, the retention times of the analytes (O^6BG and 8-oxo-O^6BG) were at 0.70 min, 2.60 min, and the IS (pCl-O^6BG) was at 1.80 min between the two analytes. In comparison to the previous method (Stefan et al., 1997), the method developed not only achieved the baseline resolution of all analytes with a much simpler elution profile, but also reduced the total run time from 11 min to 5 min.

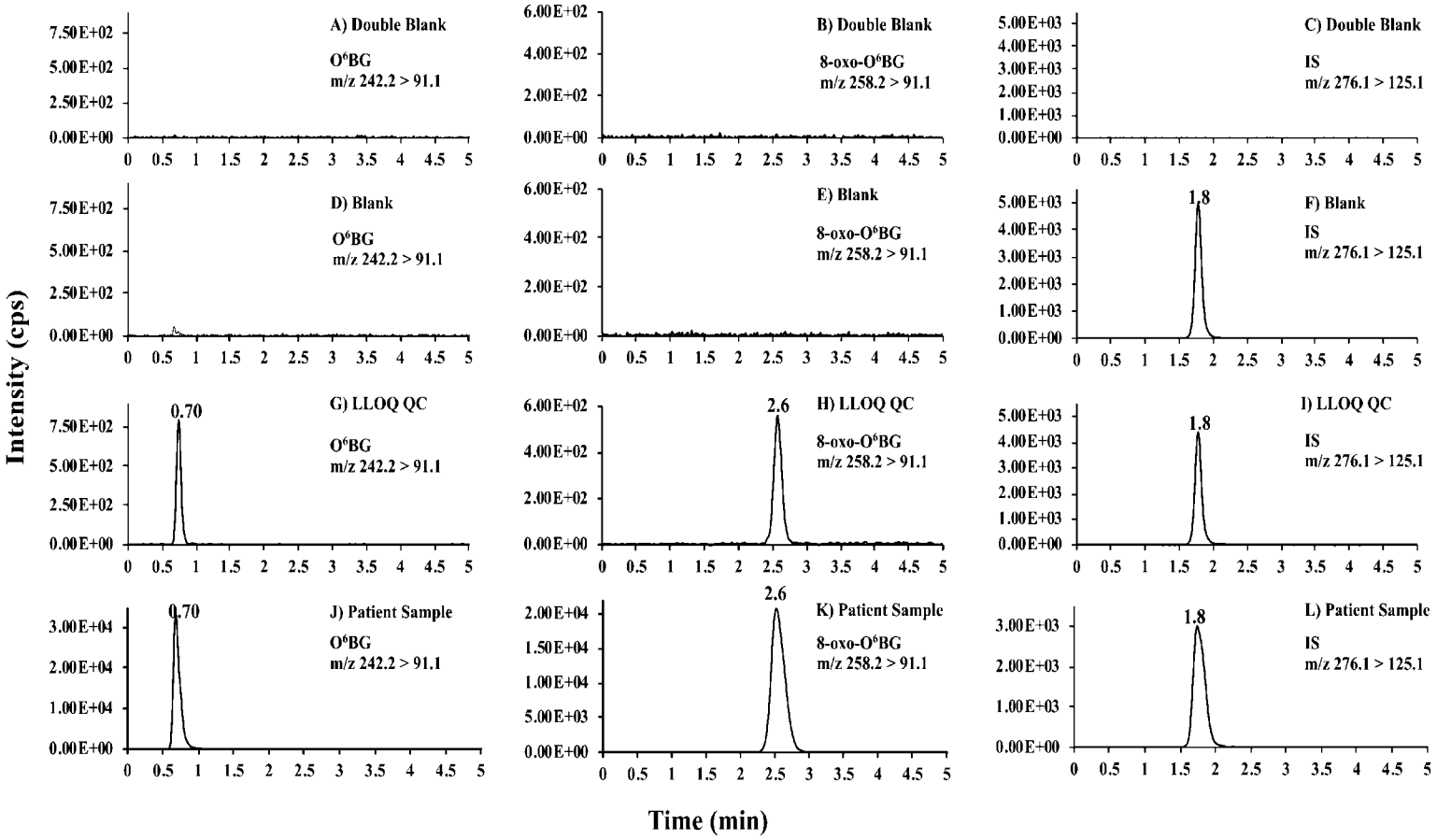

Figure. 3.3. The representative mass chromatograms of O^6BG, 8-oxo-O^6BG, and *p*Cl-O^6BG in the following samples: double blank pooled human plasma (A, B and C); blank pooled human plasma (D, E and F); human plasma at LLOQ (G, H and I); and a patient sample at 15-min time point (J, K and L).

3.3.2. Method validation

3.3.2.1. Selectivity and LLOQs

The selectivity of the method developed as illustrated in Fig. 3.3A, B and C, where there were no detectable interferences at the mass transitions and retention times of O^6BG, 8-oxo-O^6BG and pCl-O^6BG from the six individual lot blank plasmas and the pooled blank plasma, as well as from patient plasma before infusion of O^6BG. Furthermore, there were no detectable interferences from pCl-O^6BG at the mass transitions and retention times of O^6BG, 8-oxo-O^6BG (Fig. 3.3D, E, and F).

The LLOQs of the method defined as the lowest concentrations of plasma calibrators (Fig. 3.3G and H) were 1.25 ng/mL for O^6BG and 5.00 ng/mL for 8-oxo-O^6BG. As shown in Table 3.1, the accuracy and precision of the method at LLOQs from six individual lots of blank human plasma by five replicate measurements of each sample were $\leq \pm 2\%$ and $\leq 6\%$ for O^6BG, and $\leq \pm 6\%$ and $\leq 5\%$ for 8-oxo-O^6BG, respectively. These numbers were smaller than those of the industry limits set by US Food and Drug Administration ($\leq \pm 20$ and $\leq 20\%$) and implied that the actual LLOQs of the method could be lower if they were needed.

Table 3.1. Accuracy and precision of O^6BG and 8-Oxo-O^6BG at LLOQ in six individual lots of human plasma (n = 5)

Plasma matrix	O^6BG				8-oxo-O^6BG			
	$[X_N]^a$ (ng/mL)	$[\bar{X}]^b \pm SD^c$ (ng/mL)	CV^d (%)	RE^e (%)	$[X_N]$ (ng/mL)	$[\bar{X}] \pm SD$ (ng/mL)	CV (%)	RE (%)
Lot 1	1.25	1.24 ± 0.05	4	-1	5.00	4.7 ± 0.2	5	-5
Lot 2	1.25	1.22 ± 0.07	6	-2	5.00	5.1 ± 0.2	3	2
Lot 3	1.25	1.24 ± 0.02	2	-1	5.00	5.1 ± 0.2	4	2
Lot 4	1.25	1.23 ± 0.06	5	-2	5.00	5.2 ± 0.1	2	4
Lot 5	1.25	1.24 ± 0.08	6	-1	5.00	5.3 ± 0.1	2	6
Lot 6	1.25	1.24 ± 0.02	2	-1	5.00	5.1 ± 0.2	3	2

[a] $[X_N]$ = nominal concentration of analyte in plasma calibrator; [b] $[\bar{X}]$ = mean measured concentration of analyte; [c]SD = standard deviation of replicate measurements; [d]CV (%) = $\{SD/[\bar{X}]\} \times 100\%$; [e]RE = $\{([\bar{X}] - [X_N])/ [X_N]\} \times 100\%$.

3.3.2.2. Recovery and matrix effect

Recovery is a measure of an extraction efficiency of an analytical method within the limits of variability. The recoveries of O^6BG and 8-oxo-O^6BG at three different QC concentrations in human plasma were summarized in Table 3.2. The absolute recoveries of O^6BG and 8-oxo-O^6BG ranged 86-97% and 86-92%, respectively; whereas the IS normalized recoveries of O^6BG and 8-oxo-O^6BG ranged 90-96% and 90-99%. These results showed that ethyl acetate was a decent organic solvent for LLE for this work. The recoveries of analytes were consistent across the QCs and the IS normalized recoveries were closer to 100%.

Matrix effect is the effect of the coextracted matrix on the analytical signals which could be either suppressed or enhanced. If it is not corrected, the matrix effect could result in poor analytical accuracy, linearity, and reproducibility. The matrix effect in this work was assessed by matrix factor (MF). As shown in Table 3.3, the absolute MFs of O^6BG and 8-oxo-O^6BG ranged 0.96-1.02, and 0.93-1.05, respectively; whereas the IS normalized MFs of O^6BG and 8-oxo-O^6BG ranged 0.95-1.06, and 0.91-1.06. These results indicated the matrix effects on the analytical signals were negligible, which further proved the sample extraction procedure was practically effective.

Table 3.2. Recovery of O^6BG and 8-oxo-O^6BG in human pooled plasma (n = 5)

O^6BG				8-oxo-O^6BG			
$[X_N]$ (ng/mL)	$Recovery_X$[a] ± SD (%)	$Recovery_{IS}$[b] ± SD (%)	IS Normalized Recovery[c] ± SD (%)	$[X_N]$ (ng/mL)	$Recovery_X$ ± SD (%)	$Recovery_{IS}$ ± SD (%)	IS Normalized Recovery ± SD (%)
3.75	97 ± 2	102 ± 4	95 ± 6	15.0	92 ± 2	102 ± 4	90 ± 5
25.0	86 ± 1	96 ± 4	90 ± 5	100	86 ± 2	96 ± 4	90 ± 6
188	89 ± 3	93 ± 3	96 ± 6	750	92 ± 2	93 ± 3	99 ± 5

[a] $Recovery_X$ = [(mean peak area of spiked analyte in human plasma)/(mean peak area of spiked analyte in extracted human plasma)] × 100%; [b] $Recovery_{IS}$ = [(mean peak area of spiked IS in human plasma)/(mean peak area of spiked IS in extracted human plasma)] × 100%; [c] IS Normalized Recovery = ($Recovery_X$/$Recovery_{IS}$) × 100%

Table 3.3. Matrix factors of O^6BG and 8-oxo-O^6BG in six individual lots of human plasma (n = 5)

Plasma matrix	O^6BG				8-oxo-O^6BG			
	$[X_N]$ (ng/mL)	MF_X[a] ± SD	MF_{IS}[b] ± SD	IS Normalized MF[c] ± SD	$[X_N]$ (ng/mL)	MF_X ± SD	MF_{IS} ± SD	IS Normalized MF ± SD
Lot 1	3.75	0.96 ± 0.01	0.94 ± 0.02	1.02 ± 0.03	15.0	0.94 ± 0.05	0.94 ± 0.02	1.00 ± 0.07
	25.0	0.99 ± 0.01	0.96 ± 0.03	1.03 ± 0.04	100	0.94 ± 0.04	0.96 ± 0.03	0.98 ± 0.07
	188	0.99 ± 0.02	1.00 ± 0.04	0.99 ± 0.06	750	0.95 ± 0.06	1.00 ± 0.04	0.95 ± 0.10
Lot 2	3.75	1.00 ± 0.03	1.01 ± 0.02	0.99 ± 0.05	15.0	0.95 ± 0.03	1.01 ± 0.02	0.94 ± 0.05
	25.0	0.99 ± 0.02	0.96 ± 0.02	1.03 ± 0.04	100	0.98 ± 0.01	0.96 ± 0.02	1.02 ± 0.03
	188	0.98 ± 0.02	0.99 ± 0.03	0.99 ± 0.05	750	1.05 ± 0.02	0.99 ± 0.03	1.06 ± 0.05
Lot 3	3.75	0.99 ± 0.03	1.01 ± 0.01	0.98 ± 0.04	15.0	0.93 ± 0.03	1.01 ± 0.01	0.92 ± 0.04
	25.0	0.98 ± 0.01	0.96 ± 0.02	1.02 ± 0.03	100	0.94 ± 0.04	0.96 ± 0.02	0.98 ± 0.06
	188	1.02 ± 0.02	0.96 ± 0.03	1.06 ± 0.05	750	0.94 ± 0.03	0.96 ± 0.03	0.98 ± 0.06
Lot 4	3.75	1.01 ± 0.02	0.98 ± 0.04	1.03 ± 0.06	15.0	1.04 ± 0.02	0.98 ± 0.04	1.06 ± 0.06
	25.0	0.98 ± 0.04	1.02 ± 0.02	0.96 ± 0.06	100	0.98 ± 0.04	1.02 ± 0.02	0.96 ± 0.06
	188	0.98 ± 0.03	0.99 ± 0.01	0.99 ± 0.04	750	1.01 ± 0.01	0.99 ± 0.01	1.02 ± 0.02
Lot 5	3.75	0.97 ± 0.02	0.98 ± 0.02	0.99 ± 0.04	15.0	0.94 ± 0.04	0.98 ± 0.02	0.96 ± 0.06
	25.0	0.98 ± 0.03	0.99 ± 0.01	0.99 ± 0.04	100	0.99 ± 0.02	0.99 ± 0.01	1.00 ± 0.03
	188	0.99 ± 0.03	0.94 ± 0.03	1.05 ± 0.07	750	0.95 ± 0.04	0.94 ± 0.03	1.01 ± 0.07
Lot 6	3.75	1.02 ± 0.01	0.98 ± 0.03	1.04 ± 0.04	15.0	0.94 ± 0.05	0.98 ± 0.03	0.96 ± 0.08
	25.0	0.99 ± 0.02	1.02 ± 0.04	0.97 ± 0.06	100	0.93 ± 0.05	1.02 ± 0.04	0.91 ± 0.08
	188	0.96 ± 0.03	1.01 ± 0.03	0.95 ± 0.06	750	0.95 ± 0.06	1.01 ± 0.03	0.94 ± 0.09

[a] MF_X = (mean peak area of analyte in the extracted plasma)/(mean peak area of analyte in the mobile phase)
[b] MF_{IS} = (mean peak area of IS in the extracted plasma)/(mean peak area of IS in the mobile phase)
[c] IS normalized MF = MF_X/MF_{IS}

3.3.2.3. Calibration curve

The calibration equations for O^6BG and 8-oxo-O^6BG derived from three batches of calibrators in three validation days were y = 0.044 (±0.001)x + 0.069 (±0.003) with a correlation coefficient of 0.999 for O^6BG, and y = 0.186 (±0.005)x + 0.003 (±0.001) with a correlation coefficient of 0.999 for 8-oxo-O^6BG. The accuracy and precision of individual calibrators as shown in Table 3.4 were ≤ ±4% and ≤ 3% for O^6BG, and ≤ ±6% and ≤ 3% for 8-oxo-O^6BG, respectively.

3.3.2.4. Accuracy, precision and dilution integrity

Accuracy of an analytical method is described as the closeness of the mean measured obtained by the method to the nominal value (concentration) of an analyte, and precision of an analytical method is described as the closeness of individual measurement of an analyte when the method is repeatedly applied to a single sample. Dilution integrity refers to the ability to dilute a sample with blank matrix prior to the analyses of analytes at concentrations higher than those of the upper limits of quantitation (ULOQs) into the calibration ranges of the analytes and obtain an accurate estimate of the concentrations prior to dilution.

In this work, the accuracy, precision and dilution integrity of the method was assessed using low, mid, high and dilution QC samples. As shown in Table 3.5, the intra-day accuracy and precision were ≤ |2|% and ≤ 3% for O^6BG, and ≤ |5|% and ≤ 3% for 8-oxo-O^6BG; whereas the inter-day accuracy and precision were ≤ |6|% and ≤ 4% for O^6BG, and ≤ |7|% and ≤ 4% for 8-oxo-O^6BG, respectively. These results indicated the method developed was accurate and precise, and the integrity of the plasma sample was not affected by sample dilution.

Table 3.4. Accuracy and precision of O^6BG and 8-Oxo-O^6BG plasma calibrators in five validation batches

O^6BG				8-Oxo-O^6BG			
$[X_N]$[a] (ng/mL)	$[\bar{X}]$[b] ± SD[c] (ng/mL)	CV[d] (%)	RE[e] (%)	$[X_N]$ (ng/mL)	$[\bar{X}]$ ± SD (ng/mL)	CV (%)	RE (%)
1.25	1.27 ± 0.03	2	2	5.00	5.14 ± 0.06	1	3
2.50	2.41 ± 0.07	3	-4	10.0	9.70 ± 0.04	1	-3
6.25	6.25 ± 0.05	1	0	25.0	24.3 ± 0.4	2	-3
12.5	12.6 ± 0.2	2	1	50.0	53 ± 1	2	6
25.0	25.3 ± 0.5	2	1	100	102 ± 3	3	2
62.5	62 ± 1	2	0	250	254 ± 5	2	2
125	124 ± 3	2	-1	500	501 ± 9	2	0
250	248 ± 7	3	-1	1.00×10^3	$(1.02 \pm 0.01) \times 10^3$	1	2

[a]$[X_N]$ = nominal concentration of analyte in plasma calibrator; [b]$[\bar{X}]$ = mean measured concentration of analyte; [c]SD = standard deviation of replicate measurements; [d]CV (%) = (SD/$[\bar{X}]$) × 100%; [e]RE = {($[\bar{X}]$ – $[X_N]$)/ $[X_N]$} × 100%

Table 3.5. Intra- and inter-assay accuracy and precision of O^6BG and 8-oxo-O^6BG in human pooled plasma (n = 5)

Intra-assay[a]							
O^6BG				8-oxo-O^6BG			
$[X_N]$ (ng/mL)	$[\bar{X}] \pm SD$ (ng/mL)	CV (%)	RE (%)	$[X_N]$ (ng/mL)	$[\bar{X}] \pm SD$ (ng/mL)	CV (%)	RE (%)
1.25	1.24 ± 0.01	0	-1	5.00	5.0 ± 0.3	6	1
3.75	3.71 ± 0.01	0	-1	15.0	14.3 ± 0.5	3	-5
25.0	24.6 ± 0.8	3	-2	100	99 ± 1	1	-1
188	190 ± 2	1	1	750	745 ± 8	1	-1
2.00×10^3	$(2.00 \pm 0.02) \times 10^3$	1	0	8.00×10^3	$(7.99 \pm 0.02) \times 10^3$	0.3	-0.1

Inter-assay[b]							
O^6BG				8-oxo-O^6BG			
$[X_N]$ (ng/mL)	$[\bar{X}] \pm SD$ (ng/mL)	CV (%)	RE (%)	$[X_N]$ (ng/mL)	$[\bar{X}] \pm SD$ (ng/mL)	CV (%)	RE (%)
1.25	1.23 ± 0.01	1	2	5.00	5.1 ± 0.1	1	3
3.75	3.6 ± 0.1	3	-3	15.0	14.0 ± 0.5	4	-7
25.0	23 ± 1	4	-6	100	96 ± 2	2	-4
188	185 ± 4	2	-2	750	745 ± 10	1	-1
2.00×10^{3c}	$(2.01 \pm 0.01) \times 10^3$	0.5	0.5	8.00×10^{3c}	$(7.99 \pm 0.02) \times 10^3$	0.3	-0.1

[a] Measured by five replicate measurements of each QC sample within a validation batch.
[b] Measured by five parallel measurements of five identical QC samples at each concentration over five validation batches.
[c] Dilution QC was measured after 10x dilution with pooled blank human plasma.

3.3.2.5. Stability studies

The stability studies for O^6BG and 8-oxo-O^6BG were conducted, and the results were summarized in Table 3.6. Our data showed that at room temperature on the bench-top, the stock solutions and plasma QCs were stable for at least 24 h and had the recoveries of 95-98% and 93-100% for O^6BG; and 99-101% and 95-99% for 8-oxo-O^6BG. In the autosampler (post-preparative) at 4°C, the plasma QCs were stable for at least 24 h and had the recoveries of 92-99% for O^6BG, and 92-102% for 8-oxo-O^6BG. In the freeze-thaw-cycle study, the plasma QCs had the recoveries of 96-103% for O^6BG, and 96-102% for 8-oxo-O^6BG. Furthermore, in the long-term storage (65 days at -70°C), the plasma QCs had the recoveries of 95-99% for O^6BG, and 95-97% for 8-oxo-O^6BG. These data indicated that O^6BG and 8-oxo-O^6BG were stable under all test conditions and showed no sign of sample degradation.

Table 3.6. Stabilities of O^6BG and 8-oxo-O^6BG under various test conditions (n = 5)

Condition	Temperature	Sample	Recovery ± SD (%)			
			O^6BG		8-oxo-O^6BG	
			6 h	24 h	6 h	24 h
Bench-top	23°C	Stock solution[a]	95 ± 2	98 ± 1	101 ± 3	101 ± 2
		Stock solution[b]	96 ± 2	95 ± 2	99 ± 1	100 ± 3
Bench-top	23°C	Low QC[c]	100 ± 2	98 ± 4	96 ± 1	99 ± 2
		High QC[c]	93 ± 1	95 ± 3	95 ± 2	95 ± 2
Autosampler	4°C	Low QC	99 ± 2	92 ± 4	102 ± 3	93 ± 2
		High QC	96 ± 3	96 ± 2	99 ± 2	92 ± 1
3 Freeze-thaw cycles	-70°C to 23°C	Low QC	102 ± 2		96 ± 4	
		High QC	103 ± 4		101 ± 3	
Long-term storage (65 days)	-80°C	Low QC	95 ± 5		95 ± 4	
		High QC	99 ± 4		97 ± 2	

[a] The concentrations of O^6BG and 8-oxo-O^6BG stock solutions were measured after serial dilution to prepare a mixed working standard solution at concentrations of 3.75 ng/mL and 15.0 ng/mL for O^6BG and 8-oxo-O^6BG, respectively.

[b] The concentrations of O^6BG and 8-oxo-O^6BG stock solutions were measured after serial dilution to prepare a mixed working standard solution at concentrations of 188 ng/mL and 750 ng/mL for O^6BG and 8-oxo-O^6BG, respectively.

[c] The concentrations of low and high plasma QCs of O^6BG/8-oxo-O^6BG were 3.75/15.0 ng/mL and 188/750 ng/mL, respectively.

3.3.3 Method application

The applicability of method developed was tested by the measurement of O^6BG and 8-oxo-O^6BG concentrations in patient plasma samples collected from a previous phase I clinical trial of O6BG (Stefan et al., 1997). These samples were collected, prepared, and analyzed as the procedures described in Section 3.2.7. Fig. 3.4 showed the O^6BG and 8-oxo-O^6BG concentration–time profiles in a patient by a 1-h bolus infusion of O^6BG at a dose of 23.5 mg/m^2. Compared to the HPLC-DAD method developed in the previous work (Stefan et al., 1997), the LC-MS/MS method implemented in this work not only could produce comparable concentration-time profiles for O^6BG and 8-oxo-O^6BG in the patient, but also required much less sample and analysis time, and showed no interference from co-eluted compounds in sample matrix. Therefore, the LC-MS/MS method developed is a better method for the clinical study of O^6BG, especially when the patient sample size is small and analyte concentrations are low.

3.4. Conclusion

In this work, an LC-MS/MS method has been developed and validated for the measurement of O^6BG and its metabolite 8-oxo-O^6BG in human plasma, which employs LLE for sample extraction, reverse phase chromatography for analyte separation, and tandem mass spectrometry for analyte detection and quantitation. This method is rapid, sensitive and selective. It has linear calibration ranges of 1.25-250 ng/mL and 5.00-1.00 x 10^3 ng/mL for O^6BG and 8-oxo-O^6BG, respectively. The method uses only 10.0 μL of patient plasma sample per analysis and is well-suited for pediatric studies and clinical trials where the sample volume is small and analyte concentrations are low. The method

developed was tested using patient plasma samples from a prior phase I clinical trial and the results were comparable with those obtained by the LC-DAD method.

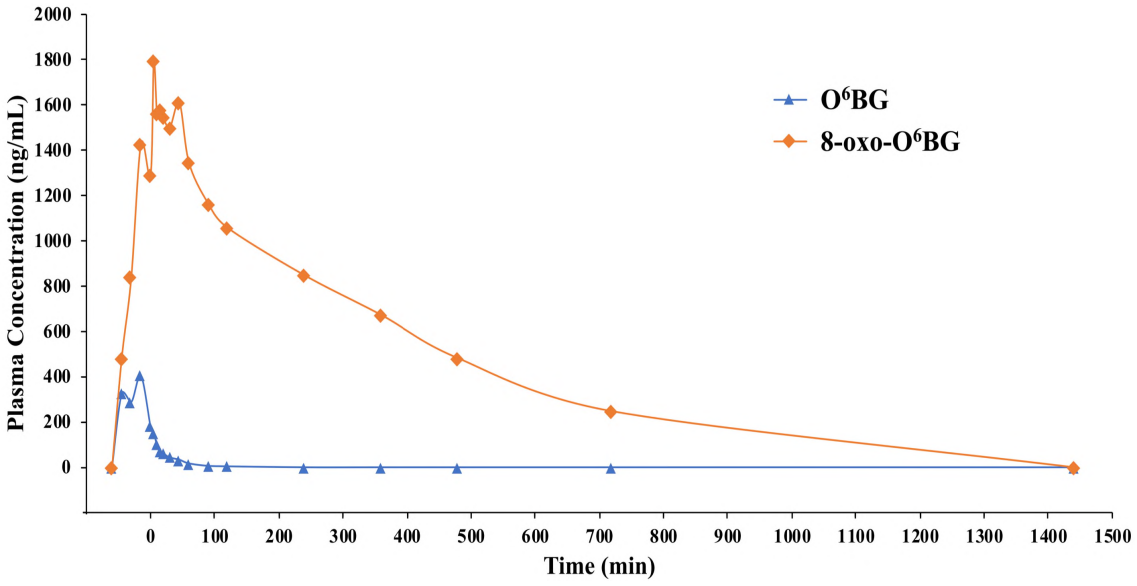

Figure. 3.4. The concentration-time profiles of O^6BG and 8-oxo-O^6BG in a patient who received a 1-h bolus IV-infusion of O^6BG at a dose of 23.5 mg/m^2.

3.5 REFERENCES

1. Housman, G.; Byler, S.; Heerboth, S.; Lapinska, K.; Longacre, M.; Snyder, N.; Sarkar, S. Drug resistance in cancer: an overview. Cancers (Basel) **2014**, 6, 1769–1792.
2. Okada, H.; Kohanbash, G.; Zhu, X.; Kastenhuber, E.R.; Hoji, A.; Ueda, R.; Fujita, M. Immunotherapeutic approaches for glioma. Crit. Rev. Immunol. **2009**, 29, 1–42.
3. Hotta, T.; Saito, Y.; Fujita, H.; Mikami, T.; Kurisu, K.; Kiya, K.; Uozumi, T.; Isowa, G.; Ishizaki, K.; Ikenaga, M. O6-alkylguanine-DNA alkyltransferase activity of human malignant glioma and its clinical implications. J. Neurooncol. **1994**, 21, 135–140.
4. Saad, A.A.; Kassem, H.S.; Povey, A.C.; Margison, G.P. Expression of O-Alkylguanine-DNA Alkyltransferase in Normal and Malignant Bladder Tissue of Egyptian Patients. J Nucleic Acids **2010**, 2010, 840230.
5. Maxwell, J.A.; Johnson, S.P.; Quinn, J.A.; McLendon, R.E.; Ali-Osman, F.; Friedman, A.H.; Herndon, J.E.; Bierau, K.; Bigley, J.; Bigner, D.D.; et al. Quantitative analysis of O6-alkylguanine-DNA alkyltransferase in malignant glioma. Mol. Cancer Ther. **2006**, 5, 2531–2539.
6. Mitra, S. MGMT: a personal perspective. DNA Repair (Amst.) **2007**, 6, 1064–1070.
7. Apisarnthanarax, N.; Wood, G.S.; Stevens, S.R.; Carlson, S.; Chan, D.V.; Liu, L.; Szabo, S.K.; Fu, P.; Gilliam, A.C.; Gerson, S.L.; et al. Phase I clinical trial of O6-benzylguanine and topical carmustine in the treatment of cutaneous T-cell lymphoma, mycosis fungoides type. Arch Dermatol **2012**, 148, 613–620.

8. Wedge, S.R.; Porteous, J.K.; Newlands, E.S. 3-aminobenzamide and/or O6-benzylguanine evaluated as an adjuvant to temozolomide or BCNU treatment in cell lines of variable mismatch repair status and O6-alkylguanine-DNA alkyltransferase activity. Br. J. Cancer **1996**, 74, 1030–1036.

9. Zhu, R.; Liu, M.-C.; Luo, M.-Z.; Penketh, P.G.; Baumann, R.P.; Shyam, K.; Sartorelli, A.C. 4-nitrobenzyloxycarbonyl derivatives of O(6)-benzylguanine as hypoxia-activated prodrug inhibitors of O(6)-alkylguanine-DNA alkyltransferase (AGT), which produces resistance to agents targeting the O-6 position of DNA guanine. J. Med. Chem. **2011**, 54, 7720–7728.

10. Long, L.; Moschel, R.C.; Dolan, M.E. Debenzylation of O(6)-benzyl-8-oxoguanine in human liver: implications for O(6)-benzylguanine metabolism. Biochem. Pharmacol. **2001**, 61, 721–726.

11. Berg, S.L.; Murry, D.J.; McCully, C.L.; Godwin, K.; Balis, F.M. Pharmacokinetics of O6-benzylguanine and its active metabolite 8-oxo-O6-benzylguanine in plasma and cerebrospinal fluid after intrathecal administration of O6-benzylguanine in the nonhuman primate. Clin. Cancer Res. **1998**, 4, 2891–2894.

12. Neville, K.; Blaney, S.; Bernstein, M.; Thompson, P.; Adams, D.; Aleksic, A.; Berg, S. Pharmacokinetics of O(6)-benzylguanine in pediatric patients with central nervous system tumors: a pediatric oncology group study. Clin. Cancer Res. **2004**, 10, 5072–5075.

13. Ewesuedo, R.B.; Wilson, L.R.; Friedman, H.S.; Moschel, R.C.; Dolan, M.E. Inactivation of O6-alkylguanine-DNA alkyltransferase by 8-substituted O6-benzylguanine analogs in mice. Cancer Chemother. Pharmacol. **2001**, 47, 63–69.

14. Tserng, K.-Y.; Ingalls, S.T.; Boczko, E.M.; Spiro, T.P.; Li, X.; Majka, S.; Gerson, S.L.; Willson, J.K.; Hoppel, C.L. Pharmacokinetics of O6-benzylguanine (NSC637037) and its metabolite, 8-oxo-O6-benzylguanine. J Clin Pharmacol **2003**, 43, 881–893.

15. Stefan, T.L.; Ingalls, S.T.; Minkler, P.E.; Willson, J.K.; Gerson, S.L.; Spiro, T.P.; Hoppel, C.L. Simultaneous determination of O6-benzylguanine and 8-oxo-O6-benzylguanine in human plasma by reversed-phase high-performance liquid chromatography. J. Chromatogr. B Biomed. Sci. Appl. **1997**, 704, 289–298.

16. Stefan, T.L.; Ingalls, S.T.; Gerson, S.L.; Willson, J.K.; Hoppel, C.L. Determination of O6-benzylguanine in human plasma by reversed-phase high-performance liquid chromatography. J. Chromatogr. B, Biomed. Appl. **1996**, 681, 331–338.

17. Long, L.; McCabe, D.R.; Dolan, M.E. Determination of 8-oxoguanine in human plasma and urine by high-performance liquid chromatography with electrochemical detection. J. Chromatogr. B Biomed. Sci. Appl. **1999**, 731, 241–249.

18. Neville, K.; Blaney, S.; Bernstein, M.; Thompson, P.; Adams, D.; Aleksic, A.; Berg, S. Pharmacokinetics of O(6)-benzylguanine in pediatric patients with central nervous system tumors: a pediatric oncology group study. Clin. Cancer Res. **2004**, 10, 5072–5075.

CHAPTER IV

FUTURE DIRECTIONS

4.1. In-Quest of biomarkers for Alzheimer's Disease in Human Plasma using Liquid Chromatography in tandem with High Resolution Mass Spectrometry (Quadrapole Time-of-Flight(Q-TOF))

4.1.1 Bioanalytical

The work in this study had detailed the workflow for the untargeted discovery of the probabilistic biomarkers in Alzheimer's disease (AD) using the lipidomics approach and bioinformatics tools [1,2]. This study was a pilot study to establish the probabilistic biomarkers in AD that are Up- and Down-regulated. We found a total of 28 statistically significant identified lipids, including LPC, PC, SM, and TG, and a total of 31 unidentified features that were Up- and Down-regulated. Thought the study is warranted on the number of study subjects in each condition (AD = 4 and NCC =3), a similar approach can be employed to study in the larger cohort for the confirmation of these probabilistic biomarkers of the AD disease. As well, this work can be extended by evaluating the

usefulness of the reported potential biomarkers in predicting the early onset of AD. It can be performed by the identification, quantitation, and validation of these plasma lipid biomarkers in AD-P and MCI-AD stages using the methodology described in this work. Longitudinal studies are to be performed to study the transitions and phenoconversion of these biomarkers in the progression of the disease. Further, using the same sample sets, targeted discovery experiments can be performed, and then targeted validation is to be performed on the panel of probabilistic biomarkers [15]. Thus, the validated biomarkers can be used as a panel for predicting the preclinical stage of the AD for the early intervention treatment. For further deeper understanding at the pathway level, pathway analysis, and correlation of the enzymes responsible for these aberrations at lipid levels are to be investigated in the AD disease models by performing biological experiments.

In this study, we were able to identify, 148 and 108 lipid species in phospholipid fraction (PL) and neutral lipid fraction (NL). Since lipids are complex molecules with fatty acids as side chains, reverse phase chromatography employed in this study suffers from not able to separate the isobaric peaks as it co-elutes the lipids of similar polarity. This issue can be addressed either by employing the ion mobility as a front end to MS detection [3–5] or by using the normal phase chromatography, HILIC chromatography [6–8], to fractionate each subclass of lipids then analyze them using reverse phase chromatography. Co-elution of the isobaric peaks challenges the MS detector to detect the low abundant oxidized species.

It is evident and established in the AD disease that neuroinflammation is the process that begins earlier the disease diagnosis [9]. During the inflammatory process, lipids undergo oxidation and form the oxidized lipids, which are indicators of the biological stress and serves as a biomarker in many acute and chronic inflammation conditions [10]. Hence there is a vast scope for the quantitation of these lipids and to compare the lipid profiles of oxidized products vs. their precursors. The availability of the isotopes labeled lipid standards, and cost serves the major

limitation for these types of studies. The current methodology fails to determine the location of the double bonds in the fatty acyl chain and the position of the fatty acids attached to the glycerol backbone in the complex lipid. Techniques like ozone induced dissociation of the double bonds [11], Silver ion chromatography [12,13], and selective deuteration [14] that assist in the location of the double bonds can be employed to address the unsaturation location in the lipids.

4.1.2 Molecular biology

By the action of the phospholipases enzymes as shown in Fig 4.1, phospholipids are constantly being remodeled in terms of fatty acyl side chains, polar head groups and generation of secondary messengers.

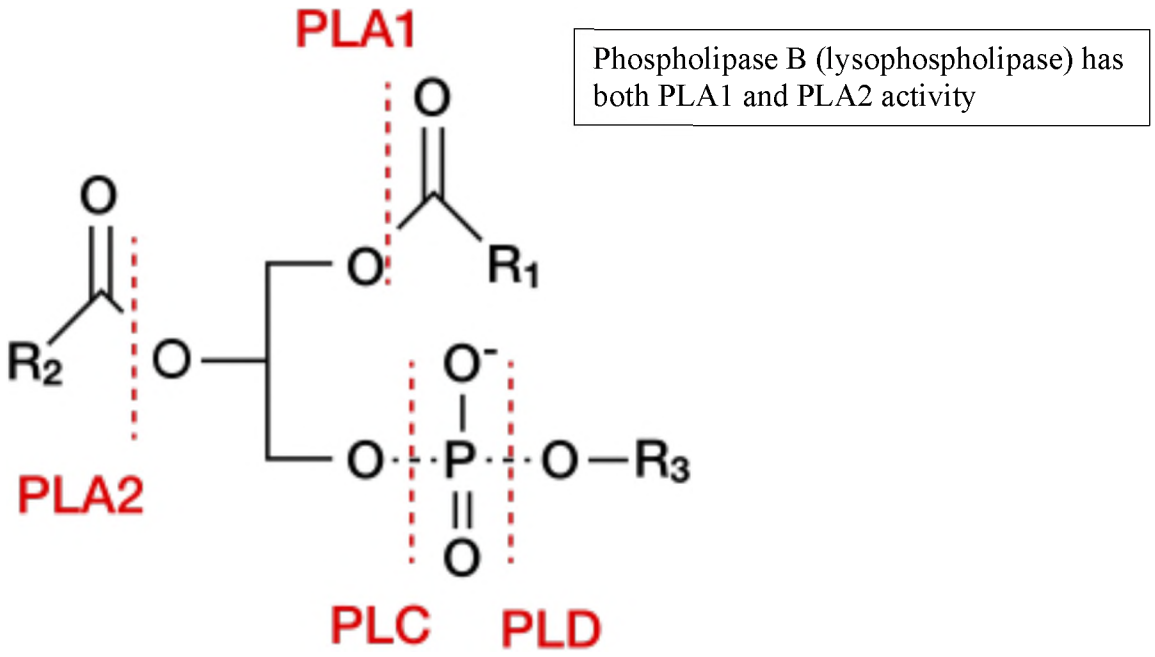

Fig. 4.1. Phospholipase enzymes and site of action.

PLA1: Phospholipase A1, PLA2: Phospholipase A2, PLC: Phospholipase C, PLD: Phospholipase D, R_1 and R_2: fatty acyl side chains, R_3: phospholipid head group

As shown in the Fig 2.5 and 2.6 , *PLD, PLA* and *PLC* genes/ enzymes play crucial role in the AD. Variants of PLD has been involved with APP and presenilin intracellular trafficking (*PLD1*) and *PLD2* has been involved with amyloid beta signaling. *PLD* hydrolyses PC to produce choline and phosphatidic acid (PA) which acts as an effector for clathrin mediated endocytosis [19] and have been implicated in AD pathogenesis. With animal models to study PLD, the enzyme is emerging as a key player in regulating phospholipids metabolism and is now a therapeutic target for several brain disorders, including AD, due to its multiple role in signal transduction pathways [20, 21]. Recently GWAS had reported the involvement of *PLD3* in AD. Phospholipase C (*PLC*) cleaves phospholipids before the phosphate group as shown in Fig 4.1 which generates intermediate signaling molecules [22, 23]. As described in section 2.4.2.1, the role of phospholipase A (PLA) variants in altering the composition of the phospholipids thus, leading to increased concentration of certain lipid sub-classes and decreased concentration of the other lipid sub-classes must be investigated by closely studying the ratio and composition of the lipids changing in AD.

The results presented in chapter 2, in this thesis have also opened the area fir future investigation which may contribute to the identification of a sensitive and specific plasma lipid AD biomarker panel. Such lipidomics studies will likely lead to a greater understanding of the pathological processes involved in AD and may identify novel targets for which therapeutic interventions are directed. The following summarizes suggested areas for further investigation:

1. Determination of PLC, PLD and PLA variants activity levels within the baseline cohort is recommended. The levels of these enzymes are to be assessed longitudinally along with the potential hall mark biomarkers of AD.

2. Assessing the levels of SMase in baseline cohort and in longitudinal studies to correlate the sphingolipids and ceramides concentrations To improve the diagnostic sensitivity and specificity of the existing lipid profiles, assessing ratios of lipid species may provide additional information..

4.2. Absolute Quantitation of O^6-Benzyl Guanine and 8-oxo-O^6-Benzyl guanine in Human Plasma using Reverse Phase Liquid Chromatography-Triple Quadrapole Mass Spectrometry (LC-MS/MS)

This work detailed the absolute quantitation of O6-Benzyl Guanine (O^6BG) and 8-oxo-O6-Benzyl guanine (8-oxo-O^6BG) in the human plasma and its application to the clinical study samples with 10.0 μL of patient sample volume diluted to 100 μL with pooled human plasma blank matrix. Since the clinical dosing range of these analytes are high, and the LC-MS/MS method is sensitive enough to go low, small sample volumes are required for the bioanalysis of these analytes in the matrices. Therefore in the future, the method could be validated using the Mitra® microsampling device (Neoteryx, LLC, CA), driven by volumetric absorptive microsampling (VAMS®) technology [16,17]. Where patients enrolled in clinical trial collects the small sample volumes in microliters (μL) from their home and shipped to the analysis site as per directed procedure, making the clinical trial process feasible and cheaper. Further, the method could be compared to using dried blood

spot samples [18]. Validating the method with these sample collection techniques enables accessible micro-sample collection for pediatric clinical studies of these analytes in the future.

4.3 REFERENCES

1. Looney, S.W.; Hagan, J.L. 4 Statistical Methods for Assessing Biomarkers and Analyzing Biomarker Data. In *Handbook of Statistics*; Rao, C.R., Miller, J.P., Rao, D.C., Eds.; Epidemiology and Medical Statistics; Elsevier, 2007; Vol. 27, pp. 109–147.
2. Research, C. for D.E. and About Biomarkers and Qualification. *FDA* **2019**.
3. Zandkarimi, F.; Brown, L.M. Application of Ion Mobility Mass Spectrometry in Lipidomics. *Adv. Exp. Med. Biol.* **2019**, *1140*, 317–326.
4. Leaptrot, K.L.; May, J.C.; Dodds, J.N.; McLean, J.A. Ion mobility conformational lipid atlas for high confidence lipidomics. *Nat Commun* **2019**, *10*, 1–9.
5. Paglia, G.; Kliman, M.; Claude, E.; Geromanos, S.; Astarita, G. Applications of ion-mobility mass spectrometry for lipid analysis. *Anal Bioanal Chem* **2015**, *407*, 4995–5007.
6. Baker, P.R.S.; Armando, A.M.; Campbell, J.L.; Quehenberger, O.; Dennis, E.A. Three-dimensional enhanced lipidomics analysis combining UPLC, differential ion mobility spectrometry, and mass spectrometric separation strategies. *J. Lipid Res.* **2014**, *55*, 2432–2442.
7. Cífková, E.; Holčapek, M.; Lísa, M.; Vrána, D.; Melichar, B.; Študent, V. Lipidomic differentiation between human kidney tumors and surrounding normal tissues using HILIC-HPLC/ESI-MS and multivariate data analysis. *J. Chromatogr. B Analyt. Technol. Biomed. Life Sci.* **2015**, *1000*, 14–21.
8. Hines, K.M.; Herron, J.; Xu, L. Assessment of altered lipid homeostasis by HILIC-ion mobility-mass spectrometry-based lipidomics. *J. Lipid Res.* **2017**, *58*, 809–819.

9. Markesbery, W.R. Oxidative stress hypothesis in Alzheimer's disease. *Free Radic. Biol. Med.* **1997**, *23*, 134–147.
10. Spickett, C.M.; Pitt, A.R. Oxidative Lipidomics Coming of Age: Advances in Analysis of Oxidized Phospholipids in Physiology and Pathology. *Antioxidants & Redox Signaling* **2015**, *22*, 1646–1666.
11. Thomas, M.C.; Mitchell, T.W.; Harman, D.G.; Deeley, J.M.; Nealon, J.R.; Blanksby, S.J. Ozone-induced dissociation: elucidation of double bond position within mass-selected lipid ions. *Anal. Chem.* **2008**, *80*, 303–311.
12. Trujillo-Rodríguez, M.J.; Anderson, J.L. Silver-based polymeric ionic liquid sorbent coatings for solid-phase microextraction: Materials for the selective extraction of unsaturated compounds. *Anal. Chim. Acta* **2019**, *1047*, 52–61.
13. Momchilova, S.M.; Nikolova-Damyanova, B.M. Advances in silver ion chromatography for the analysis of fatty acids and triacylglycerols-2001 to 2011. *Anal Sci* **2012**, *28*, 837–844.
14. Dickens, B.F.; Ramesha, C.S.; Thompson, G.A. Quantification of phospholipid molecular species by coupled gas chromatography-mass spectrometry of deuterated samples. *Analytical Biochemistry* **1982**, *127*, 37–48.
15. Mapstone, M.; Cheema, A.K.; Fiandaca, M.S.; Zhong, X.; Mhyre, T.R.; MacArthur, L.H.; Hall, W.J.; Fisher, S.G.; Peterson, D.R.; Haley, J.M.; et al. Plasma phospholipids identify antecedent memory impairment in older adults. *Nat Med* **2014**, *20*, 415–418.
16. Volumetric adsorptive microsampling-liquid chromatography tandem mass spectrometry assay for the simultaneous quantification of four antibiotics in human

blood: Method development, validation and comparison with dried blood spot - ScienceDirect Available online: https://www.sciencedirect.com/science/article/abs/pii/S0731708517307112 (accessed on Oct 12, 2019).

17. Validation and clinical application of an LC-MS/MS method for the quantification of everolimus using volumetric absorptive microsampling - ScienceDirect Available online: https://www.sciencedirect.com/science/article/pii/S1570023218312194 (accessed on Oct 12, 2019).
18. Zakaria, R.; Allen, K.J.; Koplin, J.J.; Roche, P.; Greaves, R.F. Advantages and Challenges of Dried Blood Spot Analysis by Mass Spectrometry Across the Total Testing Process. *EJIFCC* **2016**, *27*, 288–317.
19. McDermott, M.; Wakelam, M.J.O.; Morris, A.J. Phospholipase D. *Biochem. Cell Biol.* **2004**, *82*, 225–253.
20. Jin, J.-K.; Ahn, B.-H.; Na, Y.-J.; Kim, J.-I.; Kim, Y.-S.; Choi, E.-K.; Ko, Y.-G.; Chung, K.C.; Kozlowski, P.B.; Min, D.S. Phospholipase D1 is associated with amyloid precursor protein in Alzheimer's disease. *Neurobiol. Aging* **2007**, *28*, 1015–1027.
21. Oliveira, T.G.; Chan, R.B.; Tian, H.; Laredo, M.; Shui, G.; Staniszewski, A.; Zhang, H.; Wang, L.; Kim, T.-W.; Duff, K.E.; et al. Phospholipase d2 ablation ameliorates Alzheimer's disease-linked synaptic dysfunction and cognitive deficits. *J. Neurosci.* **2010**, *30*, 16419–16428.

22. Shimohama, S.; Matsushima, H.; Fujimoto, S.; Takenawa, T.; Taniguchi, T.; Kameyama, M.; Kimura, J. Differential involvement of phospholipase C isozymes in Alzheimer's disease. *Gerontology* **1995**, *41 Suppl 1*, 13–19.

23. Magno, L.; Lessard, C.B.; Martins, M.; Lang, V.; Cruz, P.; Asi, Y.; Katan, M.; Bilsland, J.; Lashley, T.; Chakrabarty, P.; et al. Alzheimer's disease phospholipase C-gamma-2 (PLCG2) protective variant is a functional hypermorph. *Alz Res Therapy* **2019**, *11*, 16.